Quantum frustration in organic Mott insulators: from spin liquids to unconventional superconductors

B. J. Powell* and Ross H. McKenzie†

Department of Physics, University of Queensland, Brisbane, 4072, Australia

(Dated: February 5, 2022)

We review the interplay of frustration and strong electronic correlations in quasi-two-dimensional organic charge transfer salts, such as $(BEDT-TTF)_2X$ and $Et_nMe_{4-n}Pn[Pd(dmit)_2]_2$. These two forces drive a range of exotic phases including spin liquids, valence bond crystals, pseudo-gapped metals, and unconventional superconductivity. Of particular interest is that in several materials with increasing pressure there is a first-order transition from a spin liquid Mott insulating state to a superconducting state. Experiments on these materials raise a number of profound questions about the quantum behaviour of frustrated systems, particularly the intimate connection between spin liquids and superconductivity. Insights into these questions have come from a wide range of theoretical techniques including first principles electronic structure, quantum many-body theory and quantum field theory. In this review we introduce some of the basic ideas of the field by discussing a simple frustrated Heisenberg model with four spins. We then describe the key experimental results, emphasizing that for two materials, κ-$(BEDT-TTF)_2Cu_2$-$(CN)_3$ and $EtMe_3Sb[Pd(dmit)_2]_2$, there is strong evidence for a spin liquid ground state, and for another, $EtMe_3P[Pd(dmit)_2]_2$, there is evidence of a valence bond crystal ground state. We review theoretical attempts to explain these phenomena, arguing that they can be captured by a Hubbard model on the anisotropic triangular lattice at half filling, and that Resonating Valence Bond (RVB) wavefunctions capture most of the essential physics. We review evidence that this Hubbard model can have a spin liquid ground state for a range of parameters that are realistic for the relevant materials. In particular, spatial anisotropy and ring exchange are key to destabilising magnetic order. We conclude by summarising the progress made thus far and identifying some of the key questions still to be answered.

Contents

*Electronic address: bjpowell@gmail.com
†Electronic address: r.mckenzie@uq.edu.au

I. INTRODUCTION

In the early 1970's, Anderson and Fazekas (Anderson, 1973; Fazekas and Anderson, 1974) proposed that the ground state of the antiferromagnetic Heisenberg spin-1/2 model on the triangular lattice did not break spin rotational symmetry, i.e., had no net magnetic moment. A state of matter characterised by well defined local moments and the absence of long range order has become known as a spin liquid (Normand, 2009). Such states, are known in one-dimensional (1d) systems, but 1d systems have some very special properties that are not germane to higher dimensions. Until very recently there has been a drought of experimental evidence for spins liquids in higher dimensions (Lee, 2008).

In 1987 Anderson (Anderson, 1987), stimulated by the discovery of high-T_c superconductivity in layered copper oxides, made a radical proposal that has given rise to lively debate ever since. We summarise Anderson's proposal as:

> The fluctuating spin singlet pairs produced by the exchange interaction in the Mott insulating state become charged superconducting pairs when the insulating state is destroyed by doping, frustration or reduced correlations.

These fluctuations are enhanced by spin frustration and low dimensionality. Furthermore, partly inspired by resonating valence bond (RVB) ideas from chemical bonding (Anderson, 2008; Shaik and Hiberty, 2008), Anderson proposed a variational wave function for the Mott insulator: a BCS superconducting state from which all doubly occupied sites are projected out.

In the decades since, there has been an enormous outgrowth of ideas about spin liquids and frustrated quantum systems, which we will review. We will also consider the extent to which several families of organic charge transfer salts can be used as tuneable systems to test such ideas about the interplay of superconductivity, Mott insulation, quantum fluctuations, and spin frustration.

A goal of this review is not to be exhaustive but rather to be pedagogical, critical, and constructive. We will attempt to follow the goals for such reviews proposed long ago (Herring, 1968).

A. Motivation: frustration, spin liquids, and spinons

1. Key questions

A major goal for this review will be to address the following questions:

  1. Is there a clear relationship between superconductivity in organic charge transfer salts and in other

strongly correlated electron systems?

2. Are there materials for which the ground state of the Mott insulating phase is a spin liquid?

3. What is the relationship between spin liquids and superconductivity? In particular, does the same fermionic pairing occur in both?

4. What are the quantum numbers (charge, spin, statistics) of the quasiparticles in each phase?

5. Are there deconfined spinons in the insulating phase of any of these materials?

6. Can spin-charge separation occur in the metallic phase?

7. In the metallic phase close to the Mott insulating phase is there an anisotropic pseudogap, as in the cuprates?

8. What is the simplest low-energy effective quantum many-body Hamiltonian on a lattice that can describe all possible ground states of these materials?

9. Can a RVB variational wave function give an appropriate theoretical description of the competition between the Mott insulating and the superconducting phase?

10. Is there any significant difference between destroying the Mott insulator by hole doping and by increasing the bandwidth?

11. For systems close to the isotropic triangular lattice, does the superconducting state have broken time-reversal symmetry?

12. How can we quantify the extent of frustration? Are there differences between classical and quantum frustration? If so what are the differences?

13. What is the relative importance of frustration and static disorder due to impurities?

14. Is the "chemical pressure" hypothesis valid?

15. Is there quantum critical behaviour associated with quantum phase transitions in these materials?

16. Do these materials illustrate specific "organising principles" that are useful for understanding other frustrated materials?

At the end of the review we consider some possible answers to these questions.
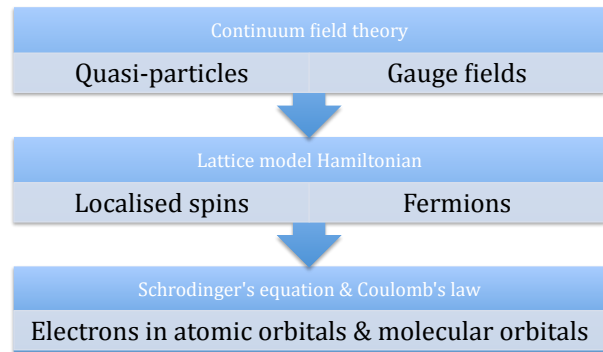
FIG. 1 The hierarchy of objects and descriptions associated with theories of organic charge transfer salts. The arrows point in the direction of decreasing length scales, increasing energy scales, and increasing numbers of degrees of freedom. At the level of quantum chemistry (Schrödinger's equation and Coulomb's law) one can describe the electronic states of single (or pairs of) molecules in terms of molecular orbitals (which can be approximately viewed as superpositions of atomic orbitals). Just a few of these molecular orbitals interact significantly with those of neigbouring molecules in the solid. Low-lying electronic states of the solid can be described in terms of itinerant fermions on a lattice and an effective Hamiltonian such as a Hubbard model (see Section VI.B). In the Mott insulating phase the electrons are localised on single lattice sites and can described by a Heisenberg spin model (see Section VI.A). The low-lying excitations of these lattice Hamiltonians and long-wavelength properties of the system may have a natural description in terms of quasi-particles which can be described by a continuum field theory such as a non-linear sigma model. At this level unexpected objects may emerge such as gauge fields and quasi-particles with fractional statistics (see Section VII).

2. A hierarchy of theories: from quantum chemistry to field theory

The quantum many-body physics of condensed matter provides many striking examples of emergent phenomena at different energy and length scales (Anderson, 1972; Coleman, 2003; Laughlin and Pines, 2000; McKenzie, 2007; Wen, 2004). Figure 1 illustrates how this is played out in the molecular crystals, which form the focus of this article, showing the stratification of different theoretical treatments and the associated objects. It needs to be emphasized that when it comes to theoretical descriptions going up the hierarchy is extremely difficult, particularly determining the quantum numbers of quasi-particles and the effective interactions between them, starting from a lattice Hamiltonian.

3. Organic charge transfer salts are an important class of materials

Organic charge transfer salts have a number of features that make them a playground for the study of quantum many-body physics. They have of several properties

that are distinctly different from other strongly correlated electron materials, such as transition metal oxides and intermetallics. These properties include:

- They are available in ultra-pure single crystals, which allow observation of quantum magnetic oscillations such as the de Haas van Alphen effect.

- The superconducting transition temperature and upper critical field are low enough that one can destroy the superconductivity and probe the metallic state in steady magnetic fields less than 20 Tesla. As a result, one can observe rich physics in experimentally accessible magnetic fields and pressure ranges

- Chemical substitution provides a means to tune the ground state.

- Chemical doping (and the associated disorder) is not necessary to induce transitions between different phases.

- These materials are compressible enough that pressures of the order of kbars can induce transitions between different ground states.

Consequently, over the past decade it has been possible to observe several unique effects due to strongly correlated electrons, sometimes phenomena that have not been seen in inorganic materials. These significant observations include:

- Magnetic field induced superconductivity.

- A first-order transition between a Mott insulator and superconductor induced with deuterium substitution, anion substitution, pressure, or magnetic field.

- A valence bond solid in a frustrated antiferromagnet.

- A spin liquid in a frustrated antiferromagnet.

- Novel critical exponents near the critical point of Mott metal-insulator transition.

- Collapse of the Drude peak in the optical conductivity (a signature of the destruction of quasiparticles) above temperatures of order of tens of Kelvin in the metallic phase.

- Bulk measurement of the Fermi surface using angle-dependent magnetoresistance.

- Low superfluid density in a weakly correlated metal.

- Multi-ferroic states.

- Superconductivity near a charge ordering transition.
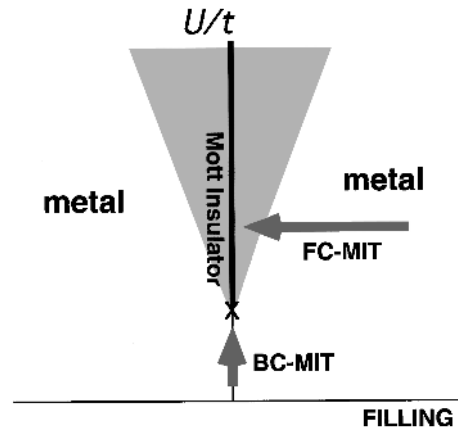
FIG. 2 Schematic phase diagram associated with the Mott-Hubbard metal-insulator transition. [Figure after Reference (Imada et al., 1998)]. The Mott insulating phase occurs at half filling and when the on-site Coulomb repulsion U is much larger than the hopping energy t and the associated band width. A transition to a metallic phase occurs either by doping away from half filling [FC-MIT= filling controlled metal-insulator transition] or by decreasing the ratio U/t [BC-MIT = bandwidth controlled metal-insulator transition]. In the cuprates a FC-MIT occurs whereas in the organic charge transfer salts considered in this review one might argue that BC-MIT occurs. On the other hand, perhaps one should consider a third co-ordinate, the frustration, in addition to the filling and band width. This would lead to the notion of a frustration controlled transition (FrC-MIT). In the Hubbard model on the anisotropic lattice at half-filling for fixed U/t increasing the hopping t'/t can drive an insulator to metal transition (compare Figure 39). [Copyright (1998) by the American Physical Society.]

Figure 2 illustrates schematically two possible different routes to destroying the Mott insulating phase, either by varying the band filling or by varying the bandwidth. Another possible route is by varying the amount of frustration of the spin interactions. An important consequence of Anderson RVB's theory of the filling controlled metal-insulator transition (FC-MIT) is that the "preexisting magnetic singlet pairs of the insulating state become charged superconducting pairs when the insulator is doped sufficiently strongly" (Anderson, 1987). It is therefore important to understand whether this extends to the bandwidth controlled metal-insulator transition (BC-MIT) were one has equal numbers of "holons" and "doublons". More generally, an important question, that has not yet received adequate attention, is what are the similarities and differences between the FC-MIT and the BC-MIT?

4. What are spin liquids?

This question has recently been reviewed in detail (Balents, 2010; Normand, 2009; Sachdev, 2009a). There are

several alternative definitions. The definition that we think is the most illuminating, because it brings out their truly exotic nature, is the following.

> A spin liquid has a ground state in which there is no long-range magnetic order and no breaking of spatial symmetries (rotation or translation) and which is not adiabatically connected to the band (Bloch) insulator.

One can write down many such quantum states. Indeed, Wen classified hundreds of them for the square lattice (Wen, 2002). But the key question is whether such a state can be the ground state of a physically realistic Hamiltonian. A concrete example is the ground state of the one-dimensional antiferromagnetic Heisenberg model with nearest-neighbour interactions. However, despite an exhaustive search since Anderson's 1987 Science paper, (Anderson, 1987) it seems extremely difficult to find a physically realistic Hamiltonian in two dimensions which has such a ground state.

As far as we are aware there is still no definitive counter-example to the following conjecture:

> Consider a family of spin-1/2 Heisenberg models on a two-dimensional lattice with short range antiferromagnetic exchange interactions (pairwise, ring exchange and higher order terms are allowed). The Hamiltonian is invariant under $SU(2) \times L$, where L is a space group and there is a non-integer total spin in the repeat unit of the lattice Hamiltonian. Let γ be a parameter which can be used to distinguish different Hamiltonians in the family (e.g., it could be the relative magnitude of different interaction terms in the Hamiltonian). Then a non-degenerate ground state is only possible for discrete values of γ (e.g., at a quantum critical point). In other words, the ground state spontaneously breaks at least one of the two symmetries $SU(2)$ and L over all continuous ranges of γ.

The requirement of non-integer spin in the repeat unit ensures that the generalisation of the Lieb-Schultz-Mattis theorem to dimensions greater than one (Alet et al., 2006; Hastings, 2004) does not apply. The theorem states that for spin-1/2 systems with one spin per unit cell on a two-dimensional lattice, if the ground state is non-degenerate and there is no symmetry breaking, one cannot have a non-zero energy gap to the lowest excited state. Note that, the triangular, kagome, and pyrochlore lattices contain one, three, and four spins per unit cell respectively (Normand, 2009). Hence, Hasting's theorem cannot be used to rule out a spin liquid for the pyrochlore lattice.

One of the best candidate counter examples to the above conjecture is the Heisenberg model on the triangular lattice with ring exchange (LiMing et al., 2000) which will be discussed in more detail in Section VI.A.

Sachdev (Sachdev, 2009b) pointed out that such Heisenberg models have possible ground states in four classes: Neel order, spiral order, a valence bond crystal, or a spin liquid. Examples of the first two occur on the square and the triangular lattices respectively. For both cases spin rotational symmetry and lattice symmetry are broken. For a valence bond crystal, only the spatial symmetry is broken. It may be that valence bond crystal ground state occurs on the anisotropic triangular lattice (cf. Section VI.A).

Normand (Normand, 2009) considered three different classes of spin liquids, each being defined by their excitation spectrum. If we denote the energy gap between the singlet ground state and the lowest-lying triplet state by Δ_T and the gap to the first excited singlet state by Δ_S. The three possible cases are:

1. $\Delta_S \neq 0$ and $\Delta_T \neq 0$.

2. $\Delta_S = 0$ and $\Delta_T \neq 0$.

3. $\Delta_S = \Delta_T = 0$.

Normand refers to the first two as Type I and Type II respectively. The third case is referred to as an Algebraic spin liquid. The case $\Delta_T = 0$ and $\Delta_S \neq 0$ is not an option because, by Goldstone's theorem, it would be associated with broken spin-rotational symmetry.

An important question is how to distinguish these different states experimentally. It can be shown that for a singlet ground state at zero temperature singlet excited states do not contribute to the dynamical spin susceptibility. If the susceptibility is written in the spectral representation, [1]

$$\chi_{-+}(\mathbf{q}, \omega) = \sum_n \exp(-\beta(E_n - E_0)) \frac{|\langle n|S^+(-\mathbf{q})|0\rangle|^2}{E_n - E_0 - \omega}, \tag{1}$$

it is clear that the matrix elements of the spin operators between the singlet ground state and any singlet excited state must be zero. This means that at low temperatures, only triplet excitations contribute to the uniform magnetic susceptibility, the NMR relaxation rate, Knight shift, and inelastic neutron scattering cross section. In contrast, both singlet and triplet excitations contribute to the specific heat capacity and the thermal conductivity at low temperatures. Hence, comparing the temperature dependence of thermal and magnetic properties should allow one to distinguish Type I spin liquids from Type II spin liquids. Furthermore, the singlet spectrum will not shift in a magnetic field but the triplets will split and the corresponding spectral weight be redistributed.

One important reason for wanting to understand these details of the spin liquid states is that the spin excitation spectrum may well be important for understanding

---

[1] Here $\beta = 1/k_B T$ is the inverse temperature and $S^\pm(\mathbf{q})$ are the spin raising/lowering operators.

unconventional superconductivity. This has led to a lot of attention being paid to a magnetic resonance seen by inelastic neutron scattering the cuprates. It is still an open question as to whether this triplet excitation is correlated with superconductivity (Chubukov et al., 2006; Cuk et al., 2004; Hao and Chubukov, 2009; Hwang et al., 2004). Strong coupling RVB-type theories focus on *singlet* excitations whereas weak-coupling antiferromagnetic spin fluctuation theories focus on *triplet* excitations. This important difference is emphasized and discussed in a review on the cuprates (Norman, 2006).

5. What are spinons?

A key question is what are the quantum numbers and statistics of the lowest lying excitations. In a Neel ordered antiferromagnet these excitations are "magnons" or "spin waves" which have total spin one and obey Bose-Einstein statistics (Auerbach, 1994). Magnons can be viewed as a spin flip propagating through the background of Neel ordered spins. They can also be viewed as the Goldstone modes associated with the spontaneously broken symmetry of the ground state.

In contrast, in a one-dimensional antiferromagnetic spin chain (which has a spin liquid ground state) the lowest lying excitations are gapless spinons which have total spin-1/2 and obey "semion" statistics, which are intermediate between fermion and boson statistics (i.e. there is a phase factor of $\pi/2$ associated with particle exchange) (Haldane, 1991). The spinons are "deconfined" in the sense that if a pair of them are created (for example, in an inelastic neutron scattering experiment) with different momentum then they will eventually move infinitely far apart. Definitive experimental signatures of this deconfinement are seen in the dynamical structure factor $S(\omega, \vec{q})$ which shows a continuum of low-lying excitations rather than the sharp features associated with spin waves. This is clearly seen in the compound $KCuF_3$, which is composed of linear chains of spin-1/2 copper ions (Tennant et al., 1995). The most definitive evidence for such excitations in a real two-dimensional material comes from Cs_2CuCl_4 (Coldea et al., 2003; Kohno et al., 2007) above the Neel ordering temperature. Below the Neel temperature these excitations become confined into conventional magnons (Fjærestad et al., 2007; Starykh et al., 2010). It is an open theoretical question as to whether there is any two-dimensional Heisenberg model with such excitations at zero temperature, other than at a quantum critical point (Singh, 2010).

What type of spinon statistics might be possible in two dimensions? Wen used quantum orders and projective symmetry groups, to construct hundreds of symmetric spin liquids, having either SU(2), U(1), or Z_2 gauge structures at low energies (Wen, 2002). He divided the spin liquids into four classes, based on the statistics of the quasi-particles and whether they were gapless:

Rigid spin liquid: spinons (and all other excitations) are fully gapped and may have either bosonic, fermionic, or fractional statistics.

Fermi spin liquid: spinons are gapless and are described by a Fermi liquid theory (the spinon-spinon interactions vanish as the Fermi energy is approached).

Bose spin liquid: low-lying gapless excitations are described by a free-boson theory.

Algebraic spin liquid: spinons are gapless, but they are not described by free fermionic and free bosonic quasiparticles.

6. Antiferromagnetic fluctuations

It has been proposed that an instability to a d-wave superconducting state can occur in a metallic phase which is close to an antiferromagnetic instability (Scalapino et al., 1986). This has been described theoretically by an Eliashberg-type theory in which the effective pairing interaction is proportional to the dynamical spin susceptibility, $\chi(\omega, \vec{q})$ (Moriya and Ueda, 2003). If this quantity has a significant peak near some wavevector then that will significantly enhance the superconducting T_c in a specific pairing channel. NMR relaxation rates are also determined by $\chi(\omega, \vec{q})$ and so NMR can provide useful information about the magnetic fluctuations. For example, a signature of large antiferromagnetic fluctuations is the dimensionless Korringa ratio that is much larger than one.

From a local picture one would like to know the strength of the antiferromagnetic exchange J between localised spins in the Mott insulating and the bad metallic phase. In RVB theory J sets the scale for the superconducting transition temperature. It is important to realise that this is very different from picture of a "glue" in the Eliashberg-type theories where superconductivity arises due to the formation of Cooper pairs between Fermi liquid quasi-particles (Anderson, 2007; Maier et al., 2008) (also see section IX.C).

7. Quantum critical points

Figure 3 shows a schematic phase diagram associated with a quantum critical point (Coleman and Schofield, 2005; Sachdev, 1999). We will discuss the relevance of such diagrams to the organic charge transfer salts below. We will see that some of the theoretical models (such as the Heisenberg model on an anisotropic triangular lattice) do undergo a quantum phase transition from a magnetically ordered to a quantum disordered phase with an energy gap to the lowest lying triplet excitation.

A particularly important question is whether any signatures of quantum critical behavior have been seen in organic charge transfer sites. Most transitions at zero temperature are first-order. Perhaps, the clearest evidence of
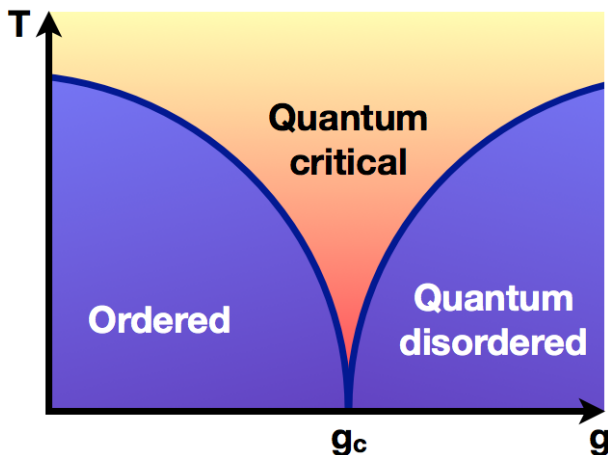
FIG. 3 Schematic phase diagram associated with a quantum critical point. The vertical axis is temperature and the horizontal axis represents a coupling constant, g. Quantum fluctuations increase with increasing g and for a critical value g_c there is a quantum phase transition from an ordered phase (with broken symmetry) to a disordered phase, usually associated with an energy gap, $\Delta \sim (g - g_c)^{z\nu}$ where z is the dynamical critical exponent and ν is the critical exponent associated with the correlation length $\xi \sim |g - g_c|^{-\nu}$. In the quantum critical region the only energy scale is the temperature and the correlation length $\xi \sim 1/T^{1/z}$. In this region there are also no quasi-particles (i.e., any singularities in spectral functions are not isolated poles but rather branch cuts).

quantum critical fluctuations come from the NMR spin relaxation rate in κ-(BEDT-TTF)$_2$Cu$_2$(CN)$_3$, which will be discussed in Section VII.D.

B. Key consequences of frustration

We briefly list some key consequences of frustration. Many of these are discussed in more detail later in the review.

- Frustration enhances the number of low energy excitations. This increases the entropy at low temperatures (Ramirez, 1994). The temperature dependence of the magnetic susceptibility is flatter and the peak occurs at a lower temperature (Section I.B.3).

- Quantum fluctuations in the ground state are enhanced due to the larger density of states at low energies. These fluctuations can destroy magnetically ordered phases (Section VI.A).

- Singlet excitations are stabilised and singlet pairing correlations are enhanced. Resonating valence bond states have a larger overlap with the true ground state of the system (Section VI.A).

- Intersite correlations are reduced which enhances the accuracy of single site approximations such as

Curie-Weiss theory and dynamical mean-field theory (Section III.D).

- In Heisenberg models frustrated spin interactions produce incommensurate correlations. These can also change the symmetry of the superconducting pairing (Powell and McKenzie, 2007), lead to new triplet excitations (phasons) (Chandra et al., 1990), and the emergence of new gauge fields which are deconfining (Section VII).

- Frustration of kinetic energy (such as in non-bipartite lattices or by next-nearest-neighbor hopping) reduces nesting of the Fermi surface and stabilises the metallic state (Section VI.B).

1. Reduction of the correlation length

The temperature dependence of the correlation length $\xi(T)$ and the static structure factor $S(\vec{Q})$, associated with the classical ordering wavevector $\vec{Q}$ has been calculated for both the triangular lattice and square lattice Heisenberg models using high-temperature series expansions (Elstner et al., 1993, 1994). For the triangular lattice the correlation length has values of about 0.5 and 2 lattice constants, at temperatures $T = J$ and $T = 0.2J$, respectively. In contrast, the model on the square lattice has correlation lengths of about 1 and 200 lattice constants, at $T = J$ and $T = 0.2J$, respectively. At $T = 0.2J$ the static structure factor has values of about 1 and 3000 for the triangular and square lattices, respectively. Hence, frustration leads to a significant reduction of the spin correlation length. These distinct differences in temperature dependence can be understood in terms of frustration producing a 'roton' like minimum in the triplet excitation spectra of the triangular lattice model (Zheng et al., 2006).

We discuss later how the temperature dependence of the uniform magnetic susceptibility of several frustrated charge transfer salts can be fit to that of the Heisenberg model on the triangular lattice with $J = 250$ K (Shimizu et al., 2003; Tamura and Kato, 2002; Zheng, Singh, McKenzie and Coldea, 2005). This implies that $\xi \simeq 2a$ at 50 K. This is consistent with estimates of the spin-spin correlation length in organic charge transfer salts from low temperture NMR relaxation rates (Yusuf et al., 2007).

2. Competing phases

One characteristic feature of strongly correlated electron systems that, we believe, should be discussed more is how sensitive they are to small perturbations. This is particularly true in frustrated systems. A related issue is that there are often several competing phases which are very close in energy. This can make variational wave functions unreliable. Getting a good variational energy

may not be a good indication that the wave function captures the key physics. Below we give two concrete examples to illustrate this point.

Firstly, consider the spin 1/2 Heisenberg model on the isotropic triangular on a lattice of 36 sites, and with exchange interaction J. Exact diagonalisation (Sindzingre et al., 1994) gives a ground state energy per site of $-0.5604J$ and a net magnetic moment (with 120 degree order as in the classical model) of 0.4, compared to the classical value of $1/2$. In contrast, a variational short-range RVB wavefunction has zero magnetic moment and a ground state energy of $-0.5579J$. Yet, it is qualitatively incorrect because it predicts no magnetic order (and thus no spontaneous symmetry breaking) in the thermodynamic limit. Note, however, that the energy difference is only $J/400$. [For details and references see Table III in (Zheng et al., 2006)].

The second example concerns the spin 1/2 Heisenberg model on the anisotropic triangular lattice, viewed as chains with exchange J' and frustrated interchain coupling J. For $J' \sim 3J$ this describes the compound Cs_2CuCl_4. The triplet excitation spectrum of the model has been calculated both with a small Dzyaloshinski-Moriya interaction D, and without ($D = 0$). It is striking that even when $D \sim J'/20$ it induces energy changes in the spectrum of energies as large as $J'/3$, including new energy gaps (Fjærestad et al., 2007). For $J' \gg J$ the ground state turns out to be "exquisitely sensitive" to other residual interactions as well (Starykh et al., 2010).

3. Alternative measures of frustration

Balents recently considered how to quantify the amount of frustration in an antiferromagnetic material (or model) and its tendency to have a spin liquid ground state (Balents, 2010). He used a measure (Ramirez, 1994) $f = T_{CW}/T_N$, the ratio of the Curie-Weiss temperature T_{CW} to the Neel temperature, T_N at which three-dimensional magnetic ordering occurs.

One limitation of this measure is that it does not separate out the effects of fluctuations (both quantum and thermal), dimensionality, and frustration. For strictly one or two dimensional systems, T_N is zero. For quasi-two-dimensional systems the interlayer coupling determines T_N. Thus, f would be larger for a set of weakly coupled unfrustrated chains than for a layered triangular lattice in which the layers are moderately coupled together.

Section II of (Zheng, Singh, McKenzie and Coldea, 2005) contains a detailed discussion of two different measures of frustration for model Hamiltonians: (1) the number of degenerate ground states, and (2) the ratio of the ground state energy to the base energy [the sum of all bond energies if they are independently fully satisfied.] This measure was introduced previously for classical models (Lacorre, 1987).

Figure 4 shows results that might be the basis of some
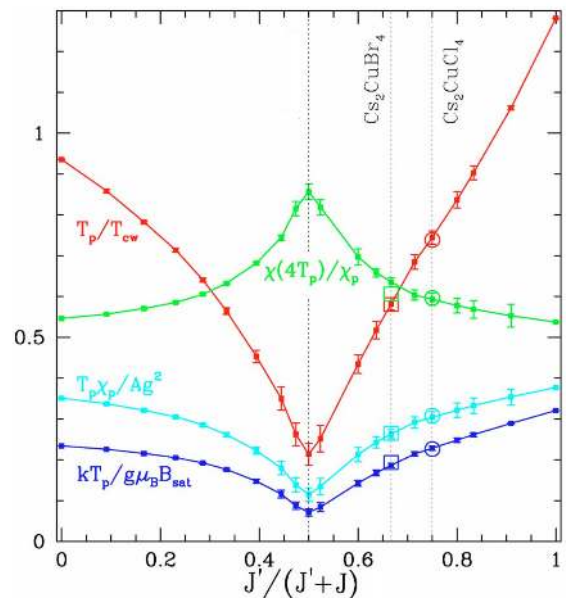
FIG. 4 Effect of frustration on the temperature dependence of the magnetic susceptibility $\chi(T)$ for the Heisenberg model on an anisotropic triangular lattice (Zheng, Singh, McKenzie and Coldea, 2005). The variation of key parameters is shown as a function of the ratio $J'/(J + J')$. T_p is the temperature at which the susceptibility is a maximum, with a value $\chi_p \equiv \chi(T_p)$. T_{cw} is the Curie-Weiss temperature which can be extracted from the high-temperature dependence of the susceptibility. B_{sat} is the magnetic saturation field and Ag^2 is the Curie-Weiss constant. All quantities were calculated by a high-temperature series expansion. All of the quantities plotted have extreme values for the isotropic triangular lattice, suggesting that in some sense it is the most frustrated. [Modified from (Zheng, Singh, McKenzie and Coldea, 2005). Copyright (2005) by the American Physical Society.]

alternative measures of frustration. The sensitivity of the temperature dependence of the susceptibility to the ratio J'/J has been used to estimate this ratio for specific materials (Zheng, Singh, McKenzie and Coldea, 2005).

In some sense then, the temperature T_p at which the susceptibility has a maximum and the magnitude of that susceptibility is a measure of the amount of frustration. This is consistent with some intuition (or is it just prejudice?) that for the anisotropic triangular lattice the frustration is largest for the isotropic case. These measures of frustration are not dependent on dimensionality and so do not have the same problems discussed above that the ratio f does. On the other hand, these measures reflect short-range interactions rather than the tendency for the system to fail to magnetically order.

Another issue that needs to be clarified is how one might distinguish quantum and classical frustration. In general the nearest neighbour spin correlation $f_s \equiv \langle \hat{\mathbf{S}}_i \cdot \hat{\mathbf{S}}_j \rangle$ will be reduced by frustration. Entanglement measures from quantum information theory can be used to distinguish truly quantum from classical correlations.

For a spin rotationally invariant state (i.e. a total spin singlet state) f_s is related to a measure of entanglement between two spins in a mixed state, known as the concurrence C by (Cho and McKenzie, 2006)

$$C = \max\{0, -2f_s - 1/2\}. \qquad (2)$$

Hence, there is maximal entanglement ($C = 1$) when the two spins are in a singlet state and are not entangled with the rest of the spins in the system. Once the spin correlations decrease to $f_s = 1/4$ there is no entanglement between the two spins.

4. Geometric frustration of kinetic energy

In a non-interacting electron model we are aware of only two proposed quantitative measures of the geometrical frustration of the kinetic energy. Both are based on the observation that, for frustrated lattices with $t > 0$, an electron at the bottom of the band does not gain the full lattice kinetic energy, while a hole at the top of the band does. Barford and Kim (Barford and Kim, 1991) suggested that for tight binding models a measure of the frustration is then $\Delta = |\epsilon_k^{max}| - |\epsilon_k^{min}|$, where ϵ_k^{max} and ϵ_k^{min} are the energies (relative to the energy of the system with no electrons) of the top and bottom of the band respectively. This frustration increases the density of states for positive energies for $t > 0$ (negative energies for $t < 0$) which represents an increased degeneracy and enhances the many-body effects when the Fermi energy is in this regime.

Together with Merino, we previously argued (Merino et al., 2006) that a simpler measure of the kinetic energy frustration is $W/2z|t|$, where W is the bandwidth and z is the coordination number of the lattice. The smaller this ratio, the stronger the frustration is, while for an unfrustrated lattice $W/2z|t| = 1$. But, for example, on the triangular lattice kinetic energy frustration leads to a bandwidth, $W = 9|t|$, instead of $12|t|$ as one might naïvely predict from $W = 2z|t|$ since $z = 6$.

We argued that geometrical frustration of the kinetic energy is a key concept for understanding the properties of the Hubbard model on the triangular lattice. In particular, it leads to particle-hole asymmetry which enhances many-body effects for electron (hole) doped $t > 0$ ($t < 0$) lattices.

It should be noted that geometrical frustration of the kinetic energy is a strictly quantum mechanical effect arising from quantum interference. This interference arises from hopping around triangular plaquettes which will have an amplitude proportional to t^3, which clearly changes sign when t changes sign. In contrast on the, unfrustrated, square lattice the smallest possible plaquette is the square and the associated amplitude for hopping around a square is independent of the sign of t as it is proportional to t^4. Barford and Kim noted that the phase collected by hopping around a frustrated cluster may be exactly cancelled by the Aharonov-Bohm phase associated with hopping around the cluster for a particular choice of applied magnetic field (Barford and Kim, 1991). Thus a magnetic field may be used to lift the effects of kinetic energy frustration. The quantum mechanical nature of kinetic energy frustration is in distinct contrast to geometrical frustration in antiferromagnets which can occur for purely classical spins.

II. TOY MODELS TO ILLUSTRATE THE INTERPLAY OF FRUSTRATION AND QUANTUM FLUCTUATIONS

We now consider some model Hamiltonians on just four lattice sites. The same Hamiltonians on an infinite lattice are relevant to the organic charge transfer salts and will be discussed in Sections VI.A and VI.B. Although such small systems are far from the thermodynamic limit, these models can illustrate some of the essential physics associated with the interplay of strong electronic correlations, frustration, and quantum fluctuations. These toy models illustrate the quantum numbers of important low-lying quantum states, the dominant short-range correlations, and how frustration changes the competition between these states. Furthermore, understanding these small clusters is a pre-requisite for cluster extensions of dynamical mean-field theory (Ferrero et al., 2009) and rotationally invariant slave boson mean-field theory (Lechermann et al., 2007) which describes band selective and momentum space selective Mott transitions. Insight can also be gained by considering two, three, and four coupled Anderson impurities (Ferrero et al., 2007). Small clusters are also the basis of the contractor renormalisation (CORE) method which has been used to study the doped Hubbard model (Altman and Auerbach, 2002) and frustrated spin models (Berg et al., 2003).

A similar approach of just considering four sites has been taken before when considering the ground state of a Heisenberg model on a depleted lattice which is a model for CaV_4O_9 (Ueda et al., 1996). The authors first considered a single plaquette with frustration, albeit along both diagonals (see also Section 3 in (Valkov et al., 2006)). Dai and Whangbo (Dai and Whangbo, 2004) considered the Heisenberg model on a triangle and a tetrahedra. Similar four site Heisenberg Hamiltonians have also been discussed in the context of mixed valence metallic clusters of particular interest to chemists (Augustyniak-Jablokow et al., 2005).

A. Four site Heisenberg model

The four site Heisenberg model illustrates that frustration can lead to energy level crossings and consequently to changes in the quantum numbers of the ground state and lowest lying excited state.

The Hamiltonian is (see Figure 5(a))

$$\hat{\mathcal{H}} = J\left(\hat{\mathbf{S}}_1 \cdot \hat{\mathbf{S}}_2 + \hat{\mathbf{S}}_2 \cdot \hat{\mathbf{S}}_3 + \hat{\mathbf{S}}_3 \cdot \hat{\mathbf{S}}_4 + \hat{\mathbf{S}}_4 \cdot \hat{\mathbf{S}}_1\right)$$
$$+ J'\hat{\mathbf{S}}_1 \cdot \hat{\mathbf{S}}_3. \tag{3}$$

It is helpful to introduce the total spin along each of the diagonals, $\hat{\mathbf{S}}_{13} = \hat{\mathbf{S}}_1 + \hat{\mathbf{S}}_3$ and $\hat{\mathbf{S}}_{24} = \hat{\mathbf{S}}_2 + \hat{\mathbf{S}}_4$, and note that these operators commute with each other and with the Hamiltonian. The total spin of all four sites can be written in terms of these operators: $\hat{\mathbf{S}} = \hat{\mathbf{S}}_{13} + \hat{\mathbf{S}}_{24}$. Thus, the total spin S, and the total spin along each of the two diagonals, S_{13} and S_{24} are good quantum numbers. The term in (3) associated with J can be rewritten as $J/2(\hat{\mathbf{S}}^2 - \hat{\mathbf{S}}_{13}^2 - \hat{\mathbf{S}}_{24}^2)$. Hence, the energy eigenvalues are

$$E(S, S_{13}, S_{24}) = \frac{1}{2}JS(S+1) + \frac{1}{2}(J'-J)S_{13}(S_{13}+1)$$
$$-\frac{1}{2}JS_{24}(S_{24}+1) - \frac{3}{4}J'. \tag{4}$$

Figure 5 (c) shows a plot of these energy eigenvalues as a function of J'/J. We note that the quantum numbers of the lowest lying excited state change when $J' = J$ and $J' = 4J$, and that the ground state changes when $J' = 2J$.

The two singlet states can also be written as linear combinations of two orthogonal valence bond states, denote $|H\rangle$ and $|V\rangle$, which descibe a pair of singlets along the horizontal and vertical directions, respectively (see Figure 5 (b)). The state with quantum numbers $(S, S_{13}, S_{24}) = (0, 0, 0)$ is

$$|0, 0, 0\rangle = \frac{1}{\sqrt{2}}\left(|H\rangle - |V\rangle\right) \tag{5}$$

and the state with $(S, S_{13}, S_{24}) = (0, 1, 1)$ state is

$$|0, 1, 1\rangle = \frac{1}{\sqrt{2}}\left(|H\rangle + |V\rangle\right). \tag{6}$$

Both of these singlet states are resonating valence bond states (see Figure 5 (b)).

The Hamiltonian has C_{2v} with the C_2 axes along each diagonal (and out of the plane). The two singlet states above have A_1 and A_2 symmetry, respectively. However, if $J' = 0$ there is C_{4v} symmetry and the $(0, 0, 0)$ and $(0, 1, 1)$ states have A_1 and B_1 symmetry, respectively. The latter, which is the ground state, connects naturally to the B_1 symmetry of a $d_{x^2-y^2}$ superconducting order parameter on the square lattice.

It is possible to relate the two singlet states to the physical states of a Z_2 gauge field on a single plaquette (see Section 3.2 of (Alet et al., 2006)). The gauge flux operator on the plaquette F_p flips the bonds between horizontal and vertical. The RVB states (5) and (6) are eigenstates of F_p with eigenvalues ± 1.
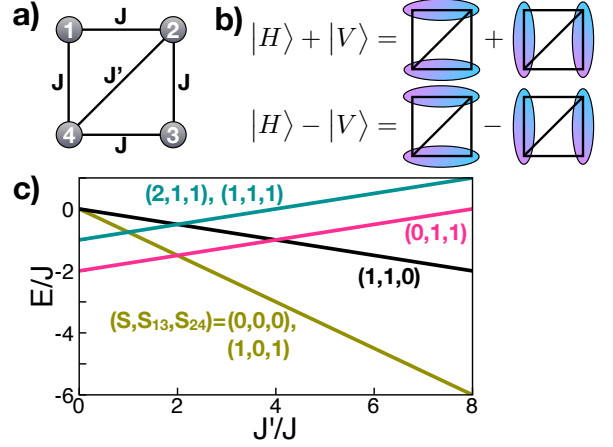
FIG. 5 Eigenstates and eigenvalues of a frustrated Heisenberg model on a single plaquette. (a) The exchange interactions in the model. (b) The two resonating valence bond states which span all the singlet states (compare equations (5) and (6)). (c) Dependence of the energy eigenvalues as a function of the diagonal interaction J'/J. Note that the quantum numbers of the lowest lying excited state change when $J' = J$ and the ground state changes when $J' = 2J$. Furthermore, the two resonating valence bond states become degenerate at $J' = 2J$.

1. Effect of a ring exchange iteraction

Consider adding to Hamiltonian (3) the term

$$\hat{\mathcal{H}}_\square = J_\square(\hat{P}_{1234} + \hat{P}_{4321}) \tag{7}$$
$$= J_\square(\hat{P}_{12}\hat{P}_{34} + \hat{P}_{14}\hat{P}_{23} - \hat{P}_{13}\hat{P}_{24} + \hat{P}_{13} + \hat{P}_{24} - 1)$$

where $J_\square$ describes the ring-exchange interaction around a single plaquette, the operator $\hat{P}_{12} = 2\hat{\mathbf{S}}_1 \cdot \hat{\mathbf{S}}_2 + 1/2$ permutes spins 1 and 2, and $\hat{P}_{1234}$ is the permutation operator around the plaquette (Misguich and L'huillier, 2005; Thouless, 1965).

Intuitively,

$$\hat{\mathcal{H}}_\square|H\rangle = 2J_\square|V\rangle \qquad \hat{\mathcal{H}}_\square|V\rangle = 2J_\square|H\rangle \tag{8}$$

Hence, the RVB states (5) and (6) are eigenstates of the ring-exchange Hamiltonian with eigenvalues $-2J_\square$ and $2J_\square$, respectively. Hence, ring exchange has a similar effect to the diagonal interaction in that it stabilises the state $|0, 0, 0\rangle$.

B. Four site Hubbard model

A comprehensive study of the $t' = 0$ model (which has C_{4v} symmetry) has been given by Schumann (Schumann, 2002). The analysis is simplified by exploiting this SU(2) symmetry associated with particle-hole symmetry (Noce and Cuoco, 1996). In particular, the Hamiltonian matrix then decomposes into blocks of dimension 3 or less. Schumann has also solved the model on a tetrahedron and a

triangle (Schumann, 2008). When $t' \neq 0$ the SU(2) symmetry is broken, but it may be that the SU(2) quantum numbers are still useful to define a basis set in which to diagonalize the Hamiltonian and see the effect of $t' \neq 0$.

Freericks, Falicov, and Rokshar studied an eight site Hubbard model with a next-nearest-neigbour hopping t' and periodic boundary conditions (Freericks et al., 1991). The model is invariant under a 128-element cluster permutation group. For $t' = t/2$ the model is equivalent to an eight site triangular lattice cluster or a face-centred-cubic cluster. They found that at half filling the symmetry of the ground state changed as a function of both t'/t and U/t [see Figure 3 in (Freericks et al., 1991)].

Falicov and Victora (Falicov and Victora, 1984) showed that the Hubbard model on a tetrahedron [which has T_d symmetry] with four electrons has a singlet ground state with E symmetry.[2] Later Falicov and Proetta (Falicov and Proetto, 1993) also showed that an RVB state with complex pairing amplitude (and which thus breaks time-reveral symmetry) and which they state has E symmetry[3] is within 0.3% of the exact ground state energy for $U = 10t$.

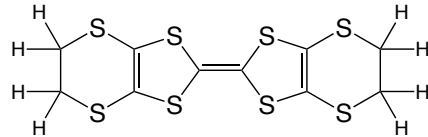More work is required to use the above results to extract insights about the role of frustration. An important question is whether results on four sites can be related to a simple picture of how $d_{x^2-y^2}$ Cooper pairing emerges on the square lattice due to antiferromagnetic interactions (Scalapino and Trugman, 1996). If so, does this pairing symmetry change with frustration, as it does for the infinite lattice, at the mean-field RVB level (Powell and McKenzie, 2007)?

III. κ-(BEDT-TTF)$_2$X

An important class of model systems for quantum frustration is the organic charge transfer salts based on the molecule bis(ethylenedithio)tetrathiafulvalene (also known as BEDT-TTF or ET; shown in Fig. 6a). These salts have been extensively studied and show a wide range of behaviours including, antiferromagnetism, spin liquids, (unconventional) superconductivity, Mott transitions, incoherent (or 'bad') metals, charge ordering and Fermi liquid behaviour. In this section we focus on the aspects most relevant to the quantum frustration in these materials, a number of other reviews focusing on different aspects of these materials are also available elsewhere (Ishiguro et al., 1998; Lang and Müller, 2003; Powell and McKenzie, 2006; Seo et al., 2006; Singleton and Mielke, 2002; Wosnitza, 2007) and in the November 2004 issue of *Chemical Reviews*. Further, although a number of crystallographic phases are observed in the BEDT-TTF salts,

---

[2] We use Mulliken notation, Falicov and Victora use Bethe notation and label this representation Γ_3, see (Lax, 1974) for details.

[3] Or Γ_{12} in the Bouckaert, Smoluchoski, Wigner notation (Lax, 1974) that Falicov and Proetta use.
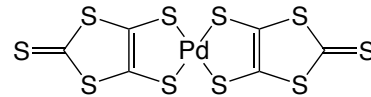
a) BEDT–TTF

b) Pd(dmit)$_2$

FIG. 6 The molecules BEDT-TTF and Pd(dmit)$_2$, which form charge transfer salts with frustrated lattices and in which the electrons are strongly correlated. BEDT-TTF denotes bis(ethylenedithio)tetrathiafulvalene, an is an electron donor. Pd(dmit)$_2$ is an electron acceptor where dmit is 1,3-dithiol-2-thione-4,5-dithiolate.

we will limit ourselves to the κ phase, which is by far the most widely studied and, in which, the most profound effects of frustration have been found.

The experimentally observed phase diagrams of two κ-BEDT-TTF salts (κ-(BEDT-TTF)$_2$Cu[N(CN)$_2$]Cl and κ-(BEDT-TTF)$_2$Cu$_2$(CN)$_3$) are shown in Figs. 7 and 8. One should note how similar these two phase diagrams are (except for the magnetic order, or lack thereof, observed in the Mott insulating phase). Two important parameters are the strength of the electronic correlations and the degree of frustration. These parameters are determined by the choice of anion, X, in κ-(BEDT-TTF)$_2$X and the applied hydrostatic pressure. Below we will focus on four of the most widely studied materials: κ-(BEDT-TTF)$_2$Cu(NCS)$_2$ and κ-(BEDT-TTF)$_2$-Cu[N(CN)$_2$]Br, which superconduct below $\sim$10 K at ambient pressure; κ-(BEDT-TTF)$_2$Cu[N(CN)$_2$]Cl, which is an antiferromagnetic Mott insulator at ambient pressure; and κ-(BEDT-TTF)$_2$Cu$_2$(CN)$_3$, which appears to be a spin liquid at ambient pressure. Both κ-(BEDT-TTF)$_2$-Cu$_2$(CN)$_3$ and κ-(BEDT-TTF)$_2$Cu[N(CN)$_2$]Cl undergo Mott transitions to superconducting states under modest pressures (a few 100 bar).

A. Crystal and electronic structure

κ-(BEDT-TTF)$_2$X salts form crystals with alternating layers of the electron donors BEDT-TTF and electron acceptors ,X, leading to a quasi-two-dimensional (q2D) band structure. Charge is transferred from organic (BEDT-TTF) layer to the anion (X) layer; for monovalent anions, which we consider here, one electron is transferred from each dimer [(BEDT-TTF)$_2$ unit] to each anion formula unit. Band structure calculations (Kandpal et al., 2009; Nakamura et al., 2009) predict that the anion layer is insulating, but that the dimer layers are
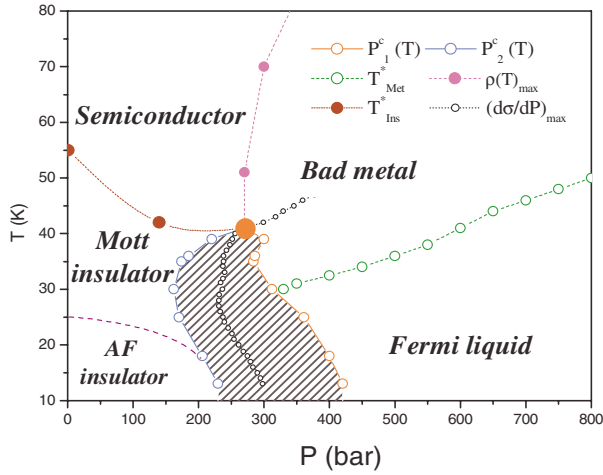
FIG. 7 Pressure-temperature phase diagram of κ-(BEDT-TTF)$_2$Cu[N(CN)$_2$]Cl. At low temperatures it undergoes a first-order Mott transition from an antiferromagnetic (AF) insulator (section III.B) to a metal when hydrostatic pressure is applied (section III.C). As the temperature is raised the line of first order transitions ends in a critical point with novel critical exponents (section III.C.1). In the insulating phase raising the temperature destroys the antiferromagnetic order. At the very lowest temperatures the metallic state becomes superconducting (section III.E). As the temperature is raised superconductivity gives way to a metal with coherent intralayer charge transport (section III.D.2) and a pseudogap (section III.D.3). Further, raising the temperature results in a loss of coherence in the intralayer transport. This incoherent metallic phase is referred to as a 'bad-metal' (section III.D). From (Limelette, Wzietek, Florens, Georges, Costi, Pasquier, Jérome, Mézière, and Batail, 2003). [Copyright (2003) by the American Physical Society.]

half-filled. Hence, these calculations predict that the organic layers are metallic, in contrast to the rich phase diagram observed (Figs. 7 and 8).

The κ phase salts of BEDT-TTF are strongly dimerised, that is the molecules stack in pairs within the crystal, cf. Fig. 9. The frontier molecular orbitals of the BEDT-TTF molecule are π orbitals, i.e., they have nodes in the plane of the molecule, cf. Fig. 11. Thus, these orbitals overlap with the equivalent orbitals on the other molecule in the dimer, cf. Fig. 11, more than they overlap with the orbitals of any other BEDT-TTF molecule. This, combined with the greater physical proximity of the two molecules within the dimer, means that the amplitude for an electron to hop between two molecules within the same dimer has a much larger magnitude than the amplitude for hopping between molecules in different dimers. This suggests that the interdimer hopping might be integrated out of an effective low energy Hamiltonian (Kino and Fukuyama, 1996; McKenzie, 1998).
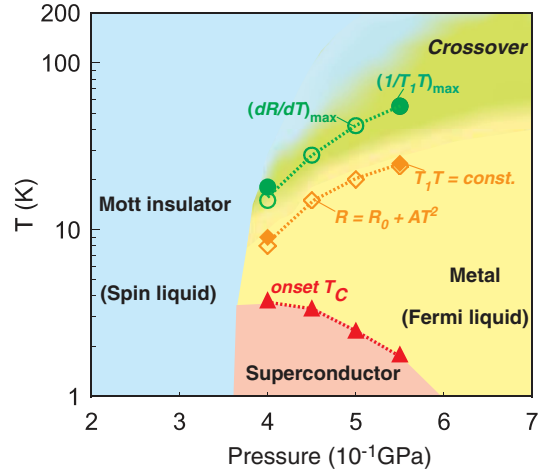
FIG. 8 Pressure-temperature phase diagram of κ-(BEDT-TTF)$_2$Cu$_2$(CN)$_3$. This is similar to that of κ-(BEDT-TTF)$_2$-Cu[N(CN)$_2$]Cl (Fig. 7), but has important differences. Most importantly the Mott insulating phase does not show any signs of long range magnetic order down to 20 mK (the lowest temperature studied; see section III.B and Fig. 12). Thus, κ-(BEDT-TTF)$_2$Cu$_2$(CN)$_3$ is believed to be a spin liquid at ambient and low pressures. Further, there is no evidence of a pseudogap in κ-(BEDT-TTF)$_2$Cu$_2$(CN)$_3$ (see section III.D.4). These differences are believed to result from the greater geometrical frustration in κ-(BEDT-TTF)$_2$Cu$_2$(CN)$_3$ (cf. Table I, Eq. (9) and Fig. 9). From (Kurosaki et al., 2005). [Copyright (2005) by the American Physical Society.]

1. Dimer model of the band structure of κ-(BEDT-TTF)$_2X$

The dimer model described above is the simplest, and most widely studied, model of the electronic structure for the κ-(BEDT-TTF)$_2X$ salts and leads to the Hubbard model on an anisotropic lattice at half filling (McKenzie, 1998; Powell and McKenzie, 2006). The Hamiltonian of this model is

$$\hat{\mathcal{H}} = -t \sum_{\langle ij \rangle \sigma} \hat{c}_{i\sigma}^\dagger \hat{c}_{j\sigma} - t' \sum_{[ij]\sigma} \hat{c}_{i\sigma}^\dagger \hat{c}_{j\sigma} + U \sum_i \hat{c}_{i\uparrow}^\dagger \hat{c}_{i\uparrow} \hat{c}_{i\downarrow}^\dagger \hat{c}_{i\downarrow}, (9)$$

where $\hat{c}_{i\sigma}^{(\dagger)}$ destroys (creates) an electron with spin σ on site (dimer) i, t and t' are the hopping amplitudes between neighbouring dimers in the directions indicated in Fig. 9, and U is the effective Coulomb repulsion between two electrons on the same site (dimer). This model is, up to an overall scale factor, governed by two dimensionless ratios: t'/t, which sets the strength of the frustration in system and U/W, which determines the strength of electronic interactions. Here, W is the bandwidth, which is determined by the values of t and t'. These two ratios can be manipulated experimentally by hydrostatic pressure,[4] P, or by studying materials with different anions,

―――――

[4] It has often been emphasised (Kanoda, 1997) that increased hydrostatic pressures correspond to decreased correlation (de-
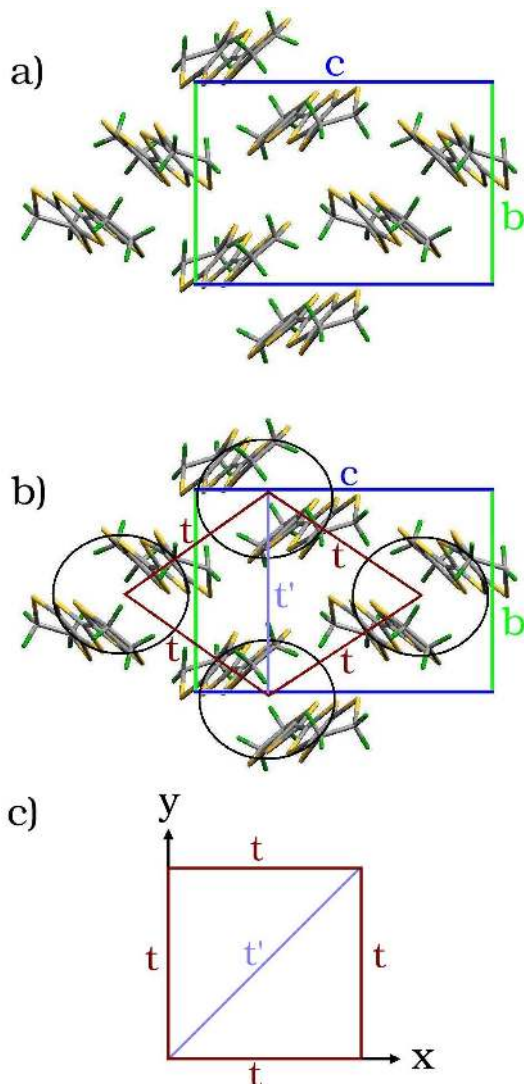
FIG. 9 Tight binding model of the electronic band-structure of a κ-type BEDT-TTF salt. Panel (a) shows a cross section of the crystal structure of κ-(BEDT-TTF)$_2$Cu(NCS)$_2$ in the organic layer. In panel (b) the black circles mark the dimers, within which the hopping integral is large and which serve as a 'site' in lattice models of the band structure. Lines indicate the inter-dimer hopping integrals in both panels (b) and (c), which are topologically equivalent. [Taken from (Powell, 2006)].

X. Varying the anions is often referred to as chemical pressure, as both degrees of freedom lead to changes in the lattice constants. However, it appears that chemical pressure causes larger variations in t'/t than hydrostatic pressure does. We will limit our discussions to monova-

lent anions,[5] in which case we have κ-(BEDT-TTF)$_2^+ X^-$, i.e., there is, on average, one hole per dimer and the appropriate dimer Hubbard model is half filled.

The anisotropic triangular lattice model extrapolates continuously between three widely studied lattice models. For $t' = 0$ it is just the square lattice. For $t' = t$ we recover the (isotropic) triangular lattice. And for $t \to 0$ one has quasi-one-dimensional chains with weak zig-zag interchain hopping. Thus, this model can be used to systematically explore the effects of frustration in strongly correlated systems and would be of significant theoretical interest even without the experimental realisations of the model in organic charge transfer salts.

In order to make a direct comparison between theory and experiment one would like to know what parameters of the anisotropic triangular lattice (i.e., what values of t, t' and U) represent specific materials. Significant effort has therefore been expended to estimate these parameters from electronic structure calculations. The first studies of the electronic structure of κ-BEDT-TTF salts where limited, by the computational power available at the time, to extended Hückel theory (Williams et al., 1992). This is a semi-empirical, i.e. experimentally parameterised, tight-binding model and ignores the role of the anions and electronic correlations. However, modern computing power means that density functional theory (DFT) calculations are no longer prohibitively expensive and several DFT studies have appeared recently.

The large unit cells and complex anions of the κ phase materials, meant that the first DFT studies of BEDT-TTF salts focused on other crystallographic phases (French and Catlow, 2004; Kasowski and Whangbo, 1990; Kino and Miyazaki, 2006; Kubler et al., 1987; Lee et al., 2003; Miyazaki and Kino, 2003, 2006; Yamaguchi et al., 2003). However, two groups have recently reported parameterisations of the tight-binding part of the Hamiltonian from DFT[6] calculations (Kandpal et al., 2009; Nakamura et al., 2009). Both groups find that the frustration parameter, t'/t, is significantly smaller than was previously thought on the basis of extended Hückel calculations (summarised in Table I). Note that the frustration is least in κ-(BEDT-TTF)$_2$Cu[N(CN)$_2$]Cl, which has an antiferromagnetically ordered ground state and greatest in κ-(BEDT-TTF)$_2$Cu$_2$(CN)$_3$, which has a spin liquid ground state. However, even κ-(BEDT-TTF)$_2$Cu$_2$(CN)$_3$ is quite far from the isotropic triangular lattice ($t' = t$), which has been taken as the basis of a number of theories of κ-(BEDT-TTF)$_2$Cu$_2$(CN)$_3$ (discussed in Section VI.A.4) on the basis of Hückel calculations (Komatsu et al., 1996).

The anisotropic triangular lattice has one site per unit cell. However, the κ-phase organics have two dimers per

---

creased U/W), but it has become increasingly clear (Caulfield et al., 1994; Kandpal et al., 2009; Pratt, 2010) that pressure may also induce changes in the frustration, t'/t.

---

[5] See (Mori, 2004) for a discussion of anions with valencies other than one.

[6] Both GGA and LDA functionals give similar results.

TABLE I Values of t'/t of selected κ-BEDT-TTF salts, calculated from Density Functional Theory (DFT). Hückel theory gives systematically smaller values of 0.75, 0.84, and 1.06, for these salts, respectively. Estimates of this parameter in the metallic phase can also be made from quantum oscillation experiments for κ-(BEDT-TTF)$_2$Cu(NCS)$_2$ (Pratt, 2010), giving $t'/t = 0.6$ in agreement with the DFT calculated value.

Material	t'/t	Reference
κ-(BEDT-TTF)$_2$Cu[N(CN)$_2$]Cl	0.4	(Kandpal et al., 2009)
κ-(BEDT-TTF)$_2$Cu(NCS)$_2$	0.6	(Kandpal et al., 2009; Nakamura et al., 2009)
κ-(BEDT-TTF)$_2$Cu$_2$(CN)$_3$	0.8	(Kandpal et al., 2009; Nakamura et al., 2009)

unit cell. This halves the Brillouin zone and causes the Fermi surface to be split into two sheets (Merino and McKenzie, 2000a; Powell and McKenzie, 2006). Thus, two orbits are observed in quantum oscillations experiments. The lower frequency orbit, known as the α pocket corresponds to a hole like orbit. A higher frequency oscillation, known as the β orbit, is only observed at higher fields and corresponds to the magnetic breakdown orbit around the Fermi surface of the dimer per unit cell model. The ratio of the areas of these orbits is strongly dependent on t'/t (Pratt, 2010). Thus, estimates of t'/t can be made from quantum oscillation or angle-dependent magnetoresistance (AMRO) experiments, which allow one to map out the Fermi surface (Kartsovnik, 2004). In κ-(BEDT-TTF)$_2$Cu(NCS)$_2$ at ambient pressure this yields $t'/t = 0.7$ (Caulfield et al., 1994), in reasonable agreement with the calculated value. In κ-(BEDT-TTF)$_2$-Cu$_2$(CN)$_3$ at 7.6 kbar one finds that $t'/t = 1.1$ (Ohmichi et al., 2009; Pratt, 2010), which is rather larger than the ambient pressure value calculated from DFT. At 0.75 GPa the DFT calculations give $t'/t = 0.75$ (Kandpal et al., 2009), which is significantly smaller than the experimental estimate. AMRO experiments give a picture of the Fermi surface that is qualitatively consistent with the calculated Fermi surface (Ohmichi et al., 1997) (see Figure 10). However, the value of t'/t has not been estimated from these measurements.

The area of the Fermi surface can be also determined by quantum oscillations. For a wide range of organic charge transfer salts the area is found to be consistent with Luttinger's theorem and the hypothesis that these materials are always at half filling (Powell and McKenzie, 2004a). This may put significant constraints on theories that the metal-insulator transition involves "self-doping" (Baskaran, 2003).

The hopping between layers is much weaker than that within the layers. This can be measured in two separate ways: from AMROs (Moses and McKenzie, 1999; Singleton et al., 2002; Wosnitza et al., 1996, 2002) or from a comparison of how disorder affects the superconducting critical temperature and the residual resistivity (Powell and McKenzie, 2004b). Both methods find that the interlayer hopping integral, $t_\perp$ is a few tens of μeV in the κ-(BEDT-TTF)$_2X$, but that $t_\perp$ is an order of magnitude larger in the β phase ET salts. DFT calculations (Lee et al., 2003) find that interlayer dispersion
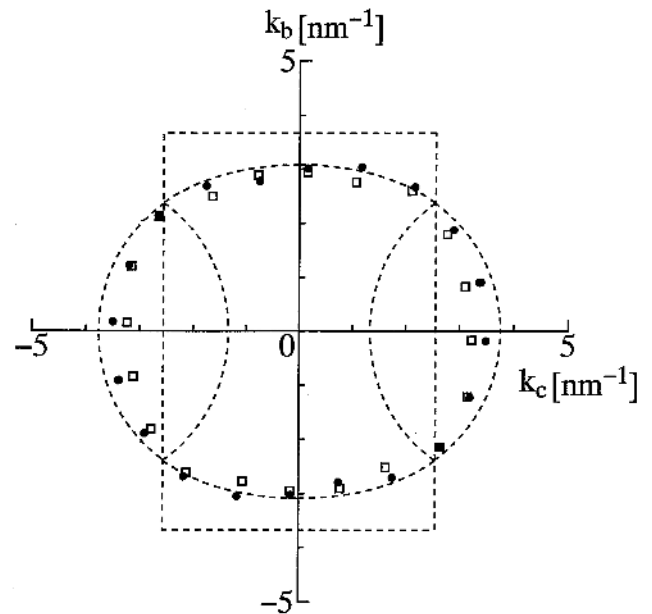
FIG. 10 The Fermi surface of κ-(BEDT-TTF)$_2$Cu$_2$(CN)$_3$ in the metallic phase at pressures of 2.1 kbar (open squares) and 7.0 kbar (closed circles), as determined by Angle-Dependent Magneto-Resistance Oscillations (AMRO) (Ohmichi et al., 1997). The dashed elliptical curves are the results of Hückel calculations.

in β-(BEDT-TTF)$_2$I$_3$ is ~ 9 meV. However, experimental estimates for the closely related material, β-(BEDT-TTF)$_2$IBr$_2$, yield $t_\perp \sim 0.3$ meV (Powell and McKenzie, 2004b; Wosnitza et al., 1996). However, one should note that the value of $t_\perp$ represents a very sensitive test of theory due its small absolute value and the small overlap of the atomic orbitals at the large distances involved in interlayer hopping.

2. The Hubbard U

There is a considerable literature that discusses the calculation of the Hubbard U in a molecular crystals. Notable systems for which this problem has been tackled include the alkali doped fullerides (Gunnarsson, 2004), oligo-acene and thiopenes (Brocks et al.,

2004), and the organic conductor tetrathiafulvalene-tetracyanoquinodimethane (TTF-TCNQ) (Cano-Cortés et al., 2007). These authors have proceeded by identifying two separate contributions to the Hubbard U:

$$U = U^{(v)} - \delta U^{(p)}, \qquad (10)$$

where $U^{(v)}$ is the contribution from the molecule (or cluster) in vacuum, and $\delta U^{(p)}$ is the reduction in the effective U when the molecule is placed in the polarisable environment of the crystal.

One might think that $U^{(v)}$ is straightforward to calculate once one has a set of suitably localised orbitals as it is just the Coulomb repulsion between two holes (or electrons) in the same orbital:

$$F_0 = \int d^3\mathbf{r}_1 \int d^3\mathbf{r}_2 \frac{\rho_\uparrow(\mathbf{r}_1)\rho_\downarrow(\mathbf{r}_2)}{|\mathbf{r}_1 - \mathbf{r}_2|}, \qquad (11)$$

where $\rho_\sigma(\mathbf{r})$ the density of spin σ electrons at the position $\mathbf{r}$ in the relevant orbital. However, this is incorrect. When one moves from a full band structure to the relevant one (or few) band model this interaction is significantly renormalised (Freed, 1983; Gunnarsson, 2004; Iwata and Freed, 1992; Powell, 2011; Scriven and Powell, 2009a). Indeed, DFT calculations for a single BEDT-TTF molecule find that the renormalised $U^{(v)}$ is about 50% smaller than F_0 (Scriven and Powell, 2009a).

The first attempts to calculate $U^{(v)}$ from electronic structure calculations were also based on the extended Hückel method. It was noted (Kino and Fukuyama, 1996) that if one models the dimer as a two site Hubbard model where each site represents a monomer then in the limit $U_m^{(v)} \to \infty$, where $U_m^{(v)}$ is the effective Coulomb repulsion between two holes on the same monomer, one finds that $U^{(v)} \to 2|t_{b_1}|$, where t_{b_1} is the intra-dimer hopping integral. Whence, calculations of t_{b_1} from the extended Hückel approximation yield estimates of $U^{(v)}$ ranging between 0.14 eV (Rahal et al., 1997) and 2.1 eV (Simonov et al., 2005). Note that this range of Hubbard Us is not caused just by changes in anions, but also the difference between different groups, who often find differences of more than a factor of two for the same material [for an extended discussion see (Scriven and Powell, 2009b)]. More recently DFT has also been used to calculate t_{b_1} and hence $U^{(v)}$ (Kandpal et al., 2009; Nakamura et al., 2009) - again there is a factor of two difference between the two different groups.

A better method of calculating $U^{(v)}$ is to note that

$$U = E_0(+2) + E_0(0) - 2E_0(+1), \qquad (12)$$

where $E_0(q)$ is the ground state energy of the molecule or cluster with charge q. This can be understood as U is the energy required to activate the charge disproportionation reaction $2(\text{BEDT-TTF})_2^+ \to (\text{BEDT-TTF})_2^0 + (\text{BEDT-TTF})_2^{2+}$. Equivalently, U is the difference in the chemical potentials for electrons and holes on the molecule or cluster. Calculations of this type for isolated BEDT-TTF monomers show that $U_m^{(v)}$ is essentially the same

for all monomers in the geometries in which they are found experimentally regardless of the anion in the salt, the crystal polymorph, or the temperature or pressure at which the crystal structure was measured (Scriven and Powell, 2009a). Remarkably, the same result holds for isolated dimers, consistent with the experimental finding that the dimer is a conserved structural motif in both the κ and β polymorphs (Scriven and Powell, 2009b).

Further, comparison of DFT calculations for monomers with those for dimers reveals that the approximation $U^{(v)} \to 2|t_{b_1}|$ is *incorrect* (Scriven and Powell, 2009b). This is because the effective Coulomb interaction between two holes on different monomers within the same dimer, $V_m^{(v)}$, is also large. Indeed, Scriven et al. found that $U_m^{(v)} \sim V_m^{(v)} \gg t_{b_1}$, in which case $U^{(v)} \simeq \frac{1}{2}(U_m^{(v)} + V_m^{(v)})$, which is in reasonable agreement with their directly calculated value of $U^{(v)}$.

To date there are no calculations of $\delta U^{(p)}$ for BEDT-TTF salts. This problem is greatly complicated for BEDT-TTF relative to the other molecular crystals previously studied (Brocks et al., 2004; Cano-Cortés et al., 2007; Gunnarsson, 2004; Tsiper and Soos, 2003) because of the (often) polymeric anions and the fact that the intermolecular spacing is small compared to the size of the molecule. Therefore, Nakamura et al. (Nakamura et al., 2009) have calculated U directly from DFT band structure calculations by explicitly integrating out high energy interband excitations to leave an effective one band model. Interestingly, in order for the value of U to converge Nakamura et al. had to include over 350 bands - corresponding to including excitations up to 16 eV above the Fermi level! Nakamura et al. find that the value of U in the Mott insulator κ-(BEDT-TTF)$_2$-Cu$_2$(CN)$_3$ (0.83 eV) is remarkably similar to that in the ambient pressure superconductor κ-(BEDT-TTF)$_2$-Cu(NCS)$_2$ (0.85 eV). However, they find that $t = 55$ meV for κ-(BEDT-TTF)$_2$Cu$_2$(CN)$_3$ and $t = 65-70$ meV for κ-(BEDT-TTF)$_2$Cu(NCS)$_2$, yielding $U/t = 15.5$ for κ-(BEDT-TTF)$_2$Cu$_2$(CN)$_3$ and $U/t = 12.0 - 12.8$ for κ-(BEDT-TTF)$_2$Cu(NCS)$_2$, consistent with the experimental finding that former material is a Mott insulator that undergoes a Mott transition under moderate pressure and the later is an ambient pressure superconductor.

However, these values are much larger than those found from comparisons of DMFT calculations to optical conductivity measurements and on κ-(ET)$_2$Cu[N(CN)$_2$]Br$_x$Cl$_{1-x}$, which suggest that $U = 0.3$ eV (Merino et al., 2008). These measurements are discussed in more detail in section III.C.

3. The (BEDT-TTF)$_2$ dimer

Significant insight can be gained from comparing (BEDT-TTF)$_2$ with the hydrogen molecule. In the molecular orbital (Hartree-Fock) picture (Fulde, 1995)

the ground state wavefunction of H_2 is

$$|\Psi\rangle = \frac{1}{2}\left(|\phi_{1\uparrow}\rangle + |\phi_{2\uparrow}\rangle\right) \otimes \left(|\phi_{1\downarrow}\rangle + |\phi_{2\downarrow}\rangle\right), \qquad (13)$$

where $|\phi_{i\sigma}\rangle$ is a basis function for an electron with spin σ centred on atom i. This provides the simplest model of the chemical bond, which results from the stabilisation of the bonding combination of atomic orbitals, and implies an increased electronic density between the two atoms. If one includes electronic interactions the picture is somewhat complicated as the wavefunction becomes correlated. These correlations can be described in the two site Hubbard model, which is a good model for the hydrogen molecule, where each atom is treated as a site (Powell, 2011). If one compares the electronic density in the HOMO of a single BEDT-TTF molecule (Fig. 11a) with that of the HOMO of the (BEDT-TTF)$_2$ dimer (Fig. 11b), it is clear that the (BEDT-TTF)$_2$ dimer wavefunction is close to being an antibonding combination of molecular wavefunctions, whereas the HOMO-1 (Fig. 11c) is close to being a bonding combination of molecular wavefunctions. In the charge transfer salt there are, on average, two electrons in the HOMO-1, but only one in the HOMO. Therefore, the net effect is bonding.

Electronic correlations also play an important role in the (BEDT-TTF)$_2$ dimer. But, as in the case of H_2, the two site Hubbard model, where each site is now an BEDT-TTF molecule, provides a good description of the electronic correlations in the (BEDT-TTF)$_2$ dimer (Powell and McKenzie, 2006; Scriven and Powell, 2009b). This shows that the physics of the (BEDT-TTF)$_2$ dimer is remarkably similar to that of the hydrogen molecule. Therefore, we can understand the (BEDT-TTF)$_2$ dimer as being held together by a 'covalent bond' not between any two atoms, but between the two BEDT-TTF molecules themselves. As one expects this 'intermolecular covalent bond' to be strong compared to the interactions between dimers, this provides a natural explanation of the conservation of the dimer motif across different materials.

B. Insulating phases

Both κ-(BEDT-TTF)$_2$Cu[N(CN)$_2$]Cl and κ-(BEDT-TTF)$_2$Cu$_2$(CN)$_3$ are insulators at ambient pressure (Ishiguro et al., 1998), and undergo a metal-insulator transition under the application of hydrostatic pressure (which we will discuss in section III.C). This can be understood straightforwardly, in terms of the half-filled Hubbard model, introduced in section III.A, as a Mott insulator phase (Kanoda, 1997; McKenzie, 1998). However, despite these similarities in the charge sector, the spin degrees of freedom in the two materials behave very differently.
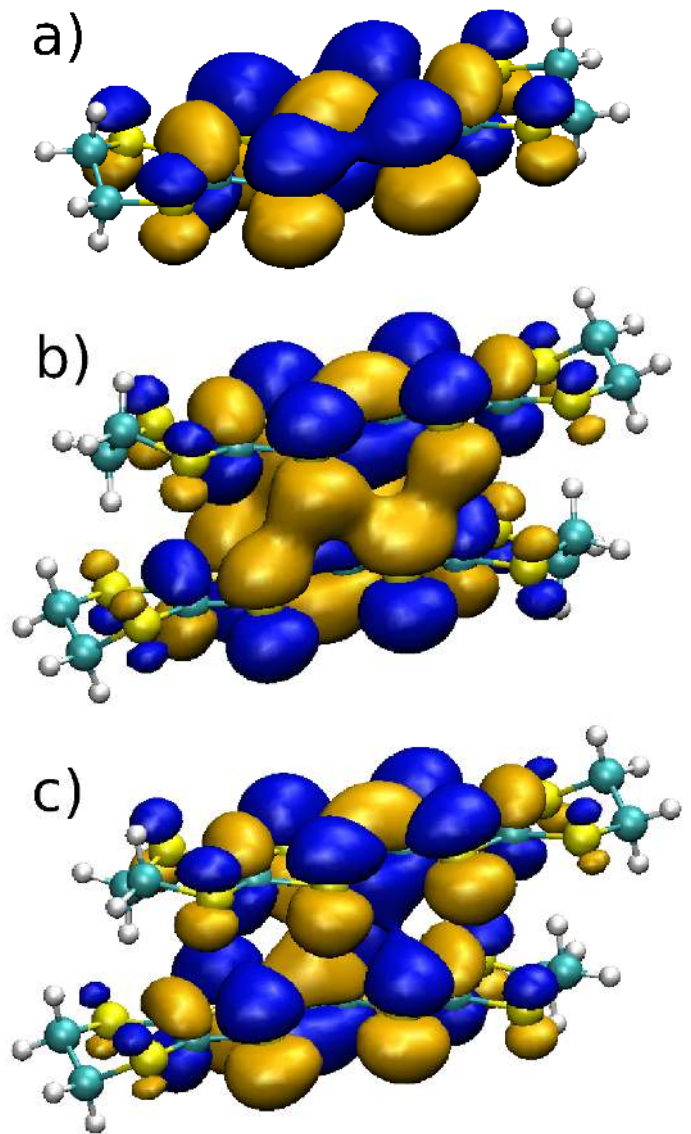
FIG. 11 The highest occupied molecular orbital (HOMO) of (a) an BEDT-TTF molecule in the geometry found in κ-(BEDT-TTF)$_2$Cu[N(CN)$_2$]Cl, (b) an (BEDT-TTF)$_2^{2+}$ dimer in the geometry found in κ-(BEDT-TTF)$_2$Cu$_2$(CN)$_3$ and (c) a neutral (BEDT-TTF)$_2$ dimer in the geometry found in κ-(BEDT-TTF)$_2$Cu$_2$(CN)$_3$. It is clear from these plots that the HOMO of the neutral dimer is the antibonding combination of the two monomer HOMOs, whereas the HOMO of the (double) cation dimer is the bonding combination of the two monomer HOMOs. Thus, the (BEDT-TTF)$_2$ dimer is held together by a 'covalent bond' between the two monomers rather than bonds between any two particular atoms. [Modified from (Scriven and Powell, 2009a) and (Scriven and Powell, 2009b)].

1. Antiferromagnetic and spin liquid phases

Shimizu *et al.* (Shimizu et al., 2003) measured and compared bulk spin susceptibilities of κ-(BEDT-TTF)$_2$-Cu[N(CN)$_2$]Cl and κ-(BEDT-TTF)$_2$Cu$_2$(CN)$_3$. Both materials are described by the Hubbard model on the

anisotropic triangular lattice, cf. Fig. 9. In the Mott insulating phase the spin degrees of freedom are described by a Heisenberg model (Section VI.A) with exchange constants, $J \sim 250$ K. However, κ-(BEDT-TTF)$_2$Cu$_2$(CN)$_3$ is significantly more frustrated than κ-(BEDT-TTF)$_2$Cu[N(CN)$_2$]Cl (as expected by electronic structure calculations, cf. Table I). κ-(BEDT-TTF)$_2$Cu[N(CN)$_2$]Cl shows a clear magnetic phase transition at ~ 27 K. This is an antiferromagnetic transition (Kanoda, 1997; Miyagawa et al., 1995) and is only visible in the bulk spin susceptibility because there is a small canting of the magnetic moment (Miyagawa et al., 2002), which gives rise to a weak ferromagnetic moment (Welp et al., 1992). In contrast, no such phase transition is visible in the susceptibility of κ-(BEDT-TTF)$_2$Cu$_2$(CN)$_3$. Analyses (Shimizu et al., 2003; Zheng, Singh, McKenzie and Coldea, 2005) of the high temperature magnetic susceptibility show that in both materials the effective Heisenberg exchange is $J \sim 250$ K. Therefore, the absence of a phase transition in κ-(BEDT-TTF)$_2$Cu$_2$(CN)$_3$ down to 32 mK (the lowest temperature studied and four orders of magnitude smaller than J) led Shimizu et al. to propose that κ-(BEDT-TTF)$_2$Cu$_2$(CN)$_3$ is a spin liquid.

The form of the temperature dependence of the susceptibility turns out to be quite sensitive to the amount of frustration (Zheng, Singh, McKenzie and Coldea, 2005) (cf. Figure 4). The values of both J and J' can be estimated by comparing the observed temperature dependence of the uniform magnetic susceptibility with high temperature series expansions (above about $J/4$). For κ-(BEDT-TTF)$_2$Cu$_2$(CN)$_3$ they agree for $J \simeq 200$ K and $J' \simeq J$. In Section VI.A.4 we discuss the possible effects of ring exchange. Consequently, it is desirable to know how they may modify the temperature dependence of the susceptibility and the values of the exchange interaction estimated from the experimental data.

Further, evidence for the absence of magnetic ordering in κ-(BEDT-TTF)$_2$Cu$_2$(CN)$_3$ comes from its NMR spectrum. Fig. 12 compares the ^{1}H NMR absorption spectrum of κ-(BEDT-TTF)$_2$Cu$_2$(CN)$_3$ with that of κ-(BEDT-TTF)$_2$Cu[N(CN)$_2$]Cl. Shimizu et al. reported that "the difference of the spectra between the two salts at high temperatures is explained by the difference in the orientation of ET molecules against the applied field and does not matter." In κ-(BEDT-TTF)$_2$Cu[N(CN)$_2$]-Cl (Fig. 12b) they observe clear changes in the NMR spectrum below $T_C \sim 27$ K. These multiple peaks are caused by the distinct crystal environments for the ^{1}H atoms due to the antiferromagnetic ordering. In contrast, no quantitative changes are observed in the spectrum of κ-(BEDT-TTF)$_2$Cu$_2$(CN)$_3$ down to 32 mK, the lowest temperature studied (Fig. 12a), consistent with an absence of long-range magnetic ordering.

No evidence of long range magnetic order is observed in the ^{13}C-NMR spectra of κ-(BEDT-TTF)$_2$Cu$_2$(CN)$_3$ down to 20 mK (the lowest temperature studied) (Fig. 12c). This is important because these experiments were carried out on samples where the ^{13}C is one of the atoms involved in the central C=C double bond. The electron density is much higher for this atom (cf. Fig. 11) than for the H atoms, which are on the terminal ethylene groups (cf. Fig. 6). Therefore the ^{13}C spectra demonstrate that the absence of long range order is genuine and not an artefact caused by low electronic density on the H atoms. We stress that 20 mK is four orders of magnitude smaller than the exchange coupling, which suggests that κ-(BEDT-TTF)$_2$Cu$_2$(CN)$_3$ may well be a true spin liquid.

The observed temperature dependence of the NMR relaxation rates for κ-(BEDT-TTF)$_2$Cu$_2$(CN)$_3$ are also inconsistent with this material having a magnetically ordered ground state. The observed (Shimizu et al., 2006) decrease of the NMR relaxation rate, $1/T_1$, and the spin echo rate, $1/T_2$, with decreasing temperature for κ-(BEDT-TTF)$_2$Cu$_2$(CN)$_3$ is distinctly different from that expected for a material with a magnetically ordered ground state. For such materials at low temperatures, both $1/T_1$ and $1/T_2$ should increase rapidly with decreasing temperature, rather than decreasing (since $1/T_1 T \sim \xi(T)^2$). The increase is seen in κ-(BEDT-TTF)$_2$Cu[N(CN)$_2$]Cl , above the antiferromagnetic ordering temperature. For materials described by the antiferromagnetic Heisenberg model on a square lattice [La$_2$CuO$_4$] (Sandvik and Scalapino, 1995) and a chain [Sr$_2$CuO$_3$] (Takigawa et al., 1997), both relaxation rates do increase monotonically as the temperature decreases.

It is noteworthy that for κ-(BEDT-TTF)$_2$Cu$_2$(CN)$_3$ at low temperatures, from 1 K down to 20 mK, it was found (Shimizu et al., 2006) that $1/T_1 \sim T^{3/2}$ and $1/T_2 \sim$ constant (see Figure 13). As discussed in Section VII.E this is similar to that expected in the quantum critical regime, (53), with the critical exponent $\eta \sim 1$, expected for a non-linear sigma model with deconfined spinons. However, the observed temperature dependence of T_1 and T_2 would lead to two different values for the exponent η.

However, caution is required in interpreting the data in Fig. 13. The observed relaxation rate is not well described by a single exponential. Shimizu et al. extracted T_1 from a fit to a stretched exponential, the exponent, α, is plotted in the inset to Fig. 13. This could be indicative of multiple relaxation rates or some other complex phenomena that has not yet been adequately explained.

There is a way to check that the NMR relaxation is actually due to spin fluctuations and not another physical mechanism. The magnitude of the relaxation rate at high temperatures can be used to provide an independent estimate of J. Data for κ-(BEDT-TTF)$_2$Cu$_2$(CN)$_3$ at ambient pressure (Kawamoto et al., 2006) gives, for the outer ^{13}C site, $1/T_1 \simeq 10 - 30$/sec in the range 100-300 K. From the $K - \chi$ plot a value of $A = 0.07$ T$/\mu_B$ is deduced for the outer site (Shimizu et al., 2003). Using the above values in the expression (37) gives $J \simeq 200 - 600$ K, consistent with the value $J = 250$ deduced from the temperature dependence of the uniform magnetic susceptibility (Shimizu et al., 2003; Zheng, Singh, McKenzie and Coldea, 2005).
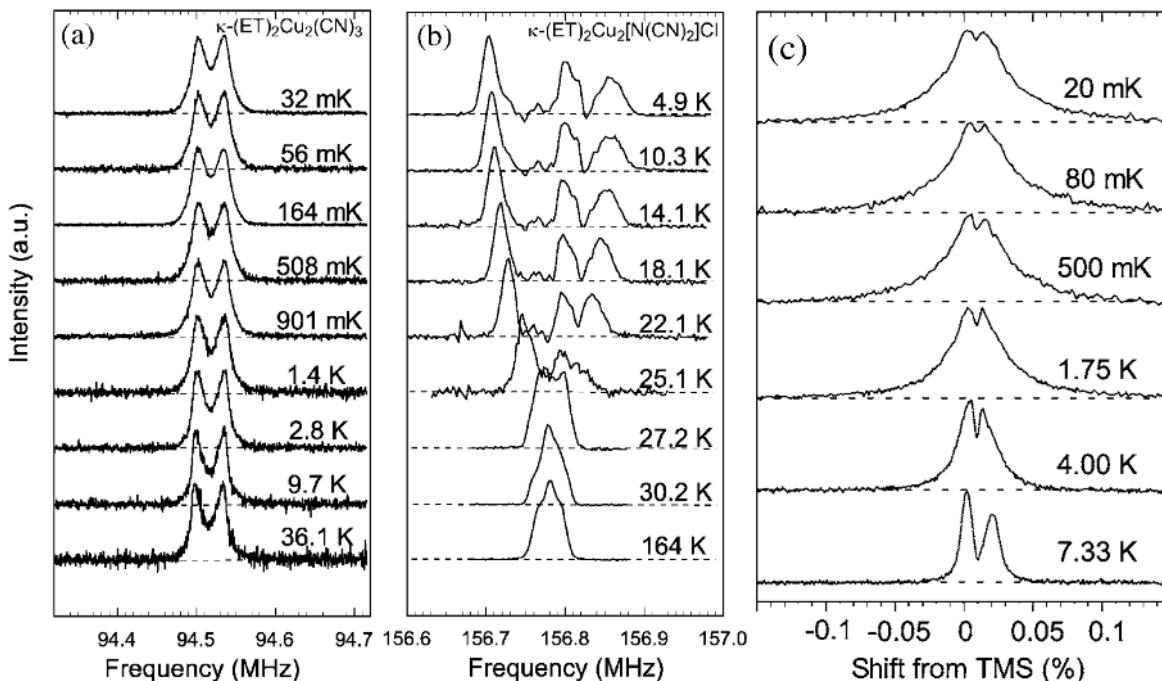
FIG. 12 The low temperature, ambient pressure ^{1}H-NMR absorption spectra of (a) κ-(BEDT-TTF)$_2$Cu$_2$(CN)$_3$ and (b) κ-(BEDT-TTF)$_2$Cu[N(CN)$_2$]Cl, and (c) the ^{13}C-NMR absorption spectra of κ-(BEDT-TTF)$_2$Cu$_2$(CN)$_3$. The antiferromagnetic phase transition at $\sim$ 27 K is clear seen in κ-(BEDT-TTF)$_2$Cu[N(CN)$_2$]Cl. In contrast, no major changes occur with temperature in κ-(BEDT-TTF)$_2$Cu$_2$(CN)$_3$, consistent with the absence of long range magnetic order. However, the spectra do broaden as T is lowered in κ-(BEDT-TTF)$_2$Cu$_2$(CN)$_3$. This broadening is seen even more dramatically in the ^{13}C-NMR spectrum of κ-(BEDT-TTF)$_2$Cu$_2$(CN)$_3$ (panel c). Again, no signs of long range magnetic order are seen down to 20 mK, a temperature that is four orders of magnitude smaller than the antiferromagnetic exchange energy, $J \approx 250$ K (Shimizu et al., 2003; Zheng, Singh, McKenzie and Coldea, 2005). [Panels (a) and (b) were taken from (Shimizu et al., 2003) and panel (c) was modified from (Shimizu et al., 2006).] [Copyright (2003,2006) by the American Physical Society.]

However, Shimizu et al. did observe a slight broadening of the ^{1}H NMR spectrum of κ-(BEDT-TTF)$_2$Cu$_2$(CN)$_3$ as the temperature is *lowered*. They observed an even more dramatic broadening in the ^{13}C NMR (Fig. 12c) (Shimizu et al., 2006). This is somewhat counter-intuitive and has provoked some theoretical interest, discussed below. Spin echo ^{13}C experiments show that the broadening is inhomogenous (T_2^*) rather than an increase in the homogeneous T_2. Similar broadenings are also seen in EtMe$_3$Sb[Pd(dmit)$_2$]$_2$ and EtMe$_3$P[Pd(dmit)$_2$]$_2$, cf. Section IV.C and Fig. 27, which could hint that this is a rather general phenomenon. It was also observed that a magnetic field induces spatially non-uniform local moments (Shimizu et al., 2006). Motrunich has given an interpretation of this observation in terms of spin liquid physics (Motrunich, 2006): the fluctuating gauge field associated with the spinons leads to the nuclear spins "seeing" a distribution in local magnetic fields.

Several model calculations have been performed to attempt to explain the large broadening by taking into account the role of disorder (Gregor and Motrunich, 2009). They found that they could only explain the experimental data for temperatures above about 5 K, if there is much larger disorder than expected and that it is strongly temperature dependent. This is in contrast

to previous work where comparable calculations for a kagome antiferromagnet could explain experimental data for ZnCu$_3$(OH)$_6$Cl$_2$ (Gregor and Motrunich, 2008). Gregor and Motrunich mention that it is hard to estimate the strength of the disorder and the role of temperature dependent screening. It is desirable to connect this work to recent estimates of the strength of disorder in the κ-(BEDT-TTF)$_2$X materials (Scriven and Powell, 2009b).

2. Is the spin liquid in κ-(BEDT-TTF)$_2$Cu$_2$(CN)$_3$ gapped?

Key questions about a spin liquid are: is it gapped and what are the nature of the low lying excitations? In particular, are there deconfined spinons? Two experiments have recently tried to address these questions in κ-(BEDT-TTF)$_2$Cu$_2$(CN)$_3$, one by measuring the specific heat (Yamashita et al., 2008), the other by measuring the thermal conductivity (Yamashita et al., 2009). However, as will now discuss, the two groups reached contradictory conclusions on the basis of these different measurements.

S. Yamashita et al. (Yamashita et al., 2008) concluded that there are gapless fermionic excitations, i.e., deconfined spinons, in κ-(BEDT-TTF)$_2$Cu$_2$(CN)$_3$ on the basis of their specific heat, C_p, measurements. A plot of C_p/T
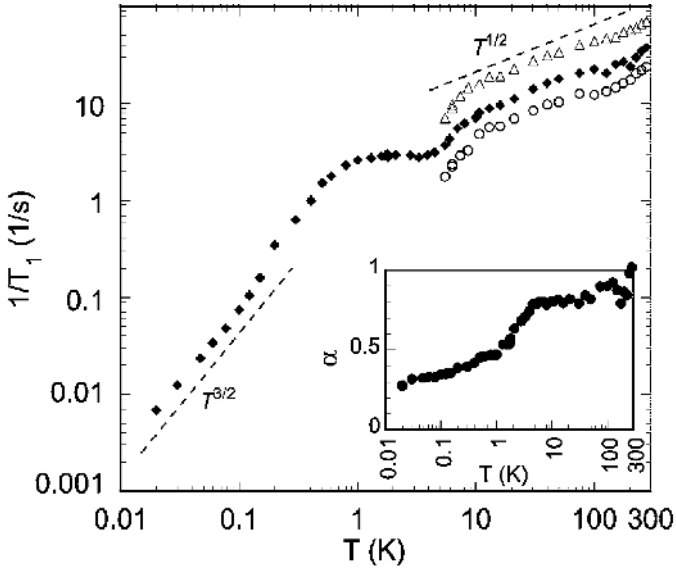
FIG. 13 Temperature dependence of the the ^{13}C-NMR relaxation rate $1/T_1$ for the spin liquid material κ-(BEDT-TTF)$_2$-Cu$_2$(CN)$_3$ at ambient pressure (Shimizu et al., 2006). Between 20 mK and 1 K $1/T_1 \sim T^{3/2}$, which suggests that the spin triplet excitation spectrum is gapless. Such a power law dependence is consistent with quantum critical behaviour. The inset shows the temperature dependence of the exponent α associated with the stretched exponential time dynamics of the spin relaxation. [Copyright (2006) by the American Physical Society.]

FIG. 14 The thermal conductivity, κ, of κ-(BEDT-TTF)$_2$-Cu$_2$(CN)$_3$ measured in two samples (A and B) and in different magnetic fields. As with the heat capacity, simple arguments suggest that, at low temperatures $\kappa/T = \alpha + \beta T^2 + \ldots$. Clearly this is not what is observed. These data suggest that $\alpha \simeq 0$ (a simple extrapolation gives $\alpha < 0$, which is unphysical). This suggests that the spin liquid state of κ-(BEDT-TTF)$_2$Cu$_2$(CN)$_3$ is gapped. However, finite temperatures do not lead to a quadratic increase in κ/T, suggesting that the low-lying excitations may be more complex that simply magnons and phonons. [Modified from (Yamashita et al., 2009).]

against T^2 is linear in the range $\sim$0.75-2.5 K, implying that $C_p = \gamma T + \beta T^3$, with $\gamma = 20 \pm 5$ mJ K^{-2} mol^{-1}. Moving to lower temperatures complicates heat capacity measurements as there is a significant Schottky anomaly. Nevertheless, the data in the temperature range 0.075 - 3 K fits well to the form $C_p = \alpha/T^2 + \gamma T + \beta T^3$ with $\gamma = 12$ mJ K^{-2} mol^{-1}. One expects a large linear term in the heat capacity if there are gapless fermionic excitations. Indeed, the values of γ estimated by S. Yamashita et al. are the same order of magnitude as those found in the metallic phases of κ-(BEDT-TTF)$_2X$ salts. Further, comparing this value with the previous measurements of the bulk magnetic susceptibility (Shimizu et al., 2003) gives a Sommerfeld-Wilson ratio, $R_W = (\pi^2 k_B^2/\mu^2)(\chi_0/\gamma)$, of order unity (Yamashita et al., 2008), which is what one would expect if the same fermions were responsible for both the linear term in the specific heat and the susceptibility (Lee et al., 2007b). In contrast, other organic charge transfer salts which undergo magnetic ordering were found to have no such linear term but to have a specific heat capacity that was quadratic in temperature.

In a discussion of these results Ramirez (Ramirez, 2008) pointed out that S. Yamashita et al.'s data is fit equally well by $C_p = \alpha/T^2 + \gamma_{2/3}T^{2/3} + \beta T^3$. This is consistent with the predictions for spinons coupled to a $U(1)$ gauge field (Montrunich, 2005) (as discussed in Section VII. Ramirez was also concerned that the entropy associated with the γ term estimated by S. Yamashita et al. is only about $\frac{R\ln 2}{40}$, which is only a small fraction of the total spin entropy. However, it is not clear to us that this should be a point of concern since for at temperatures of order $J/5$ the entropy of a Heisenberg antiferromagnet is already much less than the high temperature value due to short-range spin correlations (Elstner et al., 1994).

In contrast to the specific heat results described above M. Yamashita et al. (Yamashita et al., 2009) concluded, on the basis of thermal conductivity measurements, that the spin liquid state in κ-(BEDT-TTF)$_2$Cu$_2$(CN)$_3$ is fully gapped. As with the heat capacity, one expects that for a simple metal the thermal conductivity is given by $\kappa = \alpha T + \beta T^3 + \ldots$ (Ziman, 1960), with the fermions giving rise to the linear term and bosons, typically phonons, giving rise to the cubic term. Note particularly that, as κ is only sensitive to itinerant excitations, one does not need to subtract a Schottky term. Fig. 14 shows M. Yamashita et al.'s data in the temperature range 0.08-0.3 K plotted as κ/T against T^2. One immediately notices that the data does not lie on a straight line, which suggests that it is not dominated by phonons and therefore that M. Yamashita et al. did resolve the contribution from magnetic excitations. Further support for this assertion comes from the field dependence of the data, which one would not expect if the heat transport was dominated by phonons. However, more importantly, one should notice that an extrapolation of the data to $T = 0$ will not give a

significant κ/T (indeed the simplest extrapolation, indicated by the arrows in the figure, gives $\kappa/T < 0$, which is unphysical). Therefore, M. Yamashita *et al.* concluded that κ/T vanishes at $T = 0$ K. If correct this would imply that the spin liquid state of κ-(BEDT-TTF)$_2$Cu$_2$(CN)$_3$ is gapped.

M. Yamashita *et al.* also attempted to quantitatively analyse the very lowest temperature part of their data. One complication in this exercise was that they were unable to directly determine what fraction of the measured thermal conductivity is due to magnetic excitations and what fraction, $\kappa_{ph} = \beta T^3$, is due to phonons. M. Yamashita *et al.* found that $\kappa(T)$ cannot be well described by a power law even if κ_{ph} is large enough to represent three quarters of the measured κ at $T = 100$ mK, which seems a rather generous upper bound given their arguments (described above) that the phonons do not dominate the thermal conductivity. This suggests that the gap does not have nodes, which would give a small but non-zero intercept.

M. Yamashita *et al.* also made an Arrhenius-plot of their data. A reasonable fit was found for a value of β that implies that about one quarter of the thermal conductivity at 100 mK is due to phonons. This fit yields a gap of 0.46 (0.38) K in zero field (10 T). However, as M. Yamashita *et al.* stress, one should be cautious about taking this precise value too seriously as that fit was limited to less than a decade of temperature (0.08-0.5 K) due to the low energy scales involved and current limitations in cryogenic technology. Nevertheless, this analysis does show that, if there is a gap, it is 2-3 orders of magnitude smaller than the exchange energy $J \sim 250$ K.

Clearly, an important question is why these two experiments (specific heat and thermal conductivity) lead to such different conclusions. M. Yamashita *et al.* (Yamashita et al., 2009) argued that this disagreement results from an incorrect subtraction of the Schottky term in the heat capacity. However, this is unlikely to be the full story because the Schottky term only dominates the heat capacity below ~ 0.2 K. One point of interest is that the value of γ extracted from the heat capacity measured between ~ 0.75-2.5 K (in which no Schottky anomaly is evident) is almost twice that found from the fit of the data taken between 0.075 and 3 K. The gap estimated by M. Yamashita *et al.* is small compared to 0.75 K, so one would expect there to be high densities of thermally excited fermions in the higher temperature range. Indeed, significant densities of thermally excited fermions would remain over most of the lower temperature range.

3. The 6 K anomaly

One thing both groups (Yamashita et al., 2009, 2008) do agree on is that something interesting happens at temperatures around 6 K. S. Yamashita *et al.* found a broad 'hump' when they replot their data as $C_p T^{-3}$ against T

(in this plot the phonon term should just appear as a constant offset, while the Schottky term is not relevant at these relatively high temperatures). They also present a provocative plot of $\Delta C_p/T$ against T, where ΔC_p is the difference between the heat capacities of κ-(BEDT-TTF)$_2$Cu$_2$(CN)$_3$ and κ-(BEDT-TTF)$_2$Cu(NCS)$_2$. However, κ-(BEDT-TTF)$_2$Cu(NCS)$_2$ becomes superconducting at ~ 10 K, so its heat capacity is changing rapidly in the relevant temperature range. This makes it difficult to distinguish which of the changes in ΔC_p are due to κ-(BEDT-TTF)$_2$Cu$_2$(CN)$_3$. Note that the estimation of γ, discussed above, is from lower temperature data. However, the 'hump' appears as a change in slope of C_p/T versus T^2 around 6 K, so it is not clear that whatever causes this effect can be neglected in the estimation of γ. S. Yamashita *et al.* also found that the heat capacity is remarkably insensitive to magnetic fields (they studied fields up to 8 T).

The anomaly in the thermal conductivity is, however, very clear cut. A hump is immediately obvious in the plot of κ against T, Fig. 1 of (Yamashita et al., 2009), which begins at ~ 6 K and reachs a broad maximum at ~ 4 K. Clear anomalies have also been reported in the NMR spin-lattice relaxation rate, $1/T_1$, (Shimizu et al., 2003) and the uniaxial expansion coefficients (Manna et al., 2010) in this temperature range.

A number of theoretical explanations have been proposed for the 6 K anomaly including: pairing of spinons (Lee et al., 2007a), the formation of visons (vortices in a Z_2 spin liquid) (Qi et al., 2009), spin-chirality ordering (Baskaran, 1989) and exciton condensation (Qi and Sachdev, 2008). These theories will be discussed in section VII.H.

C. Mott metal-insulator transition

In the cuprates[7] the metal-insulator transition is driven by chemically doping charge carriers into the copper-oxygen plane of the insulating parent compound (Lee et al., 2006). This is sometimes referred to as the 'band-filling controlled Mott transition'. However, in the organics the 'parent' insulating compound can be driven metallic by decreasing U/W the ratio of the Hubbard U to the bandwidth, W. This is often referred to as the 'bandwidth controlled Mott transition' (cf. Figure 2) There are several ways to drive the bandwidth controlled Mott transition in the κ-(BEDT-TTF)$_2X$ salts:

1. *Hydrostatic pressure.* This is a beautiful realisation of Mott's original proposal (Mott, 1949) of how to drive a Mott insulator metallic. Because

---

[7] As we only refer to the cuprates here for pedagogical reasons we will neglect subtleties relating to the role of the oxygen p-levels and the distinction between charge transfer and Mott insulators (Zaanen et al., 1985).

they form rather soft crystals, only moderate pressure (sometimes as small as a few hundred bars) are required to drive very significant changes, including the Mott transition, in organic charge transfer salts.

2. *Uniaxial stress.* This seems a particularly promising approach as it holds out the prospect of also tuning the frustration, i.e., t'/t. However, this method has not yet been widely applied to the κ-(BEDT-TTF)$_2 X$ salts. For a recent review see (Kagoshima and Kondo, 2004).

3. '*Chemical pressure*'. Changes in the anion have a significant effect on the unit cell parameters - particularly in systems with polymeric anions. Thus, tuning the chemistry of the anion is remarkably similar to applying a pressure. For example, κ-(BEDT-TTF)$_2$Cu[N(CN)$_2$]Cl is an antiferromagnetic Mott insulator, but the isostructural κ-(BEDT-TTF)$_2$Cu[N(CN)$_2$]Br is a metal, which superconducts at low temperatures. A particularly elegant form of chemical pressure is to alloy the anions Cu[N(CN)$_2$]Br and Cu[N(CN)$_2$]Cl to form crystals of κ-(BEDT-TTF)$_2$Cu[N(CN)$_2$]Cl$_{1-x}$Br$_x$. We stress that as both anions are monovalent this *does not dope* the organic layer away from half filling.

4. *Deuteration of the cation.* Each BEDT-TTF molecule contains eight hydrogen atoms, cf. Fig. 6. κ-(BEDT-TTF)$_2$Cu[N(CN)$_2$]Br is extremely close to Mott transition and crystals containing the fully deuterated molecule are antiferromagnetic insulators (Taniguchi et al., 2003). Crystals of partially deuterated BEDT-TTF molecules, which can be made uniformly deuterated throughout the entire crystal, sit at different positions spanning the first order Mott transition (Taniguchi et al., 2003) and the macroscopic coexistence of the metallic and insulating phases can be seen in these crystals (Sasaki et al., 2005). No detailed explanation of how this deuteration effect operates has been presented to date. Presumably, deuteration weakens the hydrogen bonding interaction between the cation and anions because of the different quantum zero point motion (cf. (Hayashi et al., 2006)).

Although the Mott transition in organics is commonly called 'bandwidth controlled' we stress that really the important quantity is the ratio U/W, and as U is significantly renormalised by interdimer (as well as intramolecular and intradimer) processes. It has been suggested that both hydrostatic and chemical pressure may also result in variations in U (Nakamura et al., 2009; Scriven and Powell, 2009b). Further, the ratio t'/t also has an important impact on wether the ground state is metallic or insulating (Powell and McKenzie, 2007).

1. Critical exponents of the Mott transition

Much attention has focused on the Mott transition from the antiferromagnetic state to a correlated metal and superconductor. Indeed, the phase diagram of this transition in κ-(BEDT-TTF)$_2$Cu[N(CN)$_2$]Cl has been mapped out in considerable detail (Faltermeier et al., 2007; Kagawa et al., 2005, 2009; Limelette, Wzietek, Florens, Georges, Costi, Pasquier, Jérome, Mézière, and Batail, 2003; Powell and McKenzie, 2006).

Theoretical arguments predict that the Mott transition belongs to the Ising universality class (Castellani et al., 1979; Kotliar et al., 2000). These can be understood on the basis of an analogy between the Mott transition and the lattice gas (Castellani et al., 1979). Here one views the metallic phase as a liquid of doubly occupied and vacant sites [corresponding to (BEDT-TTF)$_2^0$ and (BEDT-TTF)$_2^{2+}$] moving on a background of singly occupied [(BEDT-TTF)$_2^+$] sites. The Mott insulating phase is then simply the gaseous phase of this model. Indeed, a formal basis for this analogy can be given within the dynamical mean-field approximation (Kotliar et al., 2000). In this theory the Mott critical point is described by a scalar (Ising) order parameter, which couples to the singular part of the double occupancy. Experimental support for this theory have come from measurements of the critical exponents associated with the metal-insulator transition in (V$_{0.989}$Cr$_{0.011}$)$_2$O$_3$ that suggest that this transition belongs to the 3D Ising universality class (Limelette, Georges, Jérome, Wzietek, Metcalf and Honig, 2003).

It was therefore surprising when a novel set of critical exponents ($\beta \approx 1$, $\gamma \approx 1$, $\delta \approx 2$) were reported for the metal-insulator transition in κ-(BEDT-TTF)$_2$Cu[N-(CN)$_2$]Cl (Kagawa et al., 2005, 2009). Indeed, the critical exponents found by Kagawa *et al.* from measurements of the conductivity (Kagawa et al., 2005) are far from those of the Ising model in either two- or three-dimensions. Nevertheless, the Widom scaling relation, $\gamma = \beta(\delta - 1)$, is obeyed and, when appropriately scaled, the data collapses onto two curves (one for data above the critical temperature, the other for data below the critical temperature). Kagawa *et al.* (Kagawa et al., 2009) have also reported the same order parameter exponent, β, from NMR measurements. This is interesting as NMR probes the magnetic degrees of freedom, whereas the conductivity probes the charge degrees of freedom.

A number of theories have been proposed to try and explain these results. Imada *et al.* (Imada, 2005a,b; Misawa et al., 2006) predicted exponents close to those observed by Kagawa *et al.* in a theory based on the proximity of the first order Mott transiton to a quantum critical point as the critical end point is moved to $T = 0$. Alternatively, Papanikolaou *et al.* (Papanikolaou et al., 2008) have argued that the experiments are indicative of an Ising universality class. Papanikolaou *et al.* showed that the conductivity is not only sensative to the order parameter, but can also depend on other singular variables, particularly the energy density. In the regime where the

energy density dominates they found that $\beta = 1$, $\gamma = 7/8$ and $\delta = 15/8$, consistent with the Widom scaling relation and in reasonable agrement with the experimental results. However, this theory does not explain finding that $\beta = 1$ from an NMR experiment (Kagawa et al., 2009).

Bartosch et al. have recently shown that a scaling theory based on the Ising universality class can describe the observed temperature dependence of the thermal expansion near the critical point for the fully deuterated κ-(BEDT-TTF)$_2$Cu[N(CN)$_2$]Br material (Bartosch et al., 2010). It would therefore be interesting to know what Imada et al.'s theory predicts for these experiments.

2. Optical conductivity

Faltermeier et al. (Faltermeier et al., 2007) have studied the evolution of the reflectivity and optical conductivity spectra as κ-(BEDT-TTF)$_2$Cu[N(CN)$_2$]Cl$_{1-x}$Br$_x$ as it is driven through the metal-insulator transition by increasing the Br density, x. At low temperatures, three important features can be identified in these spectra: a Drude peak and two broad peaks that are fit well by Lorentzians at around 2200 cm^{-1} and 3200 cm^{-1}.

The Drude peak is absent in the pure Cl and low Br density compounds: as expected for the Drude peak arises from Fermi liquid quasiparticle excitations, which are absent in the Mott insulating phase (Kotliar and Vollhardt, 2004). As the Br density is increased the system is driven metallic by chemical pressure and the Drude peak appears - it can be seen rather weakly for $x = 0.73$. Increasing x further increases the width of and the spectral weight under the Drude peak.

The optical spectrum of the Hubbard model at half filling and near the Mott transition is only expected to show two main features: the Drude peak in the metallic phase and a single broad peak centred on $\sim U$ and of width $\sim W$ (Kotliar and Vollhardt, 2004; Merino and McKenzie, 2000a). This broad peak corresponds to excitations that change the number of doubly occupied sites (and therefore change the number of vacant sites so as to ensure charge conservation). Therefore, Faltermeier et al.'s observation of two broad Lorentzians requires explanation.

Faltermeier et al. (Faltermeier et al., 2007) argued that the lower frequency Lorentzian is the peak predicted by the dimer Hubbard model of κ-(BEDT-TTF)$_2$-Cu[N(CN)$_2$]Cl$_{1-x}$Br$_x$. If correct, this assignment would yield a estimate of $U = 0.27$ eV, which is significantly smaller than that found from downfolding DFT calculations (Nakamura et al., 2009) (cf. section III.A). Further, Faltermeier et al. argued that the higher frequency feature is due to intra-dimer transitions.

However, Werner and Millis (Werner and Millis, 2010) have recently made significant advances in dealing with dynamical screening near the Mott transition via DMFT. Their calculations of the spectral function differ signif-
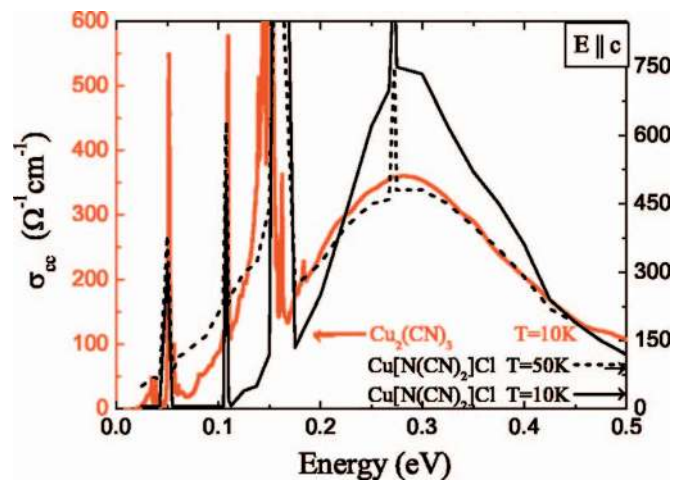
FIG. 15 Comparison of the frequency dependent conductivity in two Mott insulators, κ-(BEDT-TTF)$_2$Cu[N(CN)$_2$]Cl and κ-(BEDT-TTF)$_2$Cu$_2$(CN)$_3$ (Kézsmárki et al., 2006). The former has a ground state with Neel antiferromagnetic order and clearly has an energy gap of about 0.1 eV. In contrast, the latter compound may have a spin liquid ground state and has a much smaller energy gap. The sharp peaks are due to intramolecular vibrational modes and not the electronic degrees of freedom. [Copyright (2006) by the American Physical Society].

icantly from those with only a static U. For simple models of the frequency dependence of the effective on-site Coulomb repulsion they find two broad peaks in the spectral function at finite frequencies for a broad range of parameters. At high screening frequencies these two peaks appear to correspond to a screened-U band and a bare-U band. However, it is important to stress that Werner and Millis conclude that "peak positions in the spectral functions do not provide quantitative estimates of either the screened or unscreened U values." This may explain why Faltermeier et al.'s U value is significantly smaller than theoretical estimates. While Werner and Millis did not carry out explicit calculations of the optical conductivity, one can anticipate that dynamical screening will change the optical conductivity significantly from what is expected for a static U. Indeed, on the basis of Werner and Millis's calculations one would expect to find an additional broad peak at finite frequency in the optical conductivity, precisely as is seen experimentally. This suggests a possible reinterpretation of Faltermeier et al.'s data. An interesting question is whether this theory is capable of accounting for the observed changes in vibrational frequencies that are naturally explained by Faltermeier et al.'s theory.

The frequency dependence of the conductivity, shown in Figure 15, suggests that the charge gap in κ-(BEDT-TTF)$_2$Cu$_2$(CN)$_3$ is smaller than κ-(BEDT-TTF)$_2$Cu[N-(CN)$_2$]Cl (Kézsmárki et al., 2006). Indeed, it has been suggested that in the former compound there is a charge

gap, but that the optical conductivity has a power law dependence at low frequencies (Ng and Lee, 2007). Note, that the charge gap (the energy cost of adding an electron or hole; a signature of a Mott insulator) is a different physical quantity from the optical gap (the energy required to produce a charge neutral, spin singlet excitation, with a non-zero transition dipole moment) and so it is possible, at least in principle, that the former is non-zero and the latter is zero. However, the relative size of the energy gaps also presents a puzzle because one can also argue that κ-(BEDT-TTF)$_2$Cu[N(CN)$_2$]Cl is closer to the metallic phase than the other compound. Since κ-(BEDT-TTF)$_2$Cu[N(CN)$_2$]Cl requires a smaller pressure to destroy the Mott insulating phase (300 bar versus 4 kbar).

Motivated by these experimental results, Ng and Lee calculated the frequency dependence of the optical conductivity in a Mott insulating state which is a spin liquid with a spinon Fermi surface and coupled to a fluctuating U(1) gauge theory (Ng and Lee, 2007). (This theory is discussed further in Section VII.) They find that there is a power-law frequency dependence at low frequencies due to the conductivity of the spinons. The spinons are charge neutral and so do not couple directly to an electromagnetic field. However, they couple indirectly because the external field induces an internal gauge field in order to maintain the constraints associated with the slave-rotor representation of the electrons.

Deducing whether the experimental data shown in Figure 15 does imply zero optical gap for κ-(BEDT-TTF)$_2$-Cu$_2$(CN)$_3$ could be made more rigorous by subtracting the vibrational contributions. A robust procedure now exists for this and has been applied in the analysis of the optical conductivity of alloys of κ-(BEDT-TTF)$_2$Cu-[N(CN)$_2$]Cl and κ-(BEDT-TTF)$_2$Cu[N(CN)$_2$]Br (Dumm et al., 2009; Faltermeier et al., 2007; Merino et al., 2008).

3. The spin liquid to metal transition

κ-(BEDT-TTF)$_2$Cu$_2$(CN)$_3$ also undergoes a Mott transition under hydrostatic pressures $\sim$ 0.35 GPa (Kurosaki et al., 2005). What little is known experimentally about how the spin liquid insulator to metal transition differs from the antiferromagnetic-insulator–metal transition comes mainly from the pioneering work of Kurosaki *et al.* (Kurosaki et al., 2005). They reported measurements of the resistivity and NMR, but did not examine the critical end-point closely. Kurosaki *et al.* observed two NMR spin-lattice relaxation rates, $1/T_1$ at 0.35 GPa, i.e., close to the of metal-insulator transition. This suggests that the metal-insulator transition in κ-(BEDT-TTF)$_2$Cu$_2$(CN)$_3$ is first order and that the two rates are caused by the coexistence of the insulating and metallic phase. Note that the metal-insulator transitions in κ-(BEDT-TTF)$_2$Cu[N(CN)$_2$]Cl and (as a function of deuteration in) κ-(BEDT-TTF)$_2$Cu[N(CN)$_2$]Br are also first order. Kurosaki *et al.* also found that pressure (up

to 0.8 GPa) does not induce any significant changes in the ^{1}H NMR spectrum at 1.4 K. This shows that, at least at this temperature, pressure does not induce long range magnetic ordering and hence, one presumes, the spin liquid state remains right up until the first order Mott transition.

4. Reentrance of the Mott transition - explanation from undergraduate thermodynamics

One interesting difference between the Mott transitions in κ-(BEDT-TTF)$_2$Cu[N(CN)$_2$]Cl and κ-(BEDT-TTF)$_2$Cu$_2$(CN)$_3$ is the shape of the first order line in the (P-T) phase diagram (Kagawa et al., 2004; Kurosaki et al., 2005). For the pressure driven metal-insulator transition the Clausius-Clapeyron relation is

$$\frac{dT}{dP} = \frac{\Delta V}{\Delta S}, \tag{14}$$

where $\Delta V = V_{\text{ins}} - V_{\text{met}}$ and $\Delta S = S_{\text{ins}} - S_{\text{met}}$. As the metal is the high pressure phase one presumes[8] that $\Delta V > 0$. Therefore, the sign of dT/dP is determined by the sign of ΔS. In κ-(BEDT-TTF)$_2$Cu$_2$(CN)$_3$ $dT/dP > 0$ along the entire phase transition, cf. Fig. 8, (Kurosaki et al., 2005). In contrast, the phase transition in κ-(BEDT-TTF)$_2$Cu[N(CN)$_2$]Cl is reentrant, cf. Fig. 7, (Kagawa et al., 2004), i.e., dT/dP changes sign along the phase boundary. Therefore, at certain pressures ($\sim$ 25 MPa) isobaric cooling results in first a insulator-to-metal transition (at $T \sim 35$ K) followed by a metal-to-insulator transition (at $T \sim 20$ K). The change in sign of dT/dP occurs in the region of the phase diagram where antiferromagnetism is observed.

Fermi statistics imply that the entropy of the electrons in a metal varies linearly with temperature.[9] In the antiferromagnetic Mott insulator phase the entropy is dominated by the spin degrees of freedom. One expects the entropy to be carried by spin waves in the magnetically ordered phase, thus $S(T) \sim T^\alpha$. For a quasi-two dimensional material, such as κ-(BEDT-TTF)$_2$Cu[N(CN)$_2$]Cl, one expects that $\alpha > 1$.[10] Therefore, at low temperatures the entropy of the antiferromagnetically ordered state is proportional to T^α. At low enough temperatures this will always be less than the entropy of a Fermi liquid, which is proportional to temperature.

In a paramagnetic insulator, the entropy becomes in-

———

[8] However, some care should be exercised with this assumption. For example, famously for the ice-water transition $\Delta V < 0$.

[9] As $S(T) = \int_0^T \frac{C_v}{T} dT$ and $C_v = \gamma T$ for a gas of fermions.

[10] In the antiferromagnetically order states one finds $\alpha = 2$ in two dimensions, e.g., on the square lattice antiferromagnet, and $\alpha = 3$ in three dimensions. As κ-(BEDT-TTF)$_2$Cu[N(CN)$_2$]Cl is quasi-two dimensional an intermediate behaviour may also be possible.

dependent of temperature at high temperatures.[11] The phase diagrams of κ-(BEDT-TTF)$_2$Cu$_2$(CN)$_3$ (Kurosaki et al., 2005), κ-(BEDT-TTF)$_2$Cu[N(CN)$_2$]Cl (Kagawa et al., 2004; Lefebvre et al., 2000) and V$_2$O$_3$ (Limelette, Georges, Jérome, Wzietek, Metcalf and Honig, 2003; McWhan et al., 1973) demonstrate that $\Delta S > 0$ for the paramagnetic insulator-phase transition in all three of these materials. In principle, this argument could be quantitatively tested from measurements of the heat capacity; however, performing such measurements under pressure is extremely challenging.

For the triangular lattice Heisenberg model the entropy is much larger than that of the square lattice model (Bernu and Misguich, 2001; Elstner et al., 1994). For example, a value of $0.2R$ is obtained at temperatures of $0.5J$ and $0.15J$ respectively. For both models the entropy (and specific heat) are quadratic in temperature at low temperatures. However, the coefficient of proportionality is twenty times larger for the triangular lattice than the square lattice (Bernu and Misguich, 2001).

It is interesting to compare the experimental phase diagrams of κ-(BEDT-TTF)$_2$Cu$_2$(CN)$_3$ and κ-(BEDT-TTF)$_2$Cu[N(CN)$_2$]Cl with the cluster dynamical mean field theory (CDMFT) calculations of Liebsch et al. (Liebsch et al., 2009) for the phase diagram of the Hubbard model on an (an)isotropic triangular lattice, Fig. 16. Similar results were obtained independently for $t' = 0.8t$ by different group et al. (Ohashi et al., 2008). They find a first order Mott transition as U/W is decreased. However, they found interesting differences in the phase diagrams as the frustration, t'/t, is varied. For the isotropic triangular lattice ($t' = t$) the line of first order transitions always has a positive slope. It follows from the Clausius-Clapeyron equation (14) that the insulating state has a larger entropy than the metallic state, even at low temperatures. For $t' = 0.8t$ the slope of the phase boundary becomes negative at low temperatures, indicating that the metallic state has greater entropy at low temperatures. This is in semi-quantitative agreement with the observed temperature-pressure phase diagram of a range of organic charge transfer salts if we associate κ-(BEDT-TTF)$_2$Cu$_2$(CN)$_3$ with $t' = t$ and κ-(BEDT-TTF)$_2$Cu[N(CN)$_2$]Cl with $t' = 0.8t$. However, the parameterisation of the tight-binding model from DFT (cf. section III.A) suggest that t'/t is actually rather smaller for both materials (cf. Table I).

It is interesting to note that Liebsch et al. did not allow for long range antiferromagnetic order in their calculations. Thus, short-range magnetic fluctuations must be sufficient to account for decreased entropy in the insulating state. The parameterisations of the tight binding model for κ-(BEDT-TTF)$_2$Cu$_2$(CN)$_3$ (see section III.A.1) would put this material in the regime where

Liebsch find a reentrant phase transition. However, even more sophisticated calculations, going beyond the three site cluster Liebsch et al. studied, may result in a shift in the parameter regime in which reentrance is observed. Therefore, the lack of reentrance in the in the phase diagram of κ-(BEDT-TTF)$_2$Cu$_2$(CN)$_3$ is consistent with a spin liquid ground state.

D. Magnetic frustration in the normal state

A striking feature of the normal state is that the resistivity (Analytis et al., 2006; Kurosaki et al., 2005; Limelette, Wzietek, Florens, Georges, Costi, Pasquier, Jérome, Mézière, and Batail, 2003) Hall coefficient (Murata et al., 1990; Sushko et al., 1997; Tanatar et al., 1997) and thermopower (Buravov et al., 1992; Demishev et al., 1998; Yu et al., 1991) all vary non-monotonically with temperature (Merino and McKenzie, 2000a). This is in marked contrast to what is found in weakly correlated metals (Ashcroft and Mermin, 1976), where these quantities have a monotonic temperature dependence.

Further, at high temperatures the conductivity is less than the Mott-Ioffe-Regal limit (Analytis et al., 2006; Kurosaki et al., 2005; Limelette, Wzietek, Florens, Georges, Costi, Pasquier, Jérome, Mézière, and Batail, 2003), which would mean that, in a Drude picture, electrons are scattering more frequently than they hop from site to site (Gunnarsson et al., 2003; Merino and McKenzie, 2000a). In weakly correlated metals this only found as one approaches the Anderson transition in extremely disordered systems (Phillips, 2003). Whereas, the organics are remarkably clean systems (Analytis et al., 2006; Kartsovnik, 2004; Singleton, 2000).

A third difference between κ-(BEDT-TTF)$_2$X and weakly correlated metals is that no Drude peak is observed in the optical conductivity above a relatively low temperature ($T \gtrsim 40$ K) (Dressel et al., 1994; Eldridge et al., 1991; Faltermeier et al., 2007; Kornelsen et al., 1989; Merino et al., 2008; Tamura et al., 1991).

However, at low temperatures the mean free path returns below the Mott-Ioffe-Regal limit (Analytis et al., 2006; Kurosaki et al., 2005; Limelette, Wzietek, Florens, Georges, Costi, Pasquier, Jérome, Mézière, and Batail, 2003) and a Drude peak is seen in the optical conductivity (Dressel et al., 1994; Eldridge et al., 1991; Faltermeier et al., 2007; Kornelsen et al., 1989; Merino et al., 2008; Tamura et al., 1991). This phenomenology is observed for both κ-(BEDT-TTF)$_2$Cu$_2$(CN)$_3$ (Kurosaki et al., 2005) and its more weakly frustrated brethren.

1. Dynamical mean-field theory (DMFT)

DMFT (Georges et al., 1996; Kotliar and Vollhardt, 2004) provides both a fundamental explanation (Merino and McKenzie, 2000a) and an accurate description (Limelette, Wzietek, Florens, Georges, Costi, Pasquier,

---

[11] For a paramagnetic insulator with $T \gg J$ the entropy per spin is $S/N = k_B \ln 2$.
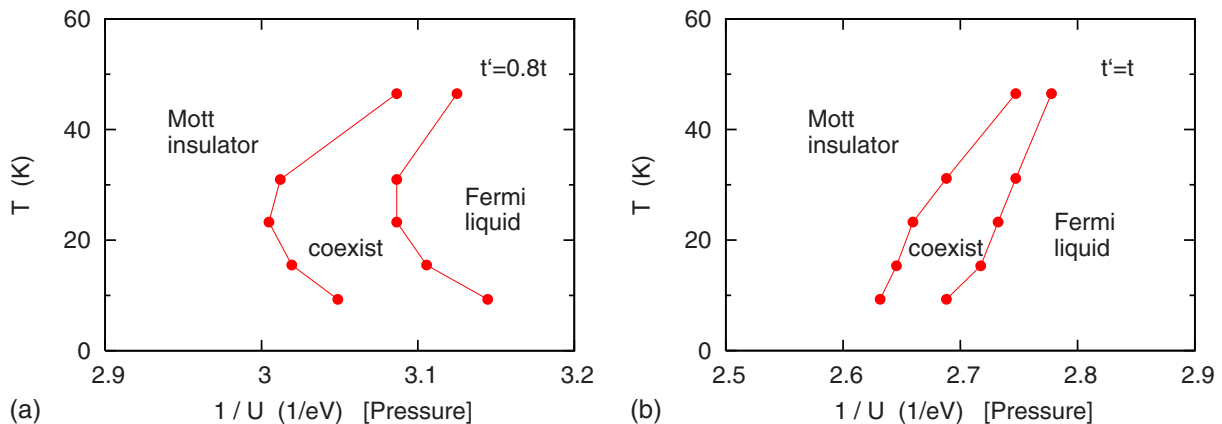
FIG. 16 Phase diagram at finite temperature from cluster dynamical mean-field theory (CDMFT) of the Hubbard model on the anisotropic triangular lattice at half filling (Liebsch et al., 2009). As U/t increases there is a first order phase transition from a metallic to a Mott insulating phase. This first order line ends at a critical point. (a) and (b) are for $t'/t = 0.8$ and 1, respectively. For $t' = 0.8t$ a reentrant Mott transition is found. This can be understood from the Clausius-Clapeyron equation (14) as showing that, at low temperatures, the insulating phase has lower entropy than the metallic phase. This would be expected if the insulating phase were magnetically ordered (see text) and can even be caused by the short range antiferromagnetic correlations associated in incipient magnetic ordering, as is the case here. At high temperatures the reverse is true, consistent with a simple paramagnetic metal. For $t' = t$ the insulating phase has higher entropy at all temperatures, consistent with a spin liquid ground state. The phase diagrams shown in panels (a) and (b) are consistent with those of κ-(BEDT-TTF)$_2$Cu[N(CN)$_2$]Cl (Fig. 7) and κ-(BEDT-TTF)$_2$Cu$_2$(CN)$_3$ (Fig. 8) respectively. [From (Liebsch et al., 2009).] [Copyright (2009) by the American Physical Society].

Jérome, Mézière, and Batail, 2003; Merino et al., 2008) of these phenomena. Merino and McKenzie (Merino and McKenzie, 2000a) found that, even without taking account of the details of the band structure, the basic features of the κ phase organics, described above, are captured by DMFT. Furthermore, these features are seen in a broad range of other strongly correlated electron materials such as transition metal oxides. In particular, DMFT predicts an incoherent or 'bad' metal at high temperatures. In this regime there are no quasiparticles (and hence no Drude peak). Incoherence implies that momentum is not a good quantum number, i.e., that electrons frequently scatter off one another, and gives rise a mean free path less than a lattice constant (Gunnarsson et al., 2003; Merino and McKenzie, 2000a).

Below a characteristic temperature, T_{coh}, DMFT predicts a Fermi liquid. Hence, the resistivity drops below the Mott-Ioffe-Regal limit and the Drude peak returns. However, the Fermi liquid is strongly correlated and the effective mass is almost an order of magnitude larger than the band mass. The change from the bad metal to the Fermi liquid is a crossover rather than a phase transition. In DMFT it is this crossover that is largely responsible for the nonmonotonicity of many response functions, including the resistivity, the thermopower and the Hall coefficient.

The success of DMFT in describing this broad range of experiments is, initially, rather puzzling. DMFT is exact in infinite dimensions or for an infinite co-ordination number. Hence, one expects DMFT to be a good approximation in the limit of large dimensions, but the κ-phase organics are quasi-two-dimensional. However,

it has recently been argued (Merino et al., 2006) that DMFT is a much better approximation for frustrated systems than unfrustrated systems as frustration suppresses long range correlations. The applicability of DMFT to low-dimensional systems with large frustration is consistent with the fact that a Curie-Weiss law holds down to a much lower temperature for frustrated magnetic models than for unfrustrated models (Ramirez, 1994; Schiffer and Daruka, 1997; Zheng, Singh, McKenzie and Coldea, 2005). Deviations from Curie-Weiss behavior result from spatially dependent correlations. Hence, the DMFT treatment of the Hubbard model on frustrated lattices is expected to be a good approximation down to much lower temperatures than it is for unfrustrated models.

Furthermore, in the "bad metal" region magnetic properties such as the uniform susceptibility and spin relaxation rate, can be described by the Heisenberg model because the electrons are essentially localized due to the proximity to the Mott insulating phase. This means that the susceptibility follows a Curie-Weiss form down to temperatures much less than the exchange energy J. The spin correlation length of the antiferromagnetic Heisenberg model increases with temperature much more slowly for the triangular lattice than the square lattice (Elstner et al., 1993, 1994). Specifically, at $T = 0.3J$ the spin correlation length is only one lattice constant for the triangular lattice. In contrast, for the square lattice the correlation length is about 50 lattice constants, at $T = 0.3J$ (Elstner et al., 1993, 1994).

Dynamical cluster approximation (DCA) calculations provide a means to systematically go beyond DMFT.

They show that for the isotropic triangular lattice the solution is remarkably similar to that found from single site DMFT. In particular, a quasiparticle peak appears at the Fermi energy. However, if the frustration is released a pseudogap opens in the one-electron spectra as a result of short range antiferromagnetic correlations (Imai and Kawakami, 2002). We will delay more detailed discussion of these results until section III.D.4.

A further hint that DMFT is a better approximation on the triangular lattice than it is on the square lattice comes from the fact that one finds that, at half filling, the Mott transition occurs at $U_c \approx 15|t|$ (Merino et al., 2006). This can be compared with more sophisticated numerical treatments which find that the Mott transition takes place at $U \approx 6 - 8|t|$ (see Section VI.A). On the square lattice it is known that perfect nesting of the Fermi surface means that the ground state is insulating for any finite U. However, DMFT predicts (Georges et al., 1996) that $U_c \gg |t|$ unless antiferromagnetism is included. Thus (without including antiferromagnetism) DMFT gives a qualitatively incorrect result for the (unfrustrated) square lattice, but a qualitatively correct result for the (frustrated) triangular lattice.

Hence, it appears that frustration plays an important role even in the normal state of the organic charge transfer salts. Counterintuitively, by suppressing long range spin correlations, frustration makes the normal state of the κ-phase organics easier to understand than would be the case without significant frustration. This may be taken as a major blessing if one compares the comparative simplicity of the normal state of the organics to the complexities of the 'normal' state of the cuprates (Lee et al., 2006). Thence, an important question is: are the differences between the normal states of the organics and the cuprates intrinsic differences between the band-width controlled Mott transition and the band-filling controlled Mott transition, or are extrinsic effects responsible for the non-Fermi liquid effects observed in the cuprates?

2. Fermi liquid regime

At low temperatures ($T < T_{coh}$) DMFT reduces to a local Fermi liquid theory and hence predicts that the temperature dependence of the resistivity is given by $\rho(T) = \rho_0 + AT^2$, where ρ_0 results from impurity scattering and the quadratic term results from electron-electron scattering. This temperature dependence is indeed seen experimentally in a range of organic charge transfer salts (Kurosaki et al., 2005; Limelette, Wzietek, Florens, Georges, Costi, Pasquier, Jérome, Mézière, and Batail, 2003; Strack et al., 2005). DMFT also predicts an enhancement of the effective mass over the band mass predicted by electronic structure calculations. This enhanced mass can be observed experimentally via the linear terms in the heat capacity, $C_v = \gamma T$. These two facts are not unrelated.

The Kadowaki-Woods ratio is defined as A/γ^2. This ratio is found to take the same value in a range of transition metals (Rice, 1968). Twenty years later it was found empirically that in a range of heavy fermions the Kadowaki-Woods ratio takes the same value (Kadowaki and Woods, 1986), albeit with several well known outliers. However, the ratio in the heavy fermions was found to be an order of magnitude larger than that in the transition metals. It was pointed out some time ago that the Kadowaki-Woods ratio is even larger in the organics (Dressel et al., 1997; Strack et al., 2005).

This large Kadowaki-Woods ratio has recently been shown to be the consequence of the details of the band structure of the organics (Jacko et al., 2009). Indeed, Jacko *et al.* found that, quite generally, the Kadowaki-Woods ratio depends on the band structure of the material in question. Jacko *et al.* proposed a new ratio, closely related to the Kadowaki-Woods ratio, that takes these band structure effects into account. They found that this ratio takes the same, predicted, value in a wide range of transition metal, heavy fermion materials, transition metal oxides and organic charge transfer salts. This new understanding of the Kadowaki-Woods ratio shows that the mass enhancement measured by the specific heat and the quadratic term in the resistivity share the same physical origin. This strongly suggests that electron-electron scattering are responsible for both effects, which had been questioned in the organics (Strack et al., 2005). As this suggests that electron-electron interactions are the strongest forces immediately above T_c, it may also imply that these same interactions are implicated in the mechanism of superconductivity in these materials.

3. NMR and the pseudogap

Beyond the arguments above that frustration enhances localisation and thus emphasises the Mott physics captured by DMFT, the properties discussed above do not depend crucially on the frustration at play in organic charge transfer salts. Therefore, to better understand the role of frustration, it is desirable to experimentally probe the spin correlations in the metallic state. The most direct method would be inelastic neutron scattering. However, this requires large single crystals, which have never been grown for organic charge transfer salts (Pintschovius et al., 1997; Taniguchi et al., 2006; Toyota et al., 1997). Therefore, the best remaining probe in nuclear magnetic resonance (NMR) spectroscopy.

Two key properties measured in an NMR experiment are the Knight shift, K_s, which is the shift in the resonance frequency due the screening of the applied magnetic field by the conduction electrons in a metal, and the spin-lattice relaxation rate, $1/T_1$, which is the characteristic time taken for spins flipped by a magnet field to return to their equilibrium distribution. In a metal, both of these quantities are related to the dynamic spin susceptibility, $\chi(\mathbf{q}, \omega) = \chi'(\mathbf{q}, \omega) + i\chi''(\mathbf{q}, \omega)$, of the elec-

trons. It may be surprising that the nuclear relaxation rate is a probe of electrons. However, this is because the total system (nuclei and their environment) must conserve energy and spin. Therefore, the nuclei can only relax by interacting with their environment. In a metal the low energy relaxation pathways are dominated by exchanging spin with the conduction electrons. Thus, one finds that (Moriya, 1963)

$$\frac{1}{T_1} = \lim_{\omega \to 0} \frac{2k_B T}{\gamma_e^2 \hbar^4} \sum_{\mathbf{q}} |A(\mathbf{q})|^2 \frac{\chi''(\mathbf{q}, \omega)}{\omega}, \qquad (15)$$

and

$$K_s = \frac{|A(\mathbf{0})|\chi'(\mathbf{0}, 0)}{\gamma_e \gamma_N \hbar^2}, \qquad (16)$$

where $A(\mathbf{q})$ is the hyperfine coupling between the nuclear and electron spins, and γ_N (γ_e) is the nuclear (electronic) gyromagnetic ratio. Note that, because of the factor T in the expression (15), $1/T_1 T$ often gives more direct access the temperature dependence of the spin fluctuations than T_1 itself.

For non-interacting electrons one finds that

$$K_s \propto N(\epsilon_F) \qquad (17)$$

and

$$\frac{1}{T_1 T} \propto N(\epsilon_F)^2, \qquad (18)$$

where $N(\epsilon_F)$ is the density of states at the Fermi level, if the hyperfine coupling is constant in reciprocal space, which is strictly true if there is only one atom per unit cell, and is an approximation otherwise. Note that both K_s and $1/T_1 T$ are independent of temperature in this approximation. Further, taking the ratio $1/T_1 T K_s^2$ removes the dependence on $N(\epsilon_F)$, which is generally not known *a priori* (Korringa, 1950). One finds that, for non-interacting electrons, the dimensionless ratio

$$\mathcal{K} \equiv \frac{\hbar}{4\pi k_B} \left(\frac{\gamma_e}{\gamma_N} \right)^2 \frac{1}{T_1 T K_s^2} = 1. \qquad (19)$$

$\mathcal{K}$ is known as the Korringa ratio. These three results: that $1/T_1 T$ and K_s are independent of T and that $\mathcal{K} = 1$ are collectively known as Korringa behaviour. Indeed, one can show (Yusuf et al., 2009) that these results hold for interacting systems provided vertex corrections to the dynamic spin susceptibility are negligible. This holds regardless of the form of the self energy, so long as it is consistent with Ward identities. However, magnetic fluctuations lead to vertex corrections to $\chi(\mathbf{q}, \omega)$ (Doniach and Sondheimer, 1998; Yusuf et al., 2009). Therefore systems with strong magnetic fluctuations do not display Korringa behaviour. In particular, $\mathcal{K} < 1$ in systems with ferromagnetic fluctuations and $\mathcal{K} > 1$ in systems with antiferromagnetic fluctuations (Doniach, 1968).
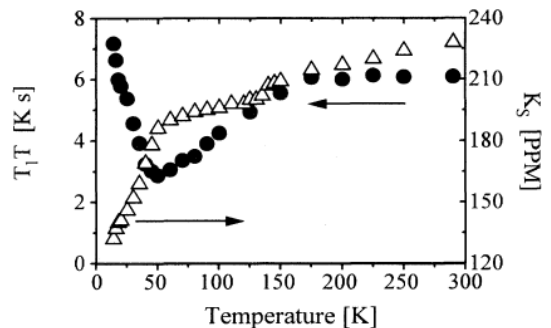

FIG. 17 NMR spectroscopy shows that there are strong spin fluctuations in κ-(BEDT-TTF)$_2$Cu[N(CN)$_2$]Br and other organic charge transfer salts. $1/T_1 T$ shows a maximum at ~ 50 K. This temperature corresponds with the temperature, T_{coh}, at which the crossover from the Fermi liquid to the bad metal is observed in the DC resistivity and the optical conductivity. Indeed this correspondence between the maximum in $1/T_1 T$ and T_{coh} is found in a wide range of BEDT-TTF salts (Powell et al., 2009). The data above 50 K is well described (Yusuf et al., 2007) by a phenomenological spin fluctuation theory (Millis et al., 1990a; Moriya and Ueda, 2000). Below 50 K there is a sudden drop in both $1/T_1 T$ and the Knight shift K_s, suggesting the a pseudogap opens (Powell et al., 2009). [Modified from (de Soto et al., 1995).] [Copyright (1995) by the American Physical Society].

There have been numerous studies of NMR in metallic organic charge transfer salts (for a review see (Miyagawa et al., 2004)). We begin by discussing investigations of the more weakly frustrated materials such as κ-(BEDT-TTF)$_2$Cu[N(CN)$_2$]Br, κ-(BEDT-TTF)$_2$Cu[N(CN)$_2$]Cl and κ-(BEDT-TTF)$_2$Cu(NCS)$_2$ (de Soto et al., 1995; Itaya et al., 2009; Kawamoto et al., 1995a,b; Mayaffre et al., 1994). These materials all show clear non-Korringa behaviours, cf. Fig. 17. As the temperature is lowered from room temperature, both $1/T_1 T$ and K_s rise to a maximum at a temperature we will denote as T_{NMR}. Below T_{NMR} both $1/T_1 T$ and K_s decrease; both drop more rapidly below the superconducting critical temperature, T_c. For weakly frustrated compounds $T_{NMR} \simeq T_{coh}$ (Itaya et al., 2009; Powell et al., 2009), the coherence temperature marking the crossover from a Fermi liquid to a bad metal, for a range of anions and pressures to within experimental error. Measurements of the Korringa ratio (de Soto et al., 1995; Itaya et al., 2009; Kawamoto et al., 1995b) find that $\mathcal{K} \gg 1$ indicating that there are strong antiferromagnetic fluctuations.

For $T > T_{NMR}$ the experimental data is naturally explained (Powell et al., 2009; Yusuf et al., 2007) by Moriya's self-consistent renormalised theory (Moriya and Ueda, 2000) in the phenomenological form used by Millis, Monien and Pines in the context of the cuprates (Millis et al., 1990a). In this model there are two contributions to the dynamic susceptibility, one arising from long wavelength background from Fermi liquid like excitations and a second contribution from spin fluctuations that is strongly peaked at some wavevector $\mathbf{Q}$ associated with

the nascent magnetic order. In the limit of strong magnetic fluctuations this model predicts that (Powell et al., 2009)

$$\frac{T_1 T}{(T_1 T)_{NMR}} = \frac{T_{NMR}}{T_{NMR} + T_x}\left(\frac{T}{T_{NMR}}\right) + \frac{T_x}{T_{NMR} + T_x} \quad (20)$$

where $(T_1 T)_{NMR}$ is the value of $T_1 T$ at $T = T_{NMR}$ and T_x sets the scale for the temperature dependence of the spin correlation length. Plotting the experimental data as $T_1 T/(T_1 T)_{NMR}$ against T/T_{NMR} indeed yields the straight line predicted above for $T > T_{NMR}$ (Powell et al., 2009). A more detailed analysis (Yusuf et al., 2007) allows one to estimate the spin correlation length, $\xi(T)$. For example, $\xi(T_{NMR}) \simeq 3a$, where a is the lattice constant, in κ-(BEDT-TTF)$_2$Cu[N(CN)$_2$]Br. It has been shown (Ding and Makivic, 1990) that, on the square lattice, the antiferromagnetic Heisenberg model has a correlation length of order $\xi(T)/a \sim 1$ for $T = J$ and of order $\xi(T)/a \sim 30$ for $T = 0.3J$. On the other hand, for the antiferromagnetic Heisenberg model on the isotropic triangular lattice, the correlation length is only of order a lattice constant at $T = 0.3J$ (Elstner et al., 1993). Therefore a correlation length of $\sim 3a$ is consistent with the intermediate value of t'/t calculated for κ-(BEDT-TTF)$_2$-Cu[N(CN)$_2$]Br (cf. section III.A) placing this compound somewhere between the square and triangular lattices.

An important question is: what causes the reduction in $1/T_1 T$, K_s and $\mathcal{K}$ for $T < T_{NMR}$? Given its successes in describing many of the phenomena discussed in this section, one should first ask what DMFT predicts. It predicts a temperature dependence that can be fit to the form (20) for all temperatures. In the bad metal phase DMFT predicts that same behaviour as the spin fluctuation theory (Pruschke et al., 1995). Therefore, for $T > T_{NMR}$, DMFT agrees with experiment qualitatively - although we are not aware of a specific quantitative comparison. However, DMFT also predicts that $1/T_1$ increases monotonically with temperature and in the Fermi liquid regime it predicts a constant Knight shift and a constant $1/T_1 T$. None of these are seen experimentally. Therefore, although DMFT may provide an adequate description of the spin physics for $T > T_{NMR}$ some additional ingredient is required for $T < T_{NMR}$. As DMFT is a purely local (single site) theory this immediately suggests that some non-local correlations are important for understanding the spin correlations.

Two pictures have been proposed to try to explain the NMR below T_{NMR}: (i) the opening of a pseudogap (Mayaffre et al., 1994; Miyagawa et al., 2002; Powell et al., 2009; Yusuf et al., 2007) and (ii) a loss of spin correlations (de Soto et al., 1995; Itaya et al., 2009; Kawamoto et al., 1995b; Lefebvre et al., 2000).

In the pseudogap scenario one assumes that non-local interactions cause a loss of spectral weight at the Fermi energy. This would lead to the suppression of both $1/T_1 T$ and K_s, cf. Eqs. (17) and (18). In context of this hypothesis it is interesting to note that the fit of the data to Eq. 20 shows that $T_{NMR} \simeq T_x$, which suggests that the

spin correlations play an important role in determining T_{NMR}. The interpretation of this result in this picture is then that the growing spin correlations cause a pseudogap to open as the temperature is lowered.

If spin correlations were to decrease below T_{NMR} this would clearly cause a reduction in $1/T_1 T$. However, it is not clear that such a decay of spin correlations would also lead to a decrease in the Knight shift as K_s is a measure of the ferromagnetic ($\mathbf{q} = \mathbf{0}$) fluctuations, cf. Eq. 16. However, if a peak in the dynamic susceptibility at $\mathbf{q} \neq \mathbf{0}$ were sufficiently broad, antiferromagnetic spin correlations could contribute significantly to the Knight shift and lead to the observed behaviour. This picture also gives a natural explanation of why the Korringa ratio decreases below T_{NMR}: because $1/T_1 T$ is more sensitive to antiferromagnetic spin fluctuations than K_s.

4. There is no pseudogap in κ-(BEDT-TTF)$_2$Cu$_2$(CN)$_3$

In contrast to the weakly frustrated materials there is no evidence for a pseudogap in κ-(BEDT-TTF)$_2$Cu$_2$-(CN)$_3$ (Shimizu et al., 2010). In the metallic state Korringa-like behaviour is seen at low temperatures: both $1/T_1 T$ and K_s are constant.

This is consistent with the finding from DCA calculations (Imai and Kawakami, 2002) that find no pseudogap on the isotropic triangular lattice. Yet when the frustration is reduced a pseudogap caused by short range antiferromagnetic correlations is found. Imai *et al.* find a pseudogap for $t' \lesssim 0.6t$ from DCA calculations, using the non-crossing approximation (NCA) to solve the effective cluster problem. While one may have some concern over whether the accuracy of the NCA is sufficient for a quantitative comparison with experiment, this result seems to fit nicely with the experimental picture of no pseudogap in κ-(BEDT-TTF)$_2$Cu$_2$(CN)$_3$ and pseudogaps in κ-(BEDT-TTF)$_2$Cu[N(CN)$_2$]Cl, κ-(BEDT-TTF)$_2$Cu[N-(CN)$_2$]Br and κ-(BEDT-TTF)$_2$Cu(NCS)$_2$ if one uses the values of t'/t calculated from DFT (Table I).

5. Other evidence for a pseudogap in the weakly frustrated materials

Independent evidence for the suppression of density of states at the Fermi level can come from the temperature dependence of the of electronic specific heat (Timusk and Statt, 1999). This probes the density of excitations within $k_B T$ of the Fermi energy. Any gap will suppress the density of states near the Fermi surface which results in the depression of the specific heat coefficient γ. Kanoda (Kanoda, 2006) compared γ for several of the κ-(BEDT-TTF)$_2 X$ salts and found that in the region close to the Mott transition, γ is indeed reduced. One possible interpretation of this behaviour is a pseudogap which becomes bigger as one approaches the Mott transition. However, other interpretations are also possible, in

particular one needs to take care to account for the coexistence of metallic and insulating phases; this is expected as the Mott transition is first order in the organic charge transfer salts (Kagawa et al., 2005; Sasaki et al., 2005). The existence of a pseudogap has also been suggested in λ-(BEDT-TSF)$_2$GaCl$_4$ (Suzuki et al., 2006) from microwave conductivity measurements. The reduction of the real part of the conductivity σ_1 from the Drude conductivity σ_{dc} and the steep upturn in the imaginary part of the conductivity σ_2 have been interpreted in terms of preformed pairs leading to a pseudogap in this material.

Scanning tunnelling microscopy (STM) has given important insights into the pseudogap phase of the high temperature superconductors (Fischer et al., 2007). Therefore, it is natural to ask what can be seen via STM in the organics. This is complicated by the difficulty in obtaining high quality surfaces in the organics and these results should be treated with caution. However, Aria *et al.* (Arai et al., 2000) did find evidence that at pseudogap opens below $T \sim 45$ K in κ-(BEDT-TTF)$_2$Cu(NCS)$_2$. This temperature scale coincides with T_{NMR}. Further the pseudogap is about five times larger than the superconducting gap. This is consistent with the observation that the pseudogap gap opens at a temperature about five times larger than the superconducting critical temperature. Further, the superconducting gap appears 'on top' of the pseudogap. This 'two gap' picture is similar to what is observed in the cuprates (Boyer et al., 2007; Fischer et al., 2007).

Clearly more work is required, from both a theoretical and experimental perspective, to resolve this issue. The most obvious theoretical avenues are to study non local correlations in the κ-(BEDT-TTF)$_2X$ salts are the cluster extensions to DMFT such as CDMFT and the DCA. These include some off-site correlations, either in real (CDMFT) or reciprocal (DCA) space. However, there are significant technical challenges to overcome to accurately calculate the properties measured in NMR spectroscopies by these methods.

6. Tests of the pseudogap hypothesis

There are a number of key experiments needed to resolve whether or not a pseudogap is present in the paramagnetic metallic phase of κ-(BEDT-TTF)$_2X$. The pressure and magnetic field dependences of the nuclear spin relaxation rate and Knight shift would be valuable in determining the pseudogap phase boundary, estimating the order of magnitude of the pseudogap, and addressing the issue how the pseudogap is related to superconductivity. In the cuprates, there have been several investigations of the magnetic field dependence of the pseudogap seen in NMR experiments. For Bi$_2$Sr$_{1.6}$La$_{0.4}$CuO$_6$ the nuclear spin relaxation rate does not change with field up to 43 T (Zheng, Kuhns, Reyes, Liang and Lin, 2005). However, since the pseudogap temperature $T^* \sim 200$ K, one may require a larger field to reduce the pseudogap. Similar re-

sults were found in YBa$_2$Cu$_4$O$_8$ (Zheng, Kuhns, Reyes, Liang and Lin, 2005). However, in YBa$_2$Cu$_3$O$_{7-\delta}$ [see especially Fig. 6 of (Mitrović et al., 2002)] a field of order 10 T is enough to start to close the pseudogap. Mitrovic *et al.* (Mitrović et al., 2002) interpreted this observation in terms of the suppression of 'd-wave' superconducting fluctuations.

The interlayer magnetoresistance of the cuprates has been used as a probe of the pseudogap. (Kawakami et al., 2005; Krusin-Elbaum et al., 2004; Morozov et al., 2000; Shibauchi et al., 2001) Moreover, it has been argued that for the field perpendicular to the layers (which means that the Zeeman effect will dominate orbital magnetoresistance effects due to the Lorentz force) the pseudogap is closed at a field given by

$$H_{PG} \simeq \frac{k_B T^*}{\hbar \gamma_e}, \qquad (21)$$

where γ_e is the gyromagnetic ratio of the electron. For the hole doped cuprates this field is ~ 100 T. In contrast, for the electron-doped cuprates this field is of the order ~ 30 T (and $T^* \sim 30 - 40$ K), and so this is much more experimentally accessible (Kawakami et al., 2005). The field and temperature dependence of the interlayer resistance for several superconducting organic charge transfer salts (Zuo et al., 1999) is qualitatively similar to that for the cuprates. In particular, for temperatures less than the zero-field transition temperature and fields larger than the upper critical field, negative magnetoresistance is observed for fields perpendicular to the layers. A possible explanation is that, as in the cuprates, there is a suppression of the density of states near the Fermi energy, and the associated pseudogap decreases with increasing magnetic field.

Angle dependent magnetoresistance has proven to be a powerful probe of Fermi surface properties in the organic charge transfer salts (Kartsovnik, 2004) and more recently in the cuprates (Abdel-Jawad et al., 2006; Kennett and McKenzie, 2007). Recently, it has been shown that an anisotropic pseudogap should produce distinct signatures in the interlayer magnetoresistance when the magnetic field is rotated parallel to the layers (Smith and McKenzie, 2009). This is a realistic and important experiment that should be done on κ-(BEDT-TTF)$_2$Cu-[N(CN)$_2$]Br.

One could also study the pressure dependence of the linear coefficient of heat capacity γ. Since γ is proportional to the density of states at the Fermi energy, a detailed mapping of $\gamma(P)$ would be an important probe for the study the pseudogap. Finally, measurements of the Hall effect have also led to important insights into the pseudogap of the cuprates (Timusk and Statt, 1999), therefore, perhaps, the time is ripe to revisit these experiments in the organic charge transfer salts.

7. The Nernst effect and vortex fluctuations above T_c

A most interesting observation, which may be related to the pseudogap, is the large normal state Nernst effect in κ-(BEDT-TTF)$_2$Cu[N(CN)$_2$]Br (Nam et al., 2007), shown in Fig. 18. In κ-(BEDT-TTF)$_2$Cu(NCS)$_2$ the Nernst signal is of order the noise in the experiment for $T > T_c$. However, a large positive Nernst signal is observed just below T_c. It is extremely likely that this arises from the motion of superconducting vortices, which freeze out at lower temperatures as the vortex lattice forms. Nam et al. point out that "there is nothing unexpected in these observations." What was unexpected however, is that in κ-(BEDT-TTF)$_2$Cu[N(CN)$_2$]-Br a Nernst signal is seen even for $T > T_c$. Nam et al. interpreted this as evidence of superconducting fluctuations that support vortices above T_c.

A large normal state Nernst effect is also seen in the underdoped cuprates (Wang et al., 2006). This has also often been interpreted as evidence for vortices above T_c. In part this was due to a misunderstanding of the "Sondheimer cancellation". Sondheimer (Sondheimer, 1948) showed that for the dispersion characteristic of free fermions, $\epsilon_{\mathbf{k}} = \hbar^2 |\mathbf{k}|^2 / 2m^*$, the normal state Nernst effect is small. This was often taken to be a general result and it was therefore assumed that a large Nernst signal was a definitive signal of vortices in the normal state. However, the Sondheimer cancellation turns out to be a special property of the free fermion dispersion relation (Behnia, 2009).

In the last few years it has become clear that there are several other effects that could give rise to large Nernst effects including an electronic nematic or Pomeranchuk phase (Daou et al., 2010; Fradkin et al., 2010; Hackl and Vojta, 2009), stripes (Hackl et al., 2010), a d-density wave (Kotetes and Varelogiannis, 2010) or even just the details of the band structure (Behnia, 2009). None of these effects have been yet been considered as possible explanations for Nam et al.'s results. Another interesting question, given that Nam et al. only see the normal state Nernst in κ-(BEDT-TTF)$_2$Cu[N(CN)$_2$]Br, which is very close to the first-order Mott transition, is: would the coexistence of small amounts of the insulating phase with the metallic phase lead to an enhanced Nernst signal.

An important consideration is that vortices can only give rise to a positive Nernst coefficient[12]. Yet, in the normal state of κ-(BEDT-TTF)$_2$Cu[N(CN)$_2$]Br Nam et al. report a *negative* Nernst coefficient above ~ 15 K. This seems to suggest that while the Nernst signal below ~ 15 K may indeed be caused by vortices, the large normal state Nernst signal above ~ 15 K arises from quasiparticles, which may give rise to a Nernst coefficient of
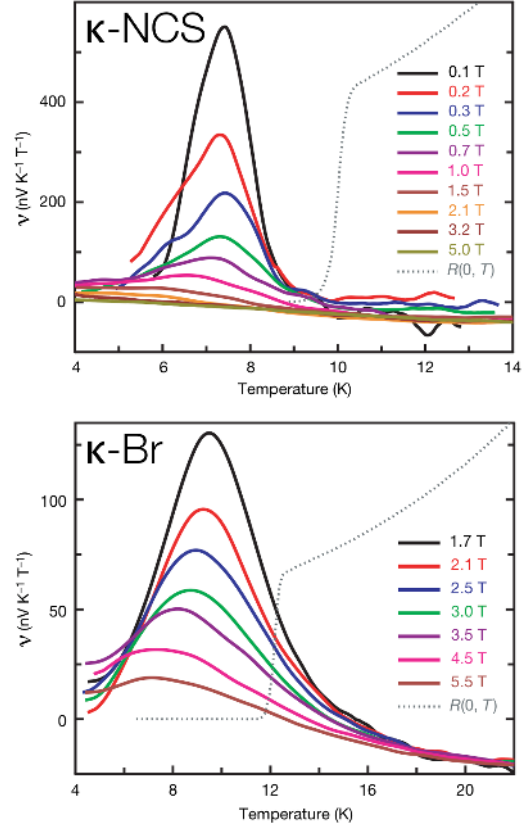
---

[12] In the convention employed by Nam et al. Note that two different sign conventions are used in the literature, which can be rather confusing. A clear discussion of this is given in (Behnia, 2009).

FIG. 18 Nernst coefficient, ν, in κ-(BEDT-TTF)$_2$Cu(NCS)$_2$ (top) and κ-(BEDT-TTF)$_2$Cu[N(CN)$_2$]Br (bottom). In κ-(BEDT-TTF)$_2$Cu(NCS)$_2$ a large Nernst coefficient is observed below the superconducting critical temperature, T_c, (for reference the temperature dependence of the zero field resistance is shown as a dotted line). Nam et al. (Nam et al., 2007) attributed this increase to the effect of vortices in the superconducting state, which are known to give a large positive contribution to N. In κ-(BEDT-TTF)$_2$Cu[N(CN)$_2$]Br the Nernst coefficient is large even above T_c, which Nam et al. interpreted as evidence of fluctuating superconductivity even above T_c. The contribution to the Nernst coefficient from quasiparticles can take either sign. Therefore, the negative Nernst coefficient at the highest temperatures in the lower panel presumably arises from quasiparticles.

either sign (Behnia, 2009).

An order of magnitude estimate of the quasiparticle contribution to the Nernst coefficient, ν, can be made from (Behnia, 2009)

$$\frac{\nu}{T} = -\frac{\pi^2}{3} \frac{k_B}{e} \frac{\mu_c}{T_F}, \tag{22}$$

where $T_F = E_F / k_B$ is the Fermi temperature, and the carrier mobility, μ_c, is given by

$$\mu_c = \frac{\tan \theta_H}{B} = \frac{e\tau}{m^*} = \frac{el}{\hbar k_F}, \tag{23}$$

where θ_H is the Hall angle, τ is the quasiparticle lifetime, and l is the mean free path. $k_F \sim \frac{\pi}{2a}$, where $a \sim 1$ nm is

a lattice constant. As the temperature is raised towards the bad metal regime the $l \sim a$. Thus, $\mu_c \sim 10^{-3}$ T^{-1}. $T_F \sim 10^3$ K (Powell and McKenzie, 2004b). Between 50 K and 20 K the resistivity decreases by an order of magnitude (Analytis et al., 2006) and hence the mean free path increases by an order of magnitude. So, at 20 K, one expects that $\nu \sim 10$ nV K^{-1} T^{-1}. (One can also construct an estimate of this order of magnitude by extrapolating from the measured scattering rate (Powell and McKenzie, 2004b) in the $T \to 0$ limit.) This is indeed the order of magnitude observed at $T \sim 20$ K in both κ-(BEDT-TTF)$_2$Cu(NCS)$_2$ and κ-(BEDT-TTF)$_2$Cu[N-(CN)$_2$]Br. Thus these two estimates suggest that the magnitude of the Nernst coefficient observed in the normal state of κ-(BEDT-TTF)$_2$Cu(NCS)$_2$ and κ-(BEDT-TTF)$_2$Cu[N(CN)$_2$]Br may be reasonable although given the multiband Fermi surface with both electron and hole sheets a more careful calculation is required to test this and to establish the sign of the quasiparticle contribution to the Nernst coefficient.

E. The superconducting state

1. κ-(BEDT-TTF)$_2$Cu$_2$(CN)$_3$

Little is known experimentally about the effects of frustration on the superconducting state of the κ-(BEDT-TTF)$_2X$ salts. In particular, there have only been a very few studies of the superconducting state of κ-(BEDT-TTF)$_2$Cu$_2$(CN)$_3$. However, this has not prevented significant interest in the effects of frustration on superconductivity from the theoretical community (Clay et al., 2008; Galitski and Kim, 2007; Gan et al., 2006; Huang et al., 2007; Kondo and Moriya, 2004; Kyung and Tremblay, 2006; Lee et al., 2007a; Powell and McKenzie, 2005, 2007; Sahebsara and Senechal, 2006; Watanabe et al., 2006; Wrobel and Suleja, 2007). Recently, Shimizu *et al.* (Shimizu et al., 2010) have reported NMR experiments under pressure in the superconducting phase. They found that $1/T_1T \propto T^2$, which is consistent with line nodes on a three dimensional Fermi surface or point nodes on a two dimensional Fermi surface. Further, Shimizu *et al.* did not observe any signs of a Hebel-Slichter peak, which suggests that the pairing has a non-*s*-wave symmetry.

Another, potentially important result is that Shimizu *et al.* only observed a very small reduction in the Knight shift of κ-(BEDT-TTF)$_2$Cu$_2$(CN)$_3$ below T_c. They suggested two possible explanations for this result. Firstly, it could be an experimental artefact due to radio frequency (rf) heating during their spin-echo experiments. Shimizu *et al.* were not able to rule this out as free induction decay experiments are complicated by the short T_2^* in κ-(BEDT-TTF)$_2$Cu$_2$(CN)$_3$ and low power rf experiments were not sufficiently sensitive in the small crystals that are currently available. Therefore larger crystals are important to rule out this trivial explanation. However, the

C_{6v}	E	C_2	$2C_3$	$2C_6$	$3\sigma_d$	$3\sigma_v$	states
A_1	1	1	1	1	1	1	s, $s_{x^2+y^2}$
A_2	1	1	1	1	-1	-1	
B_1	1	-1	1	-1	-1	1	
B_2	1	-1	1	-1	1	-1	
E_1	2	-2	-1	1	0	0	
E_2	2	2	-1	-1	0	0	$(d_{x^2-y^2}, d_{xy})$

TABLE II The character table of C_{6v}, which represents the point group symmetry of the isotropic triangular lattice.

second, more interesting, explanation is that there is little change in $1/T_1T$ below T_c because κ-(BEDT-TTF)$_2$Cu$_2$-(CN)$_3$ is a triplet superconductor. There is a small drop in K_s below T_c, which suggests that the pairing state is not purely equal spin pairing, like the A phase of ^{3}He. However, many of the plethora of exotic phases that are available to ^{3}He are ruled out (Powell, 2008) by the low symmetry of the κ-(BEDT-TTF)$_2$Cu$_2$(CN)$_3$ crystal.

A wide range of theories that invoke a magnetic pairing mechanism give rise to $d_{x^2-y^2}$ pairing on the square lattice (Lee et al., 2006; Monthoux et al., 2007). More formally one should say that the superconducting order parameter transforms like the B_1 representation of C_{4v}, which is the point group symmetry of the square lattice. The isotopic triangular lattice (i.e., $t' = t$) has C_{6v} symmetry, cf. Table II. A $d_{x^2-y^2}$ order parameter would belong to the E_2 representation of C_{6v}. This is interesting because E_2 is a two-dimensional representation, which means that one naturally expects a two component order parameter, (η_1, η_2), for which the Ginsburg-Landau free energy would be (Annett, 1990; Sigrist and Ueda, 1991)

$$\begin{aligned} F_{e_2} &= F_n + \alpha(T - T_c)(|\eta_1|^2 + |\eta_2|^2) + \beta_1(|\eta_1|^2 + |\eta_2|^2)^2 \\ &+ \beta_2(\eta_1^*\eta_2 - \eta_1\eta_2^*)^2, \end{aligned} \quad (24)$$

where F_n is the free energy of the normal state and α, β_1 and β_2 are the parameters of the theory, which need to be determined from experiment or derived from a microscopic theory.

Eq. (24) has three solutions: (i) $\vec{\eta} = (1, 0)$ or (ii) $\vec{\eta} = (0, 1)$ for $\beta_2 > 0$ (the degeneracy is lifted by sixth order terms (Annett, 1990; Sigrist and Ueda, 1991)); (iii) $\vec{\eta} = (1, i)$ for $\beta_2 < 0$. The two components of the order parameter can be associated with, say, the $d_{x^2-y^2}$ and the d_{xy} pairing channels, which gives the physical interpretation of the theory. Solution (i) corresponds to $d_{x^2-y^2}$ pairing, solution (ii) corresponds to d_{xy} pairing, and solution (iii) corresponds to $d_{x^2-y^2} + id_{xy}$ pairing, which we will refer to as the $d + id$ state. The $d + id$ state is therefore predicted for a large fraction of the possible parameter values in the theory, including the weak coupling solution (Annett, 1990; Powell, 2006; Sigrist and Ueda, 1991). The $d + id$ state is also found in microscopic calculations for the, strong coupling, resonating valence bond
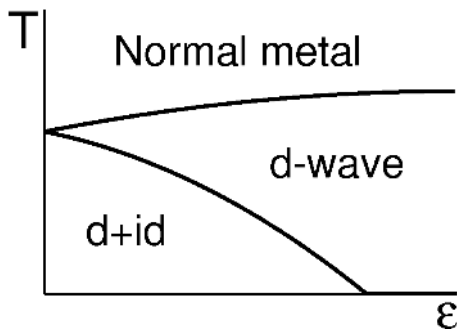
FIG. 19 Breaking the symmetry of the isotropic triangular lattice destroys the $d + id$ superconducting state in favour of a pure d-wave state. For weak symmetry breaking a double superconducting transition will occur. The symmetry breaking parameter $\epsilon \sim 1 - t'/t$. From (Powell, 2006).

(RVB) theory on the isotropic triangular lattice (Powell and McKenzie, 2007). In principle the broken time reversal symmetry of the $d + id$ state should be directly detectable via muon spin relaxation experiments (Sigrist and Ueda, 1991). However, such experiments are yet to be performed on the superconducting state of κ-(BEDT-TTF)$_2$Cu$_2$(CN)$_3$.

However, κ-(BEDT-TTF)$_2$Cu$_2$(CN)$_3$ crystals actually have C_{2h} symmetry rather than the C_{6v} symmetry of the isotropic triangular lattice. Similarly, the anisotropic triangular lattice ($t' \neq t$) has C_{2v} symmetry. It can be seen from Table III that for both C_{2h} and C_{2v} $d_{x^2-y^2}$ and d_{xy} order parameters belong to different one dimensional representations. Thus, one does not expect a two-component order parameter generically. A simple way to understand what will happen near the isotropic case is to introduce a symmetry breaking perturbation into Eq. (24) (Powell, 2006). This perturbation lifts the degeneracy and results in a double superconducting transition, see Fig. 19. Physically such a perturbation corresponds to varying t'/t away from unity, but because of its C_{2h} crystal symmetry one always excepts this perturbation to always be present in κ-(BEDT-TTF)$_2$Cu$_2$-(CN)$_3$. Therefore, if the superconducting transition of κ-(BEDT-TTF)$_2$Cu$_2$(CN)$_3$ breaks time reversal symmetry, this will be signified by a double superconducting transition, which would be visible to any number of thermodynamic probes. However, to date, no suitable experiments have been performed, presumably this is due, at least in part, to the difficulty in performing many of these measurements under pressure.

2. Weakly frustrated materials

We have given an extended review of the superconducting states of the more weakly frustrated materials, such as κ-(BEDT-TTF)$_2$Cu[N(CN)$_2$]Br and κ-(BEDT-TTF)$_2$Cu(NCS)$_2$, somewhat recently (Powell and McKenzie, 2006). We will not repeat that discus-

C_{2v}	E	C_2	σ_v	σ_v'	states
A_1	1	1	1	1	$s,\ d_{xy}$
A_2	1	1	-1	-1	$d_{x^2-y^2}$
B_1	1	-1	1	-1	
B_2	1	-1	-1	-1	

C_{2h}	E	C_2	σ_h	i	states
A_g	1	1	1	1	$s,\ d_{xy}$
A_u	1	1	-1	-1	
B_g	1	-1	-1	1	$d_{x^2-y^2}$
B_u	1	-1	-1	1	

TABLE III The character tables of C_{2v} and C_{2h}. The anisotropic triangular lattice has C_{2v} symmetry for $t' \neq t$ (cf. Fig. 9). However, the point group symmetry of κ-(BEDT-TTF)$_2$Cu$_2$(CN)$_3$ is C_{2h}. Note that for the C_{2v} point group we use the coordinate system defined in Fig. 9c, in which the C_2 axis is along the $x + y$ direction, thus the indicated transformation properties of coordinate system are different from those found in many textbooks e.g. (Lax, 1974; Tinkham, 1992).

sion here and will limit ourselves to highlighting the main issues and discuss some of the more recent results.

One key issue, that remains controversial, is the pairing symmetry. There is clear evidence from the suppression of the Knight shift below T_c that the weakly frustrated κ-(BEDT-TTF)$_2$X salts are singlet superconductors (Powell, 2006). However, no Hebel-Slichter peak is seen in $1/T_1T$ (de Soto et al., 1995; Kawamoto et al., 1995b), which suggests that the pairing state is not s-wave. Further, thermodynamic measurements down to the lowest temperatures (Taylor et al., 2007) suggest that there are nodes in the gap. Given the low symmetry of crystals of organic charge transfers salts, this evidence suggests that a $d_{x^2-y^2}$-wave state is realised in these materials (Powell, 2006). This is also natural on theoretical grounds given the proximity to antiferromagnetic order in the more weakly frustrated compounds.

In an unconventional superconductor (i.e., any superconductor in which the order parameter does not transform like the trivial representation) non-magnetic disorder suppresses the superconducting critical temperature in accordance with the Abrikosov-Gorkov forumla (Larkin, 1965; Mineev and Samokhin, 1999):

$$\ln\left(\frac{T_{c0}}{T_c}\right) = \psi\left(\frac{1}{2} + \frac{\hbar}{4\pi k_B T_c}\frac{1}{\tau}\right) - \psi\left(\frac{1}{2}\right), \quad (25)$$

where T_{c0} is the critical temperature of the clean system, $1/\tau$ is the rate at which electrons scatter from impurities and $\psi(x)$ is the digamma function. Combining this result with the Fermi liquid expression for the interlayer conductivity it can be shown (Powell and McKenzie, 2004b) that, to leading order in $1/\tau$, the suppression in T_c is
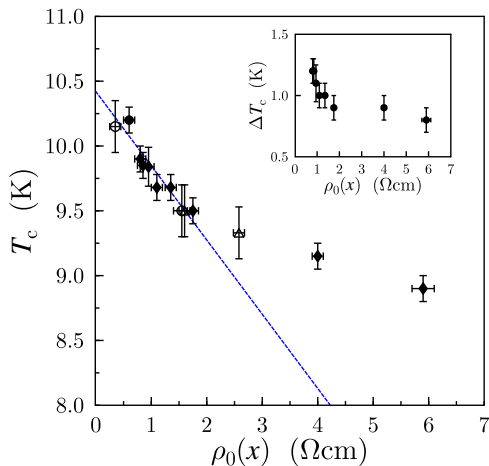
FIG. 20 Suppression of superconductivity by non-magnetic impurities. At low concentrations of impurities the data is well described by Eq. (26) with a reasonable value of $t_\perp$ (line). But, for higher impurity concentrations strong deviations from the predictions of the Abrikosov-Gorkov formula, Eq. (25) are observed. From (Analytis et al., 2006); impurities were introduced by x-ray and proton irradiation. [Copyright (2006) by the American Physical Society].

given by

$$T_c = T_{c0} - \frac{e^2 m^* c t_\perp^2}{4 k_B \hbar^3} \rho_0, \qquad (26)$$

where m^* is the effective mass, $t_\perp$ is the interlayer hopping amplitude and ρ_0 is the interlayer residual resistivity. For low impurity concentrations this linear behaviour is indeed observed in the κ-BEDT-TTF superconductors (Analytis et al., 2006; Powell and McKenzie, 2004b). Furthermore, the value of $t_\perp$ found from a fit of Eq. (26) to this data yields excellent agreement with estimates of $t_\perp$ from other experimental techniques, such as angle-dependent magnetoresistance and quantum oscillations (Analytis et al., 2006; Powell and McKenzie, 2004b). However, for higher disorder concentrations the data does *not* follow Eq. (25) (Analytis et al., 2006; Sasaki et al., 2010), cf. Fig 20. Until this deviation from the prediction of Eq. 25 is understood the question of the pairing symmetry cannot be considered to have been resolved.

Another puzzle about the superconducting state is that, at low temperatures, the in-plane penetration depth, λ has been found to vary as $\lambda \sim T^{3/2}$. As the penetration depth is proportional to the density of states with $\sim k_B T$ of the Fermi energy, one expects that $\lambda \sim \exp(-\Delta/k_B T)$ for a fully gapped superconductor, $\lambda \sim T^2$ for a 3D superconductor with point nodes and $\lambda \sim T$ for a 3D superconductor with line nodes or a 2D superconductor with point nodes (Annett et al., 1990). The observation of an intermediate power law has not yet received an adequate explanation.
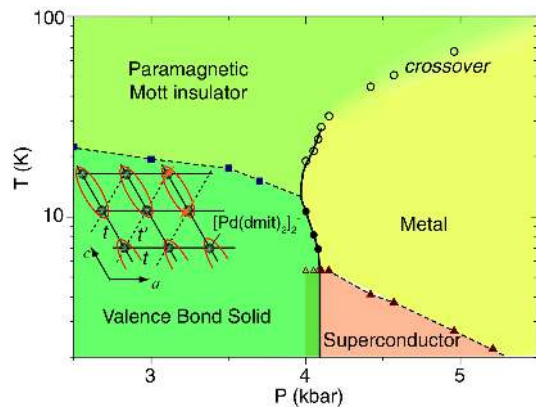

FIG. 21 Pressure-temperature phase diagram of EtMe$_3$P[Pd(dmit)$_2$]$_2$ (P-1). This is remarkably similar to the phase diagrams of κ-(BEDT-TTF)$_2$Cu[N(CN)$_2$]Cl (Fig. 7) and κ-(BEDT-TTF)$_2$Cu$_2$(CN)$_3$ (Fig. 8). However, the Mott insulator phase of P-1 shows valence bond crystalline order unlike the antiferromagnetism observed in κ-(BEDT-TTF)$_2$Cu[N(CN)$_2$]Cl and the spin liquid seen in κ-(BEDT-TTF)$_2$Cu$_2$(CN)$_3$. From (Shimizu et al., 2007a).

Another interesting issue is the zero temperature superfluid stiffness, $\rho_s(0) \propto 1/\lambda^2$, where λ is the zero temperature penetration depth. In the underdoped cuprates it is found that $\rho_s(0) \propto T_c$, which is known as the Uemura relationship. A number of explanations have be advanced to explain this, but most boil down to the idea that underdoped cuprates become normal due to a loss of phase coherence as the temperature is raised (Emery and Kivelson, 1995). This should be contrasted with the BCS theory where superconductors become normal at finite temperatures due to the suppression of pairing by the entropy associated with quasi-particle excitations. Pratt *et al.* (Pratt and Blundell, 2005; Pratt et al., 2003) have found that in a wide range of BEDT-TTF salts $T_c \propto 1/\lambda^3 \propto \rho_s(0)^{3/2}$. Furthermore, their results disagree, by orders of magnitude, with the prediction of both the BCS theory and Emery and Kivelson's theory of phase fluctuations (Powell and McKenzie, 2004a), which gives a good description of the phenomena observed in the cuprates. No theoretical explanation of Pratt *et al.*'s results has been given yet. Doing so remains a major challenge to theory and a major test for any proposed microscopic theory of superconductivity in these materials.

IV. β'-$Z[\mathbf{Pd(dmit)_2}]_2$

Organic charge transfer salts based on the Pd(dmit)$_2$ molecule, shown in Fig. 6b, are less well known, and have been less widely studied, than the κ-(BEDT-TTF)$_2 X$ materials discussed above (section III). However, the salts of Pd(dmit)$_2$ show a fascinating range of behaviours, which we review in this section. We will see that the Pd(dmit)$_2$ salts have much in common with the κ-
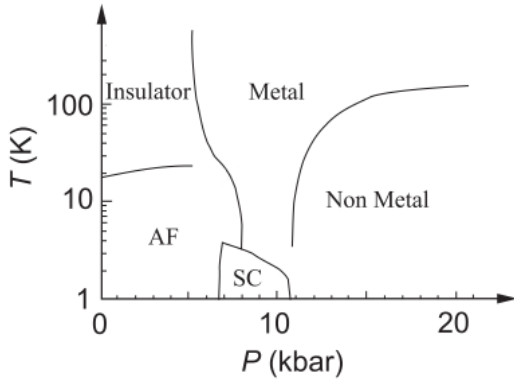
FIG. 22 Pressure-temperature phase diagram of $Et_2Me_2P[Pd(dmit)_2]_2$ (P-2). This has strong similarities to the phase diagrams of κ-(BEDT-TTF)$_2$Cu[N(CN)$_2$]Cl (Fig. 7), κ-(BEDT-TTF)$_2$Cu$_2$(CN)$_3$ (Fig. 8) and P-1 (Fig. 21). An important difference is that P-2 shows long range antiferromagnetism, like κ-(BEDT-TTF)$_2$Cu[N(CN)$_2$]Cl. The high pressure non-metal phase is associated with a change in crystal structure (Yamaura et al., 2004). Modified from (Yamaura et al., 2004).
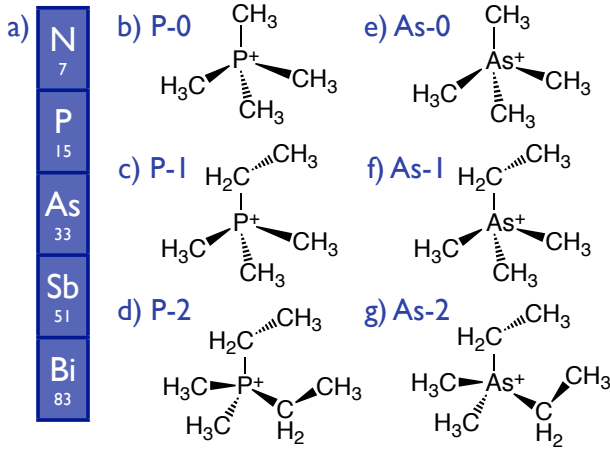

FIG. 23 Typical cations in charge transfer salts with Pd(dmit)$_2$ (shown in Fig. 6b) are shown in panels (b)-(g). These cations share the PnMe$_{4-n}$Et$_n$ motif, where Pn is a group V element (pnictogen), panel (a), Me is a methyl group (CH$_3$) and Et is an ethyl group (C$_2$H$_5$). We use the shorthand Pn-n for the salt PnMe$_{4-n}$Et$_n$[Pd(dmit)$_2$]$_2$

(BEDT-TTF)$_2$X salts, as is apparent from their similar phase diagrams (compare Figs. 21 and 22 with Figs. 7 and 8)

In this section we will discuss many materials with rather similar chemical formulae. To simplify our discussion we introduce the following nomenclature: Et$_n$Me$_{4-n}$$Pn$[Pd(dmit)$_2$]$_2$ will be written as Pn-n, where Pn is a pnictogen, Et is the ethyl group, C$_2$H$_5$, and Me is the methyl group, CH$_3$, cf. Fig. 23.

A. Crystal and electronic structure

The Pd(dmit)$_2$ molecule is shown in Fig 6b. A number of other M(dmit)$_2$ molecules, where M is a transition metal, can also form charge transfer salts. An interesting example is Ni(dmit)$_2$, whose salts have quasi-one-dimensional properties; in contrast to the quasi-two-dimensional behaviour found in salts of Pd(dmit)$_2$. These differences arise because of subtle changes in the molecular orbitals of the dimers of these two molecules as we will discuss below.

Most of the crystals that we will discuss below take the so-called β' phase, shown in Fig. 24. An important feature of this structural motif is that the Pd(dmit)$_2$ molecules are arranged in dimers. Electronic structure calculations show that the amplitude for hopping between two monomers within a dimer is much larger than the amplitude for hopping between two monomers in different dimers (Canadell, 1999; Miyazaki and Ohno, 1999). This arises not only from the greater proximity of the two monomers in a dimer, but also because of the shape of the relevant molecular orbitals, which have a large contribution from the π orbitals. Thus, the face-to-face stacking within a dimer leads to a large overlap. In Section III.A we discussed a simple model for the electronic structure of a BEDT-TTF dimer. This model is based on a single molecular orbital (the HOMO) on each BEDT-TTF molecule. We will now discuss a similar model for the electronic structure of $[M(\text{dmit})_2]_2$. However, the model for M(dmit)$_2$ differs from that for BEDT-TTF in several important ways because more than one molecular orbital on each M(dmit)$_2$ molecule is involved. Our discussion is based on extended Hückel calculations (Canadell, 1999), although we also note that DFT calculations (Miyazaki and Ohno, 1999) give the same qualitative picture.

M(dmit)$_2$ is an electron acceptor molecule and on average the dimer has a net charge of -1 in the crystal. Thus naïvely one might expect that the extra electron resides in the bonding combination of monomer LUMOs. However, electronic structure calculations find that there is significant hybridisation between the two monomer HOMOs, which complicates this picture. A simple, noninteracting model for the dimer is

$$
\begin{aligned}
\hat{\mathcal{H}}_{[M(dmit)_2]_2} &= \Delta \sum_{i=1}^{2} \sum_{\sigma} \left(\hat{L}_{i\sigma}^\dagger \hat{L}_{i\sigma} - \hat{H}_{i\sigma}^\dagger \hat{H}_{i\sigma} \right) \\
&\quad -t_H \sum_{\sigma} \left(\hat{H}_{1\sigma}^\dagger \hat{H}_{2\sigma} + \hat{H}_{2\sigma}^\dagger \hat{H}_{1\sigma} \right) \\
&\quad -t_L \sum_{\sigma} \left(\hat{L}_{1\sigma}^\dagger \hat{L}_{2\sigma} + \hat{L}_{2\sigma}^\dagger \hat{L}_{1\sigma} \right), \quad (27)
\end{aligned}
$$

where $\hat{H}_{i\sigma}$ creates an electron with spin σ in the HOMO of the ith monomer and $\hat{L}_{i\sigma}$ creates an electron with spin σ in the LUMO of the ith monomer. The solution of this model is trivial; and sketched in Fig. 25. It is clear that with five electrons, as is approporate
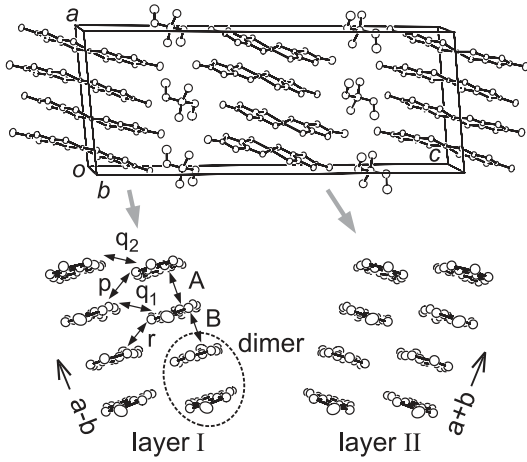
FIG. 24 The crystal structure of β'-Et$_2$Me$_2$P[Pd(dmit)$_2$]$_2$ (P-2). Note that there are two organic layers per unit cell. In the first layer the molecules stack along the $\mathbf{a} - \mathbf{b}$ direction, whereas in the second layer the molecular stacks are orientated along the $\mathbf{a} + \mathbf{b}$ direction. From (Yamaura et al., 2004).

FIG. 25 Sketch of the solution of the two site–two orbital model for a [Pd(dmit)$_2$]$_2$ dimer [Eq. (27)]. In salts formed with the monovalent cations, which we discuss here, the dimer has, on average, five electrons. (a) For $2\Delta > t_H + t_L$ (weak dimerisation) both the bonding and antibonding combinations of the molecular HOMOs are fully occupied, and the bonding combination of the molecular LUMOs contains one electron. Therefore, in the crystal, the half-filled metallic band will result primarily from the hybridisation of these LUMO antibonding orbitals. This case is believed to be relevant to the salts of Ni(dmit)$_2$ (Miyazaki and Ohno, 1999). The shape of the molecular orbitals gives rise to a quasi-one-dimensional band structure in these compounds. (b) For $2\Delta < t_H + t_L$ (strong dimerisation) the antibonding combination of the molecular HOMOs is pushed above the bonding combination of molecular LUMOs. Thus, the half-filled metallic band in the crystal will be formed from predominately from these HOMO antibonding orbitals. This is believed to be the case relevant to the salts of Pd(dmit)$_2$. The structure of the molecular HOMOs gives rise to a quasi-two-dimensional band structure with the topology of the anisotropic triangular lattice, cf. Fig. 24. In order for these single band descriptions to be relevant to the real materials $|2\Delta - t_H - t_L|$ must be larger than the other energy scales relevant to the problem. If this is not the case multiband effects may have important consequences.

for $[M(\text{dmit})_2]_2^-$, one of the energy levels will be partially occupied. However, which state this is is dependent on the ratio $(t_H + t_L)/\Delta$. There are two regimes: (a) strong dimerisation $(t_H + t_L > 2\Delta)$: the antibonding combination of monomer HOMOs contains one electron, while the bonding combination of monomer LUMOs contains two electrons (Fig. 25a); and (b) weak dimerisation $(t_H + t_L < 2\Delta)$: the antibonding combination of monomer HOMOs contains two electrons, while the bonding combination of monomer LUMOs contains one electron (Fig. 25b). In either, case a one band description will only be justified if $|t_H + t_L - 2\Delta|$ is sufficiently large compared to the other energy scales relevant to the problem.

Of course, once other orbitals, electron-electron interactions and the weak (almost symmetry forbidden) hybridisation between the HOMO on one monomer and the LUMOs on the other are included the situation becomes significantly more complicated. However, DFT calculations (Miyazaki and Ohno, 1999) suggest that the cartoon sketched above does capture many of the important physical features of both the [Pd(dmit)$_2$]$_2$ and the [Ni(dmit)$_2$]$_2$ dimers. Furthermore, these calculations suggest that [Pd(dmit)$_2$]$_2$ corresponds to case (a) (strong dimerisation) whereas [Ni(dmit)$_2$]$_2$ corresponds to case (b) (weak dimerisation). Hence the metallic band in salts of [Pd(dmit)$_2$]$_2$ results primarily from the antibonding combination of monomer HOMOs whereas the metallic band in salts of [Pd(dmit)$_2$]$_2$ results primarily from the bonding combination of monomer LUMOs. This may sound like a trivial detail but it has important consequences for the physics of these salts. In particular, the bands formed (predominately) from the bonding combination of LUMOs in $X[\text{Ni(dmit)}_2]_2$ are quasi-one-dimensional, whereas the bands formed (predominately) from the antibonding combination of HO-
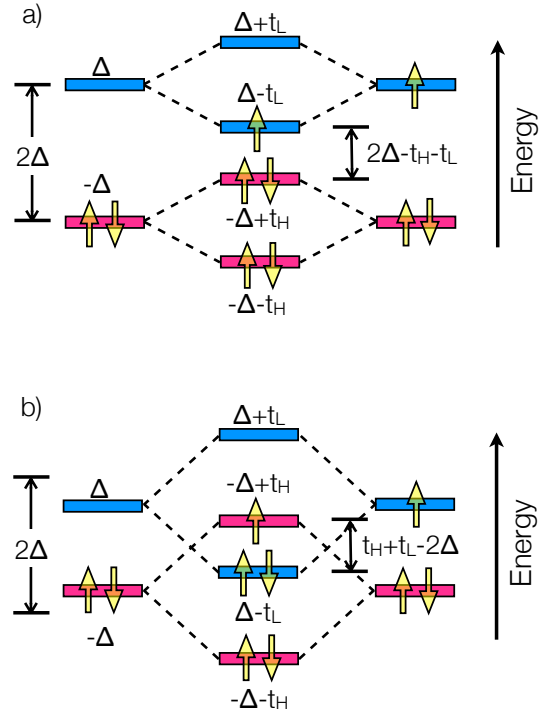
MOs in $X[\text{Pd(dmit)}_2]_2$ are quasi-two-dimensional. Thus, the profound differences in the observed behaviour of the salts of Ni(dmit)$_2$ and Pd(dmit)$_2$ results from a rather small structural change (the degree of dimerisation). The differences between in the band structures of the Ni and Pd compounds have been nicely illustrated by comparative DFT calculations for Me$_4$N[Pd(dmit)$_2$] and Me$_4$N[Ni(dmit)$_2$] (Miyazaki and Ohno, 1999).

If one takes the dimers as a basic building block for the electronic structure, then the band structure of the $Et_nMe_{4-n}Pn[Pd(dmit)_2]_2$ salts is described by an anisotropic triangular lattice, cf. Fig. 26. To date the only parameterisations of this anisotropic triangular lattice come from Hückel calculations (Canadell, 1999). Miyazaki and Ohno (Miyazaki and Ohno, 1999) reported that their DFT band structures could be described by a fit to a tight-binding model for this lattice, but did not report the values of t'/t obtained from these fits. Given the Hückel methods systematic overestimation of t'/t in the κ-$(BEDT\text{-}TTF)_2X$ salts, (cf. Section III.A), one should exercise care when dealing with the Hückel parameters for $Et_nMe_{4-n}Pn[Pd(dmit)_2]_2$ salts.

Because of the 2:1 ratio of anions to cations and the monovalency of $Et_nMe_{4-n}Pn$ cations the anisotropic triangular lattice model of the $Et_nMe_{4-n}Pn[Pd(dmit)_2]_2$ salts is half filled. Therefore, both Hückel and DFT calculations predict a metallic state. In contrast, these materials are found to be insulating at ambient pressure (Kato, 2004), and many undergo a metal-insulator transition under hydrostatic pressure and/or uniaxial stress. This suggests Mott physics is at play and hence that electron-electron interactions are vitally important. Therefore, the simplest model that may be compatible with the above considerations is the Hubbard model on an anisotropic triangular lattice (cf. Section VI.B). Nothing is reliably known about the importance of longer range electron-electron interactions or electron-phonon interactions.

B. Frustrated antiferromagnetism

At ambient pressure the β'-$Me_{4-n}Et_nPn$-$[Pd(dmit)_2]_2$ salts are Mott insulators (Kato, 2004). A large number of these materials order antiferromagnetically at low temperatures. To date relatively little is known about this antiferromagnetic state, for example, no experiments have investigated the ordering wavevector. Nevertheless, it is known that changing the cation does vary the Néel temperature, T_N. Indeed Shimizu et al. (Shimizu et al., 2007b) have argued that there is a correlation between T_N and the ratio t'/t calculated from extended Hückel theory. However, given the issues with the values of these parameters obtained from Hückel theory, see Sections III.A and IV.A, and the small changes in t'/t invoked in this comparison it is not clear how much confidence one should invest in this claimed correlation at present. Certainly the values calculated from Hückel are systematically larger than than those found from DFT in the κ-$(BEDT\text{-}TTF)_2X$ salts (see Section III.A). Nevertheless, one might hope that the trend that increasing t'/t supresses T_N may prove to be robust if higher level band structure calculations were performed.

The bulk magnetic susceptibility of many of the antiferromagnetic compounds has been studied at length (Tamura and Kato, 2002). Fits to high temperature series expansions for the magnetic susceptibility reveal several interesting trends (Tamura and Kato, 2002; Zheng, Singh, McKenzie and Coldea, 2005). Firstly, for all of the materials for which such fits have been performed, strong frustration is found ($0.85 < J'/J < 1.15$; one should note however that this method has difficulty in determining whether J'/J is greater or less than one). Secondly, for all of these materials a fit assuming an isotropic triangular lattice (i.e. $J' = J$) gives $J = 250 - 260$ K. Hence, it should be noted that in these magnetically ordered materials $k_BT_N \ll J$, consistent with strong geometrical frustration.

C. Spin liquid behaviour in β'-Me_3EtSb-$[Pd(dmit)_2]_2$ (Sb-1)

The bulk magnetic susceptibility, χ, measured at high temperatures in Sb-1 is remarkably similar to the high temperature magnetic susceptibility in the frustrated antiferromagnets discussed above. $\chi(T)$ has a broad maximum around 50 K (Itou et al., 2008) and fits well to high temperature series expansions for the isotropic triangular lattice with $J \simeq 240$ K. However, no magnetic phase transition has been observed in Sb-1 down to the lowest temperatures studied [1.37 K (Itou et al., 2008)], i.e., temperatures two orders of magnitude smaller than J.

Itou et al. (Itou et al., 2008) also observed an inhomogeneous broadening of the NMR spectra at low temperatures, see Fig. 27. They argued that this broadening is due to static local fields, but that, given the measured value of the hyperfine coupling constant, the broadening is too narrow to be understood in terms of long range magnetic order or spin glass behaviour. This is particularly interesting because it is very similar to what is observed in κ-$(BEDT\text{-}TTF)_2Cu_2(CN)_3$, cf. Fig. 12, raising the possibility of a common origin. At these low temperatures the recovery curve for the ^{13}C nuclear magnetic moment is *not* described by a single exponential, suggesting that the nuclei see more than one environment.

It is also interesting to compare the findings of NMR experiments with the measurements of χ. At high temperatures $1/T_1T \propto \chi$ (Itou et al., 2008). However, at low temperatures $1/T_1$ saturates to a constant; this is very different from what would be expected for a system with a spin gap (where one expects $1/T_1T \to 0$ as $T \to 0$). However, as noted above, in this low temperature regime the recovery of the magnetization is not described by a single exponential, making the estimation of T_1 rather difficult and raising questions about the interpretation of the estimated value of $1/T_1T$.

A recent report of measurements of the thermal conductivity of Sb-1 gives several important insights into the nature of the spin liquid state in Sb-1 (Yamashita et al., 2010). Figure 28 shows the temperature dependence of the thermal conductivity $\kappa(T)$. The non-zero intercept of $\kappa(T)/T$ as the temperature approaches zero is a clear
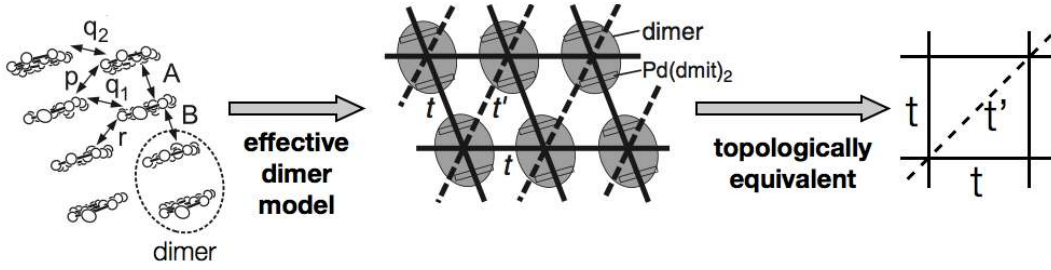
FIG. 26 The anisotropic triangular lattice in crystals of $Et_nMe_{4-n}Pn[Pd(dmit)_2]_2$. The left panel shows the a cross section of the organic layer, with a dimer ringed. The largest intermolecular hopping integrals are marked following the notation common in the Hückel literature. The central panel shows the structure of the effective dimer model. Here the dimers are represented by a single orbital, cf. Fig. 25. This can be mapped, without loss of generality, onto the same anisotropic triangular lattice model as we discussed for the κ-(BEDT-TTF)$_2X$ salts in Section III. This model is half filled, so a large Hubbard U must be associated with the dimers in order to cause the (Mott) insulating phase observed experimentally. [Modified from (Yamaura et al., 2004) and (Shimizu et al., 2007b).]
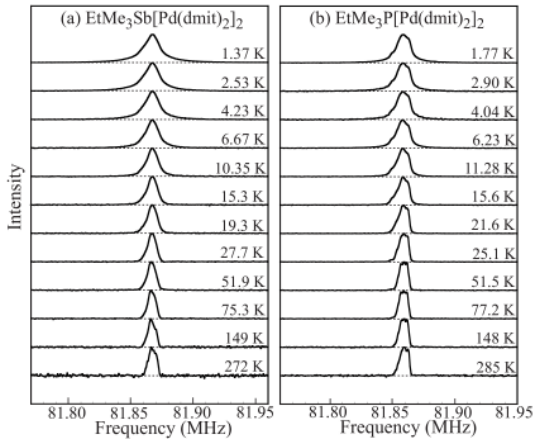

FIG. 27 Comparison of the ^{13}C-NMR spectra of (a) Sb-1 which is a spin liquid and (b) P-1 which forms a valence bond crystal at low temperatures. Both sets of spectra look remarkably similar, showing no signs of long range ordering, but an inhomogeneous broadening that increases as the temperature is lowered. A similar broadening is observed in the spin liquid state of κ-(BEDT-TTF)$_2$Cu$_2$(CN)$_3$, cf. Fig. 12. From (Itou et al., 2008). [Copyright (2008) American Physical Society].

FIG. 28 Temperature dependence of the thermal conductivity of several different frustrated materials. For κ-(BEDT-TTF)$_2$Cu$_2$(CN)$_3$ and Sb-2 the $\kappa/T \to 0$ as $T \to 0$ indicating that the excitations are gapped. However, for Sb-1 the spectrum appears to be gapless at κ/T tends to a finite number as $T \to 0$. Indeed the residual value of κ/T is comparable to that observed in the metallic state of other organics (Belin et al., 1998). The inset shows the same data on a linear scale From (Yamashita et al., 2010).

signature of gapless excitations. The magnitude of the intercept is comparable to its value in the metallic phase of other organic charge transfer salts, and an order of magnitude larger than what one gets in the d-wave superconducting state due to nodal quasi-particles (Belin et al., 1998).

Another important finding reported in this paper is that a spin gap is observed in the magnetic field dependence of thermal conductivity. At first sight this is rather puzzling as the temperature dependence of the thermal conductivity (Fig. 28) clearly shows that there are gapless excitations. However, one should note that excitations with any spin state can be excited thermally, whereas a field does not affect singlet excitations, cf. Section I.A.4. Therefore, these two results combined suggest that there are gapless singlet excitations, but a gap

to the lowest lying triplet (or higher spin) excitations. Thus, these results suggest that P-1 is what Normand has called a 'Type-II' spin liquid (Normand, 2009), see Sections I.A.4 and VI.A for further discussion.

Recently Katsura et al. (Katsura et al., 2010) predicted that there would be a sizeable thermal Hall effect in quantum spin liquids with deconfined spinons. This motivated measurements of the thermal conductance tensor in a magnetic field perpendicular to the layers (Yamashita et al., 2010). Within error the thermal Hall angle was zero.

FIG. 29 Opening of a spin gap in P-1. (a) At high temperatures the spin susceptibility is similar to the other $Pd(dmit)_2$ salts and can be fit to high temperature series expansions of t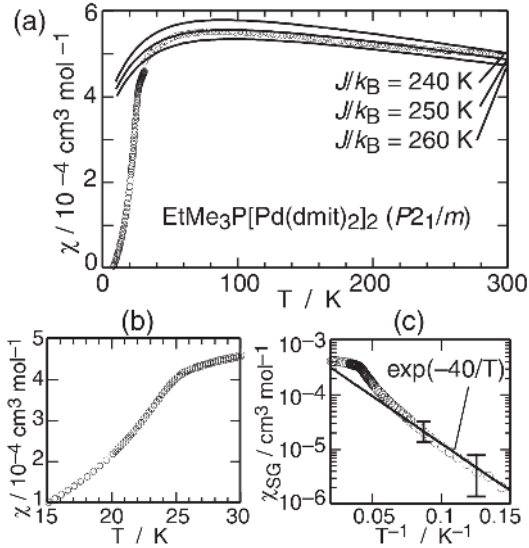he Heisenberg model on the isotropic triangular lattice with $J \sim 250$ K. But, below ~ 25 K a sudden drop is seen (b). At low temperatures the susceptibility appears to be activated consistent with the opening of a spin gap. From (Tamura, Tajima and Kato, 2005).

D. Is there a valence bond crystal or spin Peierls state in β'-Me$_3$EtP-[Pd(dmit)$_2$]$_2$ (P-1)?

P-1 shows an unusual phenomenology at low temperatures. As with the other $Pd(dmit)_2$ salts discussed above at high temperatures the bulk magnetic susceptibility is well described by high temperature series expansions for the Heisenberg model on the anisotropic triangular lattice, in this case with $J \simeq 250$ K, cf. Figure 29. One should note here that a Curie term (corresponding to about one $S = 1/2$ spin per 300 formula units) and a constant term (the value of which was not reported) have been subtracted from the experimental data before this comparison was made. However, below 25 K an exponential decrease in χ is observed (Tamura, Tajima and Kato, 2005), cf. Figure 29. The low temperature susceptibility is consistent with the opening of a spin gap of $\Delta = 40 \pm 10$ K, although Tamura et al. stress that this value is quite sensitive to the details of the values of the Curie and constant terms subtracted from the experimental data. One should also note that this fit was carried out over less than one decade in temperature.

X-ray crystallography (Tamura, Tajima and Kato, 2005) reveals structural changes in P-1 at approximately the same temperature as the spin gap opens. Satellite peaks indicating a doubling of the periodicity in the crystallographic c direction (which lies in the highly conducting plane) grow rapidly below 25 K, see Fig. 30. In the high temperature phase the distance between neighbouring $Pd(dmit)_2$ molecules in different dimers is, uni-
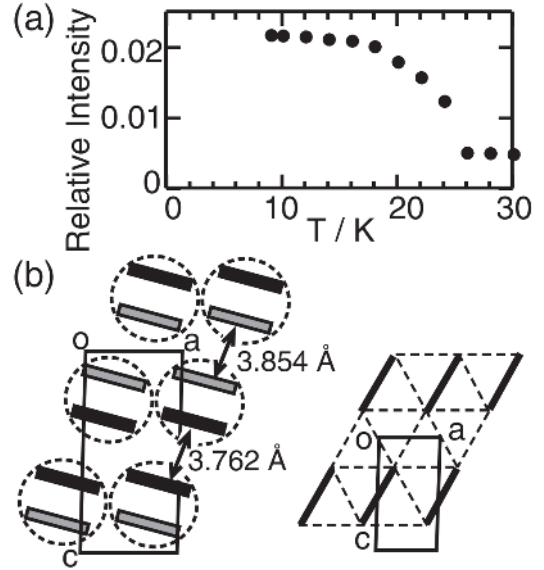

FIG. 30 Lattice distortion at low temperatures in P-1. At high temperatures all of the dimers in P-1 are uniformly spaced (3.82 Å apart). However, below ~ 25 K at lattice restructuring occurs and the dimers 'pair-up' (we will avoid the word dimerise here[13]). Below the same temperature significant changes in the magnetic susceptibility are observed, cf. Fig 29, which suggest that a spin gap opens. Both effects are large suggesting that neither is a secondary effect induced by the bilinear coupling between the order parameters. This conclusion would imply that neither the simple valence bond crystal nor the simple spin-Peierls transition is a sufficient description. Panel (a) shows the growth of the Bragg peak associated with this distortion at low temperatures, while panel (b) shows the distorted crystal lattice. From (Tamura, Tajima and Kato, 2005).

formly, 3.82 Å. In the low temperature, spin gapped, phase there are two crystallographically distinct types of $[Pd(dmit)_2]_2$ dimer with the distances between molecules in the two different dimers now being 3.76 Å and 3.85 Å. Thus the $[Pd(dmit)_2]_2$ dimers have paired up.[13]

The ^{13}C NMR spectrum of P-1, Fig. 27 (Itou et al., 2008), broadens slightly below 25 K consistent with the increased number of environments for the nuclei. It is interesting to note how similar the NMR spectra for P-1 and Sb-1 are, in marked contrast to the very different behaviours of the low temperature bulk magnetic susceptibility.

There are two natural explanations for this pairing of dimers occurring concomitantly with the opening of the spin gap: a valence bond crystal or a spin Peierls distortion. Although these two possibilities are quite different

---

[13] If we treat the $[Pd(dmit)_2]_2$ dimers as 'sites' one would conventionally say that the sites have dimerised, but this can get a little confusing as we are already using the word 'dimer' as a synonym for site.
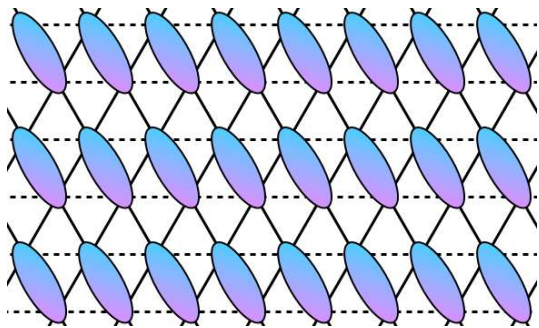
FIG. 31 Sketch of a valence bond crystal. Coloured elipses indicate singlet correlations between pairs of sights. Note that this state breaks both the rotational and translational symmetries of the underlying lattice, although a particular combination of the two remains unbroken. This should be contrasted with a valence bond liquid, that does not break these symmetries. On possible configuration of such a valence bond liquid is shown in Fig. 34.

theoretically, the experimental consequences of these differences are rather subtle. It is therefore helpful to examine each possibility briefly. The key issue is whether a spin-lattice coupling is *necessary* for formation of the spin gap. In other words, does the lattice distortion cause the gap or does the formation of spin singlets due to frustration cause the lattice distortion? Similar issues have been discussed for Heisenberg models relevant to CaV_4O_9 (Starykh et al., 1996) and Li_2VOSiO_4 (Becca and Mila, 2002).

The valence bond crystal (VBC) is a purely electronic phenomena. The VBC has been postulated as a possible ground state for various frustrated Heisenberg models (or related spin Hamiltonians) (Normand, 2009) including the model on the anisotropic triangular lattice that is relevant here (cf. Section VI.A). In the VBC state pairs of spins form singlets. These singlets are arranged periodically so as to break the translational symmetry of the underlying lattice (cf. Fig. 31). Note that the lattice degrees of freedom do not play any explicit role in stabilising the VBC state. However, in any real material the spin-phonon coupling will drive a lattice distortion that decreases the distance between the the sites within a singlet.

In contrast to the VBC, the spin Peierls distortion involves the lattice in an essential way. The spin Peierls distortion is usually conceived as a one-dimensional (1D) phenomena. The uniform one dimensional Heisenberg chain has gapless excitations. However, dimerisation of the lattice opens a gap in the excitation spectrum and lowers the ground state energy. This decrease in energy is greater than the cost in elastic energy associated with the lattice distortion and so if the spin-phonon coupling is non-zero there is a spontaneous dimerisation of the lattice (Cross and Fisher, 1979).

An appropriate order parameter for the VBC state is $\phi = \sum_i \sum_{n.n.} \langle \hat{\mathbf{S}}_i \cdot \hat{\mathbf{S}}_{i+1} - \hat{\mathbf{S}}_i \cdot \hat{\mathbf{S}}_{i-1} \rangle$ where $\mathbf{S}_i$ is the spin operator on site i and the sites $i+1$ and $i-1$ are nearest

neighbours of site i, but in opposite directions, the sum over n.n. indicates that this sum runs over all such pairs of nearest neighbours. An order parameter for the spin-Peierls transition is $\lambda = \sum_i \sum_{n.n.} \langle \hat{\mathbf{r}}_i \hat{\mathbf{r}}_{i+1} - \hat{\mathbf{r}}_i \hat{\mathbf{r}}_{i-1} \rangle$, where $\mathbf{r}_i$ is the position of site i. These order parameters couple at bilinear order in a Landau theory. Thus, the simplest Landau theory will be

$$\Delta F = \alpha \phi^2 + \beta \phi^4 + a \lambda^2 + b \lambda^4 + s \phi \lambda, \qquad (28)$$

where ΔF is the difference between the energies of the high and low symmetry phases, and α, β, a, b and s are the parameters of the theory. Thus, if one order parameter becomes finite it acts as a 'field' for the other implying that the second will take, at least, a small non-zero value. Therefore the observation that both λ and the spin gap become non-zero at ~ 25 K is not overly surprising. However, both the gap and the lattice distortion are large $\Delta/k_B T_c = 1.6 \pm 0.4$,[14] and $\lambda = 0.1$ Å, i.e., 2.4% of the average interdimer spacing This is comparable to or larger than the amplitudes of the distortions observed in many organic spin Peierls systems (Dumoulin et al., 1996; Foury-Leylekian et al., 2004; Moret et al., 1986; Visser et al., 1983). This may indicate that neither effect is simply parasitic on the other, in which case one would expect the parasitic order parameter to be small, and hence that the low temperature phase is stabilised cooperatively by both the lattice and electronic degrees of freedom and not properly characterised as either a spin-Peierls or a VBC state.

A key question is why this large spin gap is observed in P-1, but not in other $Et_nMe_{4-n}Pn[Pd(dmit)_2]_2$ salts. Tamura *et al.* proposed that an essential ingredient is the crystal structure of P-1. Most $Et_nMe_{4-n}Pn[Pd(dmit)_2]_2$ salts form the so-called β' structure, which displays a $C2/c$ space group (Kato, 2004). The unit cells of these materials each contain two organic layers, cf. Fig. 24. These planes are crystallographically equivalent and related by an axial glide along the c-axis (interlayer direction). This glide maps the $\mathbf{a} + \mathbf{b}$ direction, in which the dimers stack, in one plane onto the $\mathbf{a} - \mathbf{b}$ plane in the next. This results in what is known as a 'solid crossing' crystal structure, cf. Fig 24. However, P-1 forms crystals with $P2_1/m$ symmetry (Kato et al., 2006). This unit cell also contains two crystallographically equivalent organic layers, but now they are related by b-mirror and b-screw symmetries (in this structure the b-axis is the interlayer direction) rather than a glide plane. Thus, both layers stack in the same $(\mathbf{a} + \mathbf{c})$ direction. Other than the loss of the glide plane, the crystal structure of P-1 is remarkably close to the β' structure. Thus Tamura *et al.* argued that the solid crossing in the β' phase means that if there were Peierls distortion along the dimer stacking direction

----

[14] Note that this is close to the size of the gap predicted by weak coupling theories: the weak-coupling BCS gap in a superconductor or spin density wave is $\Delta/k_B T = 1.76$.
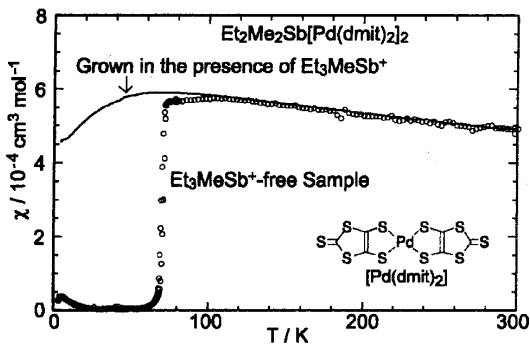
FIG. 32 The paramagnetic to non-magnetic transition in Sb-2. A rather similar transition is also seen in Cs-00. The microscopic nature of this transition is not clear. However, it is clear that small amounts of non-magnetic impurities in the cation layer completely suppress the non-magnetic phase. From (Tamura et al., 2006).

in a β'-$Et_nMe_{4-n}Pn[Pd(dmit)_2]_2$ salt this would lead to large internal strains within the crystal as the distortion would alternate along the $\mathbf{a} + \mathbf{b}$ and $\mathbf{a} - \mathbf{b}$ directions in the neighbouring planes. No detailed calculation has yet investigated whether this could be energetically unfavourable enough to prevent the opening of the spin gap. However, if there are many competing ground states it is possible that a small increase in the ground state energy of the spin Peierls/VBC phase, such as that caused by the internal strains invoked by Tamura et al., could be enough to suppress this phase in favour of some other.

The above proposal requires that the elastic coupling between layers be sufficiently large that it can change the ground state. An alternative hypothesis is that the intralayer anisotropy J'/J varies enough between the different materials that the ground state is different. In Section VI.A (see especially Figure 38) it will be seen that a significant spin gap only occurs for a narrow parameter range ($J'/J \simeq 0.7 - 0.9$) of the Heisenberg model on a triangular lattice.

E. Paramagnetic to non-magnetic transition in $Et_2Me_2Sb[Pd(dmit)_2]_2$ (Sb-2) and $Cs[Pd(dmit)_2]_2$ (Cs-00)

Rather similar phase transitions are seen at ~ 70 K in Sb-2 and ~ 65 K in $Cs[Pd(dmit)_2]_2$ (henceforth Cs-00). In Cs-00 the resistance shows a clear metal-insulator transition at this temperature (Underhill et al., 1991). This is accompanied by a sudden drop in the bulk magnetic susceptibility (Underhill et al., 1991), which is ~ 3.5 emu/mol, independent of temperature, for $T > 65$ K and zero to within experimental error for $T < 65$ K. In Sb-2 a non-metal to insulator transition corresponding to "steep rise of resistivity with decreasing temperature" was reported by Tamura et al. (although they did not show the data) concomitant with the sudden drop in the bulk magnetic susceptibility, shown in Fig. 32 (Tamura et al., 2006).

Nakao and Kato (Nakao and Kato, 2005) have shown that these phase transitions are both associated with changes in crystal structure. At room temperature both Sb-2 and Cs-00 form crystals with the $C2/c$ crystal structure of the β' phase, cf. section IV.D and Fig. 24. At temperatures just above the phase transition critical temperature, T_c, additional incommensurate satellite reflections are seen in both materials via x-ray scattering (Nakao and Kato, 2005). These become fully developed Bragg peaks below T_c, indicative of a change in the crystal structures. In their low temperature phases both P-2 and Cs-00 have crystals with $P2_1/c$ symmetry. The most dramatic change associated with this is a doubling of the unit cell along the (in plane) b-axis. This leads to there being two crystallographically distinct dimers, labelled X and Y in Fig. 33, per unit cell, which are arranged in alternating rows perpendicular to the stacking direction. The bond lengths within the X dimers are significantly different from those within the Y dimers (Nakao and Kato, 2005).

The optical conductivities of both Sb-2 (Tamura, Takenaka, Takagi, Sugai, Tajima and Kato, 2005) and Cs-00 (Underhill et al., 1991) are also very similar and show dramatic changes below T_c. Above T_c Cs-00 displays a Drude peak and a much stronger broad Lorentzian peak centred around ~ 1 eV. Below T_c the Drude peak is absent, consistent with the metal-insulator transition observed in the dc conductivity. No major qualitative changes are observed in the high energy feature between the spectrum recorded at 80 K and that at 50 K. However, by 20 K this peak has split into two distinct features. This is consistent with there being two distinct dimers in the crystals at these temperatures. Tamura et al. only reported the optical conductivity of Sb-2 for frequencies greater than 5×10^3 cm^{-1}, so it is not possible for us to discuss the Drude peak in this material, although one presumes it will be absent. However, otherwise the high frequency conductivity is remarkably similar to that of Cs-00. At 100 K (and higher temperatures) there is a single broad feature, which can be fit to a single Lorentzian. But, at 50 K and 4 K (the only temperatures below T_c for which the optical conductivity was reported) two narrower Lorentzian peaks were observed.

Both Underhill et al. and Tamura et al. interpret the peaks in the high energy optical conductivity in terms of intradimer transitions (from the HOMO-bonding level to the HOMO-antibonding level and the LUMO-bonding level to the LUMO-antibonding level, cf. Fig. 25). This neglects correlations, which we have seen are important in these materials. However, one can describe the transition as an intra-dimer charge transfer transition, which yields similar results (Merino and McKenzie, 2000c). Underhill et al. argued that the transition involved a charge density wave coupled to a secondary order parameter. Alternatively, Kato's group (Nakao and Kato, 2005; Tamura and Kato, 2004; Tamura, Takenaka, Takagi, Sugai, Tajima and Kato, 2005) have argued that the low-energy phase is charge ordered, with com-
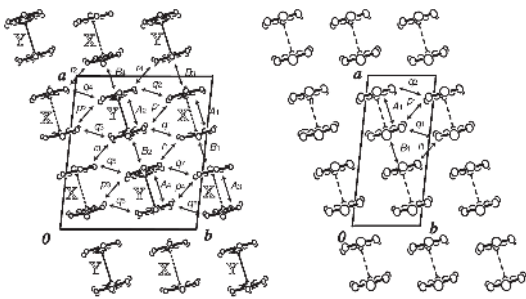
FIG. 33 Lattice reconstruction in the low temperature non-magnetic phase of Sb-2. At the temperature where the sudden drop in the bulk susceptibility is observed (Fig. 32) the crystal changes symmetry from $C2/c$ to $P2_1/c$. This results in the low temperature unit cell (left) being double the size of the high temperature unit cell (right). In the high temperature unit cell both dimers are crystallographically equivalent. But in the low temperature unit cell there are two crystallographically inequivalent dimers (labelled X and Y). The bond lengths are distinctly different in the X and Y dimers, suggesting significant charge disproportionation. From (Nakao and Kato, 2005).

plete charge disproportionation between $[Pd(dmit)_2]_2^0$ X dimers (cf. Fig. 33) and $[Pd(dmit)_2]_2^{+2}$ Y dimers. One way to test this hypothesis would be to study how the phonon frequencies shift at the transition. Nevertheless, no investigations of the interesting physics in Cs-00 and Pb-2 using quantum many-body theory have yet been reported.

It is also interesting to note that there is at least two differences between the phase transition in Sb-2 and Cs-00 (Nakao and Kato, 2005). Firstly, in Sb-2 the additional Bragg peaks grow sharply at the phase transition and hysteresis is observed, suggesting a first order transition. In contrast, in Cs-00 no hysteresis is observed and the additional Bragg peaks grow continuously suggesting a second order phase transition. Secondly, the paramagnetic to non-magnetic transition in Cs-00 is associated with a metal to insulator transition (Underhill et al., 1991), whereas Sb-2 is insulating in both phases (Tamura et al., 2006). These differences, and the possible connection between them, have not, yet, been explained.

1. Et$_3$MeSb impurities in Et$_2$Me$_2$Sb[Pd(dmit)$_2$]$_2$ (Sb-2)

The first crystals of Sb-2 to be grown were electrocrystallised out of a solution containing Et$_3$MeSb$^+$ ions as well as Et$_2$Me$_2$Sb$^+$ ions (Aonuma et al., 1997). These materials did *not* show the phase transition described above, cf. Fig. 32. Rather, the bulk magnetic susceptibility, χ, in these samples is remarkably similar to that of the spin liquid Sb-1. In both materials χ has a broad maximum around 50 K. And the exchange interaction extracted from fits to $\chi(T)$ is $J \simeq 240$ K for both Sb-1 (Itou et al., 2008) and Sb-2 (Tamura and Kato, 2002; Zheng, Singh, McKenzie and Coldea, 2005). Indeed, no magnetic

phase transition was observed in these Sb-2 salts grown in the presence of Et$_3$MeSb down to the lowest temperatures studied [4.3 K (Nakamura et al., 2001)], which is temperatures two orders of magnitude smaller than J.

Nakao and Kato (Nakao and Kato, 2005) have grown crystals of Sb-2 from electrolytes consisting of different ratios of Et$_2$Me$_2$Sb$^+$ to Et$_3$MeSb$^+$. For a 10:1 ratio the T_c of the nonmagnetic phase was supressed by ~ 5 K relative to samples grown electrolytes free of Et$_3$MeSb$^+$. However, a 2:1 ratio completely suppresses the phase transition.

Note that Et$_2$Me$_2$Sb and Et$_3$MeSb are isoelectronic, so Et$_3$MeSb should be a non-magnetic impurity. Nakao and Kato's results could suggest that the low temperature phase in Sb-2 is extremely sensitive to disorder. However, they also found that the inclusion of Et$_3$MeSb leads to a significant expansion of the unit cell, as one would reasonably expect given that an ethyl group is approximately twice as large as a methyl group. Compared to the Et$_3$MeSb free crystal, the unit cell is 0.11% larger in crystal grown from the 10:1 electrolyte and 0.25% larger in the crystal grown from the 2:1 electrolyte (Nakao and Kato, 2005). They also found that the unit cells of the earlier crystals were 0.35% larger than those of the Et$_3$MeSb free crystal suggesting that these first crystals contained significant concentrations of Et$_3$MeSb. However, no direct measurements of the concentrations of Et$_3$MeSb in an Sb-2 crystal have yet been reported.

It has not yet been possible to grow crystals of Sb-3 as Et$_3$MeSb[Pd(dmit)$_2$]$_3$ is preferentially formed (Nakao and Kato, 2005). Clearly, it would be very interesting to know how Sb-3 behaved at low temperatures.

Whether impurity physics or the lattice expansion is the dominant effect of Et$_3$MeSb impurities, it is clear that there is a rather subtle competition between the low temperature phase in Sb-2 and spin liquid behaviour. This is rather surprising as the critical temperature in Et$_3$MeSb free Sb-2 is quite large, 70 K.

It would be extremeley interesting to understand this physics. Not only for its intrinsic interest, but also in relation to the spin liquid state in κ-(BEDT-TTF)$_2$Cu$_2$-(CN)$_3$ and Sb-1.

F. Mott transition under hydrostatic pressure and uniaxial stress

Most studies of Et$_n$Me$_{4-n}$Pn[Pd(dmit)$_2$]$_2$ salts under hydrostatic pressure or uniaxial stress have been limited to measurements of the resistivity. Thus, there has been a mapping out of the phase diagram in terms of the insulating, metallic and superconducting states. In this section we review these phase diagrams and discuss the few pioneering studies to go beyond resistivity measurements.

P-0 and As-0 do not exhibit a metal-insulator transition under even the highest pressures studied (~ 17 kbar) (Kato, 2004). This suggests that they are further

into the Mott insulating regime than many other salts of $Pd(dmit)_2$, which are driven metallic under these pressures. This is rather counterintuitive as these materials have small anions (containing only methyl groups and no ethyl groups), which one would naïvely associate with a large 'chemical pressure'. However, a uniaxial strain along the b axis of > 7 kbar drives As-0 metallic (Kato et al., 2002). In contrast uniaxial strains along the a and c axes do not drive the system metallic (Kato et al., 2002), indeed moderate strains (~ 2 kbar) the these directions drive As-0 deeper into the insulating state. Kato et al. argued that that applying a stress along the a axis increases the dimerisation and so increases U, while strain along the b axis moves the dimer stacks closer together and thereby increases W. This argument make two implicit assumptions: (i) that a single orbital description of the electronic structure of these materials is appropriate; (ii) that they are in the limit $(U_m - V_m) \gg 2t_A$ and hence that $U \simeq 2t_A$, where U is the effective Coulomb repulsion between two electrons on the same $[Pd(dmit)_2]_2$ dimer, U_m is the Coulomb repulsion between two electrons on the same $Pd(dmit)_2$ molecule, V_m is the Coulomb repulsion between two electrons on different molecules within the $[Pd(dmit)_2]_2$ dimer, and t_A is the hopping integral between the two molecules in the dimer. It is not clear, at present, that either of these assumptions is valid.

Kato et al. (Kato et al., 1998) measured the resistivity of P-2 under pressure in order to map out its phase diagram (Fig. 22). They found that the ambient pressure insulating phase can be driven into a metallic state (which superconducts below ~ 4 K) by pressures above 9 kbar. However above ~ 12 kbar an insulating state is observed again. Yamaura et al. (Yamaura et al., 2004) found that the high pressure insulating phase is driven by a change in the crystal structure of P-2 from the usual β' phase with $C2/c$ symmetry and four crystallographically equivalent dimers per unit cell, cf. Fig. 24, to a phase with $P\bar{1}$, with two crystallographically *inequivalent* dimers per unit cell. As the two inequivalent dimers are in different layers this means that the layers are inequivalent. However, no detailed theory of why this causes an insulating state has yet been reported.

It is interesting to note that in the metallic state of P-2 the resistivity (Kato et al., 1998) does not have the non-monotonic temperature dependence associated with the 'bad-metal' regime, so typical of the κ-ET$_2X$ salts. Nor is there any sign of a bad metal in the metallic phases of Sb-0 [above ~ 9 kbar (Kato et al., 1996)]. There is a small peak around 50 K in As-0 under a uniaxial strain ~ 7 kbar along the b axis (Kato et al., 2002), but it appears rather less pronounced than one sees in κ-(BEDT-TTF)$_2X$.

Both Shimizu et al. (Shimizu et al., 2007a) and Itou et al. (Itou et al., 2009) have investigated the metal-VBC/spin Peierls insulator transition in P-1, which occurs under ~ 4 kbar of hydrostatic pressure (Fig. 21). Shimizu et al. found clear evidence that the transition is first order from sharp discontinuities and hysteresis in

the resistivity. They also found that a magnetic field destabilises the insulating phase in favour of the metallic phase. Whence, they were able to show, from a Clausius-Clapeyron analysis, that the magnetisation, $M = \chi B$, in the insulating phase is less than that in the metallic phase, consistent with the proposed non-magnetic VBC state. This is consistent with the results of Itou et al. from NMR spectroscopy. They did not observe any signs of magnetic ordering under pressure and concluded that the VBC/spin Peierls state persists over the entirety of the insulating region of the phase diagram. This means that the VBC/spin Peierls phase directly abuts the superconducting phase, raising interesting questions about the role of spin correlations in mediating this superconductivity. In particular this means that P-1, like the spin liquid compounds Sb-1 and κ-(BEDT-TTF)$_2$Cu$_2$-(CN)$_3$, provides an interesting contrast to the, more common, case of superconductivity near an antiferromagnetic Mott insulator (Itou et al., 2009; Powell and McKenzie, 2007). Nevertheless, both of these insulating states have large singlet fluctuations, and so, may actually have rather similar relationships to their nearby superconducting phases. In the low temperature insulating phase Itou et al. find that the spin lattice relaxation cannot be fit to a single exponential suggesting that the systems is rather inhomogeneous. Similar effects are also observed in the spin-Peierls phase of CuGeO$_3$ (Itoh et al., 1995; Kikuchi et al., 1994). Itou et al. propose that this is because unpaired spins strongly influence the relaxation rate. However, this would appear to be a rather subtle question, and it would be interesting to know if specific microscopic theories can account for this effect.

The resistivity in the metallic state of P-1 (Shimizu et al., 2007a) is remarkably similar to the resistivity in the metallic states of the κ-(BEDT-TTF)$_2X$ compounds (cf. section III.D), suggesting the same bad metal physics is likely to be at play. However, $1/T_1T$ is constant at low temperatures[15] (Itou et al., 2009) suggesting that there is no pseudogap in P-1.

One puzzling result is that in the metallic state of P-1 the in-plane (a-axis) resistivity is only described by the usual Fermi liquid form, $\rho_\parallel(T) = \rho_{\parallel 0} + AT^2$, at the highest pressures studied ~ 8 kbar (Shimizu et al., 2007a). At lower pressures and for temperatures in the range of about 2-20 K the data can be fit to the form $\rho_\parallel(T) = \rho_{\parallel 0} + AT^\epsilon$ with $2 < \epsilon < 3$. This may suggest that near the Mott transition the electrons scatter off an additional mode as well the direct electron-electron scattering that gives rise to the quadratic temperature dependence of the resistivity in Fermi liquid theory. For example, below their Debye temperature phonons give rise to an electron-phonon scattering rate $1/\tau_{e-ph} \propto T^5$

_____

[15] For $P = 4.8$ kbar below ~ 20 K, for $P = 6.0$ kbar below ~ 100 K, for $P = 8.0$ kbar below ~ 200 K. Data extends down to 2 K for all pressures.

(Ashcroft and Mermin, 1976). If both electron-electron and electron-phonon scattering gave rise to similar scattering rates this could appear as a intermediate power law over a limited temperature range, like those discussed above. On the other hand, it may be that one is fitting at temperatures above that at which simple Fermi liquid applies. At the lower pressures the resistivity increases rapidly above about 30 K, corresponding to the destruction of quasi-particles, which suggests that the T^2 behaviour may not last as high as 20 K even at 8 kbar.

Shimizu *et al.* also note that the value of A they observe is a factor of about fifty times smaller than that found in the metallic phase of the κ-(BEDT-TTF)$_2X$ salts. They suggest that this is because the electron-electron interactions are weaker. However, this seems unlikely as metallic P-1 is on the border of a Mott transition. A number of material specific factors are important in determining the value of A (Jacko et al., 2009), therefore these effects are probably responsible for the smaller value of A in P-1. Also, caution is in order since accurately measuring the intralayer resistivity in layered materials can be difficult because of uncertainties about the actual current path through the sample.

At low temperature P-1 superconducts. T_c is suppressed from its maximum value, ~ 5 K, near the Mott transition by the application of greater pressure (Shimizu et al., 2007a). However, very little is known about the superconducting state in any of the Pd(dmit)$_2$ salts. This is at least in part due to the fact that the superconducting state is only observed under pressure, making many experiments difficult. Most of the reports of superconductivity simply consist of resistivity measurements. However, (Ishii et al., 2007) did observe the Meissner effect in P-1, from which they were able to show that the superconductivity is a bulk effect.

V. NUCLEAR MAGNETIC RESONANCE AS A PROBE OF SPIN FLUCTUATIONS

The experimental data for $1/T_1T$ for most of the materials of interest show two regimes: $T > T_{\mathrm{NMR}}$ in which $1/T_1T$ increases as temperature decreases and $T < T_{\mathrm{NMR}}$ where $1/T_1T$ is rapidly suppressed as the temperature is further lowered. The spin fluctuation models that we discuss below predict that $1/T_1T$ is a monotonic decreasing function of temperature and so cannot describe the data below T_{NMR}. Hence our discussion is confined to the $T > T_{\mathrm{NMR}}$ regime, where the data for a wide range of materials can be fit to the form (Powell et al., 2009; Yusuf et al., 2007)

$$\frac{1}{T_1T} = \left(\frac{1}{T_1}\right)_\infty \frac{1}{(T + T_x)}. \qquad (29)$$

This temperature dependence is obtained for three different spin fluctuation models described below. This then raises the question of which model gives the physically appropriate picture.

1. Long-range antiferromagnetic spin fluctuation model

A phenomenological antiferromagnetic spin fluctuation model was introduced by Moriya in his self-consistent renormalization (SCR) theory (Moriya and Ueda, 2003) and was used by Millis, Monien and Pines (MMP) (Millis et al., 1990b) to describe NMR in the metallic state of the cuprates. Together with Yusuf we recently applied this model to describe NMR relaxation in the metallic phase of several superconducting organic charge transfer salts from the family, κ-(BEDT-TTF)$_2X$ (Powell et al., 2009; Yusuf et al., 2007).

The dynamic susceptibility is assumed to have the form

$$\chi(\mathbf{q}, \omega) = \frac{\chi_Q(T)}{1 + \xi(T)^2|\mathbf{q} - \mathbf{Q}|^2 - i\omega/\omega_{\mathrm{SF}}(T)} \qquad (30)$$

where $\chi_Q(T)$ is the static spin susceptibility at a non-zero wavevector $\mathbf{q} = \mathbf{Q}$, $\omega_{\mathrm{SF}}(T)$ is the characteristic spin fluctuation energy which represents damping in the system near $\mathbf{q} = \mathbf{Q}$, and $\xi(T)$ is the temperature dependent correlation length. When there are long-range antiferromagnetic fluctuations, (i.e., $\xi(T) \gg a$) the spin relaxation rate (15) is given by

$$\frac{1}{T_1T} = \frac{2\pi k_B |A|^2}{\gamma_e^2 \hbar^4 q_c^2} \frac{\chi_Q(T)}{\omega_{\mathrm{SF}}(T)\xi(T)^2} \qquad (31)$$

where $q_c \sim \pi/a$ is the cut-off wavevector when one integrates over the Brillouin zone. This expression can be simplified further by making the scaling assumptions $\chi_Q = \alpha(\xi/a)^{2-\eta}$ and $\omega_{\mathrm{SF}} = \alpha'(\xi/a)^{-z}$ where α and α' are temperature independent constants and a is the lattice spacing. Following MMP (Millis et al., 1990b), we assume a relaxational dynamics of the spin fluctuations, which are described by a dynamic critical exponent $z = 2$, and the mean-field value of the anomalous critical exponent $\eta = 0$. Within these approximations, the relaxation rate, can be written as

$$\frac{1}{T_1T} = \frac{k_B |A|^2}{\gamma_e^2 \hbar^3} \frac{\chi_Q(T)}{T_0} \qquad (32)$$

where the temperature scale, T_0 defined by Moriya and Ueda (Moriya and Ueda, 2003) is

$$T_0 \equiv \frac{\omega_{\mathrm{SF}}(q_c\xi(T))^2}{2\pi} = \frac{\alpha'}{2\pi}(q_c a)^2. \qquad (33)$$

In passing we note that this temperature scale is of particular physical significance because Moriya and Ueda (Moriya and Ueda, 2003) find that for a wide range of unconventional superconductors their transition temperature increases monotonically with T_0.

We further assume that the temperature dependence of the correlation length $\xi(T)$ is (Millis et al., 1990b; Moriya and Ueda, 2003)

$$\frac{\xi(T)}{\xi(T_x)} = \sqrt{\frac{2T_x}{(T + T_x)}}. \qquad (34)$$

For this form, T_x represents a natural temperature scale and $\xi(T)$ is only weakly temperature dependent for $T \ll T_x$. The static susceptibility associated with the antiferromagnetic fluctuations then has the temperature dependence

$$\chi_Q(T) = \chi_Q(T_x)\frac{2T_x}{T + T_x}. \tag{35}$$

Then the relaxation rate has the temperature dependence (29) with

$$\left(\frac{1}{T_1}\right)_\infty = \frac{2k_B|A|^2}{\gamma_e^2\hbar^3}\chi_Q(T_x)\frac{T_x}{T_0}. \tag{36}$$

2. Quantum critical spin fluctuation model

Sachdev has interpreted the observed temperature dependence of $1/T_1$ in the cuprates $La_{2-x}Sr_xCuO_4$ in terms of quantum criticality (see Figure 4 of (Sachdev, 2000)). He notes that theoretical calculations for non-linear sigma models associated with the Heisenberg model on the square lattice that in the quantum critical regime $1/T_1$ becomes independent of temperature. Making this identification requires that there is a quantum phase transition as a function of the doping near $x = 0.075$. A connection can be made to the MMP model if we assume that T_x defines the temperature scale above which the crossover to quantum critical behavior occurs (cf. Figure 3).

3. Local spin fluctuation model

The local spin fluctuation model presents a physically different picture for the high temperature relaxation rate because the spin fluctuations are local, in contrast, to the long-range fluctuations in the two models above. It can be shown that, in the high-temperature limit, the uniform magnetic susceptibility of a spin-1/2 Heisenberg antiferromagnetic system is given by a Curie-Weiss expression. For the triangular lattice this form holds down to much lower temperatures than for the square lattice because the frustration increases the domain of validity of the single site approximation associated with the Curie-Weiss theory (Merino et al., 2006; Zheng, Singh, McKenzie and Coldea, 2005) (cf. Figure 4). In the same high temperature limit the NMR relaxation rate is given by (Gulley et al., 1970; Moriya, 1956; Singh and Gelfand, 1990)

$$\left(\frac{1}{T_1}\right)_\infty = \frac{\sqrt{\pi}|A|^2}{z\hbar J} \tag{37}$$

where A is the hyperfine interaction and z is the co-ordination number of the lattice. The derivation of this result involves a short time expansion of the electronic spin correlation function, which is assumed to decay in a Gaussian manner. For Sb-1 it was shown that the magnitude of $1/T_1$ is consistent with the above expression with independent estimates of A (from the scale of the susceptibility and the Knight shift) and J (from the temperature dependence and magnitude of the susceptibility) (Itou et al., 2008).

VI. QUANTUM MANY-BODY LATTICE HAMILTONIANS

A. Heisenberg model for the Mott insulating phase

In Section III.A we argued that from a quantum chemical perspective that the simplest possible effective Hamiltonian for the organic charge transfer salts is a Hubbard model on the anisotropic triangular lattice at half filling. This means that in the Mott insulating phase the spin degrees of freedom can be described by a Heisenberg model on an anisotropic triangular lattice (McKenzie, 1998). This lattice can also be viewed as a square lattice with interactions along one diagonal. The Hamiltonian is

$$\hat{\mathcal{H}} = J\sum_{\langle ij \rangle}\hat{\mathbf{S}}_i \cdot \hat{\mathbf{S}}_j + J'\sum_{\langle\langle ik \rangle\rangle}\hat{\mathbf{S}}_i \cdot \hat{\mathbf{S}}_k \tag{38}$$

where J describes the exchange interaction in the vertical and horizontal directions and J' is the interaction along the diagonal (compare equation (3)). This model interpolates between the square lattice ($J' = 0$), the isotropic triangular lattice ($J' = J$), and decoupled chains ($J = 0$). We will also consider the above Hamiltonian with an additional ring-exchange interaction $J_\square$ for every square plaquette and given by (7).

Extensive studies of the above Hamiltonian have been made of the case $J_\square = 0$ and for $J' = J, J_\square \neq 0$, which we review below. We are unaware of any studies of the full two-dimensional model with $J' \neq J, J_\square \neq 0$. Below we do briefly discuss some very recent studies of related two- and four-rung ladder models for these parameters.

Below we discuss studies giving a ground state with no magnetic order when $J'/J \simeq 0.7 - 0.9, J_\square = 0$, and $J' = J, J_\square > 0.05J$. In both cases there is an energy gap to the lowest lying triplet state. In the former case the state is a valence bond crystal with dimer order on horizontal (or vertical) bonds. In the second case there is believed to be no dimer order. The observed ground state of P-1 is consistent with the valence bond crystal state. It is not possible to clearly identify the ground state of κ-$(ET)_2Cu_2(CN)_3$ with either of these two non-magnetic states. We discuss this in Section VI.A.3, below.

1. RVB states

A recent field-theoretic perspective on RVB states and their excitations has been given (Sachdev, 2009a). Becca et al. have given a nice review of variational RVB wave
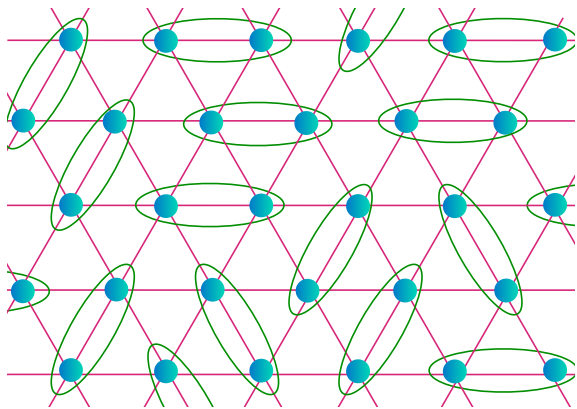
FIG. 34 One possible dimer covering of the triangular lattice. Each oval represents a singlet pairing of the spins on the two sites enclosed within the oval. Short range RVB states consist of superpositions of such states. (Figure provided by S. Sachdev).

functions for frustrated Heisenberg spin models (Becca et al., 2009). They show that these wave functions become close to the true ground state wave function as the frustration increases. Figure 35 shows this for the case of the frustrated Heisenberg model (the $J_1 - J_2$ model) on the square lattice. The upper panel shows the energy difference between a projected BCS wave function and the exact ground state for a lattice of 6×6 sites. The lower panel shows the magnitude of the overlap of these two states. A number of different numerical techniques find that there is Neel order for $0 \leq J_2/J_1 \leq 0.5$ and that there is no long-range magnetic order for $0.5 \leq J_2/J_1 \leq 0.7$ (Becca et al., 2009).

There are two main classes of RVB wave functions (Becca et al., 2009). States in the first class are sometimes called short-range RVB states. They are similar to the RVB states introduced by Pauling into quantum chemistry (Anderson, 2008; Shaik and Hiberty, 2008). The simplest possible state consists of an equal superposition of all possible dimer coverings of the lattice, $\{c\}$, where each dimer corresponds to a local spin singlet,

$$|\Psi_{SRVB}\rangle = \sum_c |\Psi_c\rangle. \tag{39}$$

Figure 34 shows one possible dimer covering of the triangular lattice. Generalisations of the wavefunction (39) have unequal coefficients for the different dimer coverings and also longer range singlet pairings. It is non-trivial but possible to show that certain parametrisations of this class become equivalent to the second class below (Becca et al., 2009).

The second class of RVB wave functions consist of Gutzwiller projected BCS states similar to that first introduced by Anderson (Anderson, 1987)

$$|\Psi_{pBCS}\rangle = \Pi_i(1 - \alpha n_{i\uparrow}n_{i\downarrow})|BCS\rangle \tag{40}$$

where $|BCS\rangle$ is a BCS state with a variational pairing function and α is a Gutzwiller variational parameter ($0 \leq$
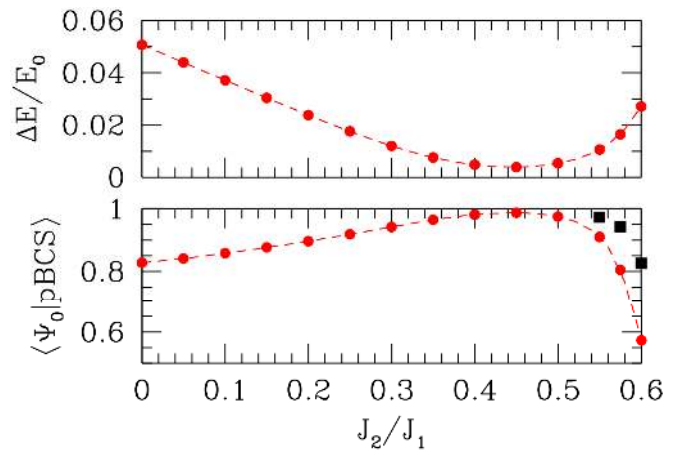

FIG. 35 Frustration stabilises RVB and spin liquid states (Becca et al., 2009). The upper panel shows the energy difference between a projected BCS wave function and the exact ground state for a lattice of 6×6 sites for the $J_1 - J_2$ model on a square lattice. (J_1 and J_2 are the nearest and next-nearest neighbour interactions, respectively). The lower panel shows the magnitude of the overlap of these two states.

$\alpha \leq 1$) which determines the number of doubly occupied sites. $\alpha = 1$ when no doubly occupied states are allowed.

2. Isotropic triangular lattice

The clear consensus from a wide range of studies is that the true ground state for $J' = J$, $J_\square = 0$ is not a spin liquid but a Neel antiferromagnet with 120 degree order. Table III in (Zheng et al., 2006) gives a summary of the results and relevant references from studies using a wide range of numerical methods and approximation schemes. Thus, the conjecture of Anderson and Fazekas (Anderson, 1973; Fazekas and Anderson, 1974) that this model has a spin liquid ground state turns out to be incorrect. Nevertheless, variational short-range RVB states have been found to be close to the exact ground state for small lattices (Sindzingre et al., 1994). Specifically, they give comparable short-range spin correlations. For example, for a 12-site lattice the nearest, next-nearest neighbour, and next-next-nearest neighbour spin correlations for the exact ground state are $\langle \vec{S}_r \cdot \vec{S}_0 \rangle = $ -0.2034, 0.1930, and -0.0511, respectively. For comparison an equal superposition RVB state gives values of -0.2032, 0.2065, and -0.075. Furthermore, we will see below that small perturbations of the Hamiltonian, such as spatial anisotropy or ring exchange terms can lead to a ground state with no magnetic order.

3. Role of spatial anisotropy ($J' \neq J$)

It turns out that spatial anisotropy can destroy the magnetic order present when $J' = J$. The model Hamil-

tonian (38) has been studied by a wide range of techniques: linear spin-wave theory (Merino et al., 1999; Trumper, 1999), series expansions (Fjærestad et al., 2007; Zheng et al., 1999), large-N expansion of an sp(N) Schwinger boson theory (Chung et al., 2001), mean-field RVB theory (Hayashi and Ogata, 2007), variational Monte Carlo of Gutzwiller projected BCS states (Heidarian et al., 2009; Yunoki and Sorella, 2006), pseudo-fermion functional renormalistion group (Reuther and Thomale, 2010) and the density matrix renormalisation group (Weng et al., 2006). The weakly coupled chain regime $J' \gg J$ has been studied by perturbing about the exact ground state single chains (Kohno et al., 2007). Most studies agree that for $0 \leq J'/J \lesssim 0.5$ the Neel state with ordering wavevector (π, π) is stable and that a spiral ordered state is stable for $J' \sim J$. However, whether the ground state is a spin liquid in the regimes $J' \gg J$ and $J'/J \sim 0.6 - 0.9$ is controversial. The phase diagram of the model deduced from series expansions (Zheng et al., 1999) is shown in Figure 36. Comparing the solid and dashed curves in Figure 36 shows that quantum fluctuations tend to make the excitation spectrum more commensurate than the order found in the classical Hamiltonian. In particular, deviations of the wavevector $\vec{Q} = (q, q)$ from the commensurate values $q = \pi, 2\pi/3, \pi/2$, are reduced. The reduction of deviations from commensurability by quantum fluctuations is also found in renormalisation group analysis of the corresponding non-linear sigma models (Apel et al., 1992). There, it is found that quantum fluctuations drive the system towards a fixed point with $O(4)$ symmetry, and at which the spin wave anisotropy is reduced. Hence, quantum fluctuations will reduce the incommensurability. This is an example of "order through disorder" as the "disorder" due to the quantum fluctuations stabilises the "order" associated with commensurate spin correlations (Chandra et al., 1990; Chubukov and Jolicoeur, 1992).

Figure 37 shows the magnitude of the magnetic moment associated with the magnetic order, calculated from series expansions. For the range $0.65 < J'/J < 0.95$ the most stable state has dimer order, a valence bond crystal with bonds along either the horizontal or vertical direction (i.e., associated with the J interaction). There is an energy gap to the lowest triplet excited state, and its magnitude as a function of J'/J is shown in Figure 38.

The ground state of the dmit material P-1 is reminiscent of this valence bond crystal state. The pattern of bond ordering is consistent with that deduced from x-ray scattering (see Figure 30) and the measured energy gap [$40 \pm 10K \simeq (0.15 \pm 0.05)J$ (see Figure 29)] is comparable to that shown in Figure 38. This identification would require that the hopping integrals in the corresponding Hubbard model have $t'/t \simeq 0.8 - 0.95$, which is significantly smaller than the value of 1.1 (Shimizu et al., 2007b) estimated from Hückel calculations. However, DFT calculations for the κ-(ET)$_2$X family (Kandpal et al., 2009; Nakamura et al., 2009) find that the Hückel method tends to over-estimate this ratio. This
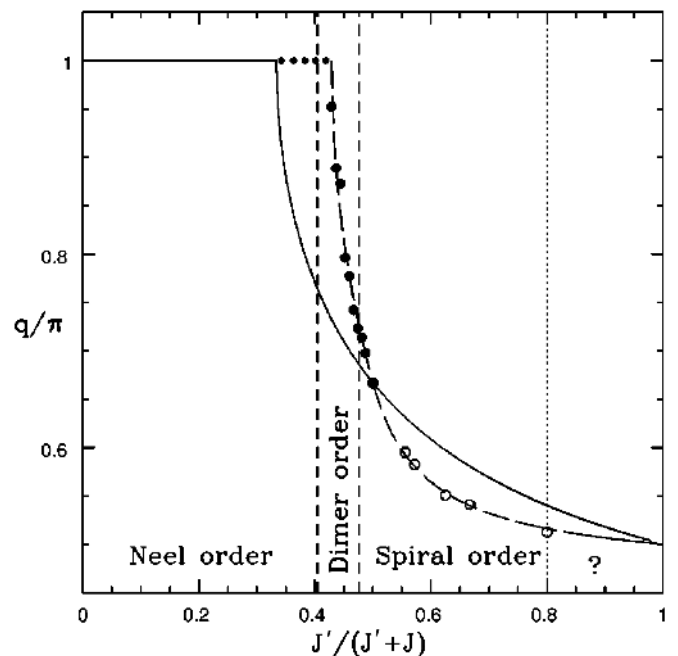

FIG. 36 Phase diagram and incommensurability of spin correlations for the Heisenberg model on the anisotropic triangular lattice (Zheng et al., 1999). The solid curve shows the classical ordering wavevector (q, q) as a function of the diagonal interaction $J'/(J' + J)$. The circles show the value of q which defines the location of the minimum energy gap to a triplet excited state. These are calculated from series expansions relative to different reference states (Zheng et al., 1999). Incommensurate (spiral) antiferromagnetic order occurs for $J' > 0.95J$. The antiferromagnetic order is unstable for the range $0.6 < J'/J < 0.95$. The series cannot determine the ground state for weakly coupled chains with $J'/J > 4$. Modified from (Zheng et al., 1999). [Copyright (1999) by the American Physical Society.]

underscores the need for DFT calculations on the dmit materials.

It is not clear that the possible spin liquid state in κ-(ET)$_2$Cu$_2$(CN)$_3$ can be identified with this valence bond crystal (VBC) state. The NMR, specific heat, and thermal conductivity show no evidence of a spin gap at temperatures less than 1 K which is two orders of magnitude smaller than J. The only possibility consistent with the existence of the VBC phase would be that this material lies close to one of the quantum critical points associated with the transition between the VBC and the magnetically ordered states.

4. Ring exchange

As the band-width controlled Mott metal-insulator transition is approached from the metallic side the charge fluctuations increase and the average double occupancy increases (see, for example, Figure 4 in (Ohashi et al., 2008)). Hence, for a Mott insulating state close to the
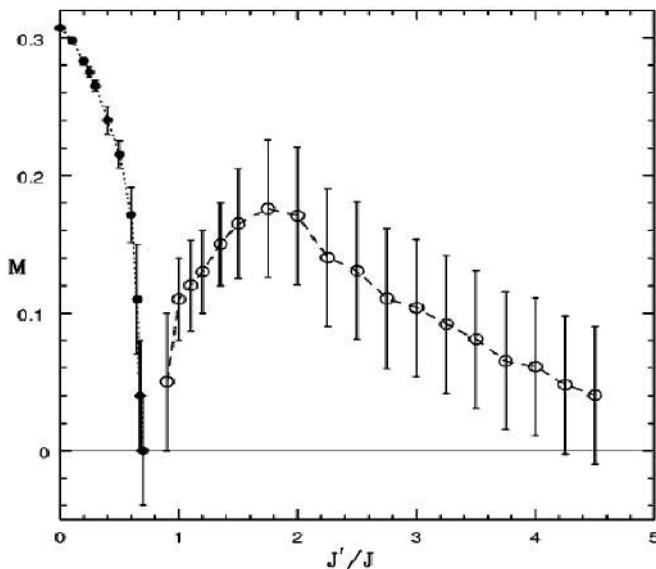
FIG. 37 Magnitude of the magnetic order parameter (magnetic moment) as a function of the diagonal interaction J'/J. [In our notation $J_1/J_2 = J'/J$.] This is calculated from a series expansion (Zheng et al., 1999). For $J' < 0.6J$ the frustration associated with J' reduces the magnitude of the Neel ordering. Incommensurate (spiral) antiferromagnetic order occurs for $J' > 0.95J$. The antiferromagnetic order is unstable for the range $0.6 < J'/J < 0.95$. This behaviour is also qualitatively reproduced by linear spin-wave theory (Merino et al., 1999; Trumper, 1999). This shows just how sensitive the ground state is to the spatial anisotropy. This is the parameter regime relevant to many of the compounds discussed in this review. [Copyright (1999) by the American Physical Society.]
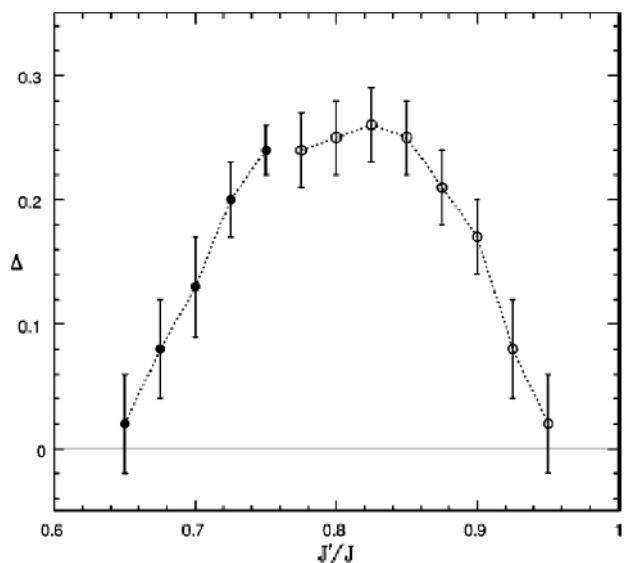

FIG. 38 Dependence of the triplet energy gap on the diagonal coupling in the valence bond solid phase (with dimers in either the horizontal or vertical direction relative to the "square" lattice, i.e., dimers are associated with the J interaction), calculated in a dimer series expansion (Zheng et al., 1999). For $0.65 < J'/J < 0.75$ the gap occurs at the wavevector $(0, \pi)$, whereas for larger J'/J it is at an incommensurate wavevector. Together with Figure 37 this suggests that the model undergoes quantum phase transitions at $J'/J \simeq 0.65$ and 0.95. Modified from (Zheng et al., 1999). [Copyright (1999) by the American Physical Society.]

metallic phase in the Hamiltonian one needs to include the ring exchange terms which arise from the charge fluctuations. A strong coupling expansion to fourth order in t/U for the Hubbard model gives $J_\square/J = 5(t/U)^2$ (Delannoy et al., 2005; MacDonald et al., 1990; Yang et al., 2010).

Even well into the Mott insulating phase the ring exchange terms can have both qualitative and quantitative effects. For example, in La_2CuO_4 ring exchange interactions modify the dispersion relation of triplet spin excitations near the zone boundary (Coldea et al., 2001).

The Heisenberg model on the isotropic triangular lattice (i.e. $J' = J$) with ring exchange has been studied using exact diagonalisation (LiMing et al., 2000), a Gutzwiller projected Fermi sea of spinons (Motrunich, 2005), and variational Monte Carlo for projected BCS states (Grover et al., 2010). Exact diagonalisation calculations on lattices of up to 36 sites suggest these ring exchange terms can lead to a spin liquid ground state for $J_\square > 0.05J$ (LiMing et al., 2000; Misguich and L'huillier, 2005). Furthermore, in this state there are a large number of singlet excitations below the lowest energy triplet excited state (LiMing et al., 2000). The presence of a spin gap for triplet excitations (estimated to be about

$0.07J$ for $J_\square \simeq 0.1J$) implies that the NMR relaxation rates would approach zero exponentially with decreasing temperature.

It has also been proposed that the ground state of κ-$(BEDT\text{-}TTF)_2Cu_2(CN)_3$ is a spin liquid with a spinon Fermi surface (Lee and Lee, 2005; Motrunich, 2005), with spinons that are coupled to gauge field fluctuations. This is discussed further in Section VII.C below.

Variational Monte Carlo calculations were recently performed for Gutzwiller-projected BCS states where different possible types of pairing were considered (Grover et al., 2010). A mean-field theory on these states for the Heisenberg model without ring exchange gives a BCS state with broken time-reversal symmetry (known as the chiral spin liquid). The form of the fermion pairing function is $d_{x^2-y^2} + id_{xy}$ which belongs to the E representation of the C_{6v} point group symmetry of the lattice. We now summarise some of the main results of the variational Monte Carlo study (Grover et al., 2010). (i) In contrast to mean-field theory, it is found that for ring exchange strengths in a small range the pairing function is purely $d_{x^2-y^2}$. (ii) The authors suggest that under increasing pressure (increasing t/U) the Mott insulator will be destroyed leading to a superconducting state with the same $d_{x^2-y^2}$ pairing. This is qualitatively different to what one gets with a mean-field RVB theory of the model without

the ring exchange (Powell and McKenzie, 2007). (iii) This ground state cannot explain why the observed low temperature specific heat of κ-(ET)$_2$Cu$_2$(CN)$_3$ is weakly dependent on magnetic field. (iv) The "Amperean pairing" theory proposed earlier (Lee et al., 2007b) does not have this problem, but has difficulty describing the superconducting state which develops under pressure.

Several important issues are not addressed in this paper. First, in the range $J_\square/J \simeq 0.05-0.1$ exact diagonalisation calculations on small lattices give a different spin liquid ground state, one with an energy gap to triplet excitations, and many singlet excitations inside the gap (Yang et al., 2010). Second, the NMR relaxation rate $1/T_1$ for κ-(ET)$_2$Cu$_2$(CN)$_3$ is observed to have a power law temperature dependence consistent with gapless excitations. Third, the estimate of the spinon scattering rate due to impurities ($\sim$ 1.5 K) can be compared to estimates of the scattering rate associated with charge transport in the metallic phase of similar organic charge transfer salts. Table I in (Powell and McKenzie, 2004b) gives estimates of this scattering rate which are an order of magnitude smaller than the proposed spinon scattering rate (Grover et al., 2010). However, given that the quasi-particles being scattered are different we should not necessarily expect them to have the same scattering rate, but a complete theory should describe this difference.

For a Hubbard model the requirement $J_\square/J > 0.05$ needed for a spin liquid ground state corresponds to $U < 10|t|$. A crucial question is then how large is the critical value $U_c/|t|$ at which the metal-insulator transition occurs? In order for a Heisenberg model to be relevant the system must still be in the insulating phase for $U < 10|t|$. Below, we see that most estimates of $U_c/|t|$ lie in the range 5-8, depending on the numerical method used. Spatial anisotropy (i.e., $t' < t$) reduces the critical value. A comparison (Merino et al., 2008) of the measured optical conductivity for the alloy κ-(BEDT-TTF)$_2$Cu[N(CN)$_2$]Br$_x$Cl$_{1-x}$ with $x = 0.73$ (which lies just on the metallic side of the Mott transition) with that calculated from dynamical mean-field field theory (DMFT) found good agreement for $U/|t| \simeq 10$ (see, also, the discussion in section III.C.2). Hence, this is roughly consistent with the ring exchange term being sufficiently large to produce a spin liquid state.

Motrunich found a low variational energy for a projected spinon Fermi sea state (Motrunich, 2005). He combined this with a slave particle-gauge theory analysis, to argue that the spin liquid has spin correlations that are singular along surfaces in momentum space, i.e., "Bose surfaces." A density matrix renormalisation group (DMRG) study of a frustrated ladder model (corresponding to two coupled chains in the anisotropic triangular lattice model) with ring exchange has produced a rich phase diagram (Sheng et al., 2009). In particular, when $J \sim J'$ a ring exchange interaction $J_4 \sim 0.2J$ can lead to a "spin-Bose metal" phase. This is a spin liquid state with gapless excitations at specific wave vectors. This underscores the need for a study of the full Heisenberg model with both $J' \neq J$ and $J_\square \neq 0$. A recent study was made of the model on a four rung ladder with $0 \leq J'/J \leq 1$ and $0 \leq J_\perp \leq J$ using DMRG and variational Monte Carlo of a projected Fermi sea (Block et al., 2010). The phase diagram contained rung, VBC, and spin-Bose metal phases. The latter has three gapless modes and power law spin correlations at incommensurate wavevectors. Spatial anisotropy increased the stability of the VBC state.

A recent definitive study (Yang et al., 2010) of the Hubbard model on the isotropic triangular lattice used a high powered perturbative continuous unitary transformation to derive an effective spin Hamiltonian in the Mott insulating phase, up to twelfth order in t/U. They find that as U/t decreases, at $U/|t| \simeq 10$, there is a first-order phase transition from the 120 degree Neel ordered phase to a spin liquid phase (no net magnetic moment) and large numbers of singlet excitations below the lowest lying triplet excitation. This spin liquid state is identified with the "spin Bose metal" proposed by Motrunich (Motrunich, 2005). The first-order transition from the magnetically ordered state to the spin liquid is also associated with a small jump in the double site occupancy. It is also found that the transition to the metallic state does not occur until U/t decreases to about $6-8$. Hence, there is a significant range of U/t for which the Mott insulator is a spin liquid.

5. Dzyaloshinski-Moriya interaction

In crystals which lack inversion symmetry relativistic effects lead to an additional interaction between spins which breaks spin-rotational invariance and is known as the Dzyaloshinski-Moriya interaction. The DM interaction has been characterised in the insulating phase of κ-(BEDT-TTF)$_2$Cu[N(CN)$_2$]Cl and has a magnitude of about $D \simeq 5$ K (Smith et al., 2004). Even though it is small compared to the nearest neighbour exchange the DM interaction can have a significant effect on frustrated systems. For example, for the kagome lattice it can induce a quantum phase transition from a spin liquid state to an ordered state for $D > 0.1J$ (Cépas et al., 2008). For the anisotropic triangular lattice, even when $D \sim J/20$ the DM interaction induces energy changes in the spectrum of energies as large as $J/3$, including new energy gaps (Fjærestad et al., 2007). A detailed analysis of the effect of the DM interaction in the weakly coupled chain limit has also been given (Starykh et al., 2010).

6. The effect of disorder

Gregor and Motrunich (Gregor and Motrunich, 2009) studied the effects of nonmagnetic impurities in the Heisenberg model on the triangular lattice with the goal of understanding the large broadening of ^{13}C NMR lines in κ-(BEDT-TTF)$_2$Cu$_2$(CN)$_3$. They used a high-

temperature series expansion to calculate the local susceptibility near a nonmagnetic impurity, for temperatures down to $J/3$. At low temperatures they assumed a gapless spin liquid described by a Gutzwiller projected spinon Fermi sea. In both temperature regimes, they found that the value of the local susceptibility decays to the uniform value within a few lattice spacings. Hence a low density of impurities cannot explain the observed line broadening. This analysis needs to be combined with independent estimates of the strength of disorder in these materials (Scriven and Powell, 2009a).

B. Hubbard model on the anisotropic triangular lattice

The Hamiltonian (9) depends on three parameters: t, t', and U. Estimates of values for these parameters from quantum chemistry and electronic structure calculations were discussed in Section III.A.1. The key open questions concerning the model are whether it has superconducting and spin liquid ground states for physically reasonable parameter values.

1. Phase diagram

We have already discussed the phase diagram at nonzero temperature in section III.C.4. The zero temperature phase diagram of the Hubbard model on the anisotropic triangular lattice has also been studied by a wide range of techniques including: exact diagonalization (Clay et al., 2008; Koretsune et al., 2007), slave bosons/RVB mean-field theory (Gan et al., 2005; Powell and McKenzie, 2005, 2007), large-N expansion of a sp(N) theory (Chung et al., 2001), weak-coupling renormalisation group (Tsai and Marston, 2001), variational quantum Monte Carlo on Gutzwiller projected BCS states (Liu et al., 2005; Tocchio et al., 2009; Watanabe et al., 2008) cluster and cellular dynamical mean-field theory (Kyung, 2007; Kyung and Tremblay, 2006; Liebsch et al., 2009; Ohashi et al., 2008; Parcollet et al., 2004), slave rotor representation (Lee and Lee, 2005; Lee et al., 2007b), path-integral renormalisation group (Morita et al., 2002), cluster variational approach (Sahebsara and Sénéchal, 2008), and dual fermions (Lee et al., 2008).

There is little consensus on the phase diagram in the physically important region near the Mott transition, and particularly where there are several competing magnetic phases (i.e., $0.7t < t' < t$). This lack of consensus arises for two reasons: one mundane and the other profound. The first is that not all approaches allow for all possible states. The second is that there are very small differences in energy between the competing phases. Different computational methods and approximation schemes will get different values for these small differences in energy and so produce different phase diagrams.

The fact that in the organic charge transfer salts there is a first order phase transition between superconduct-
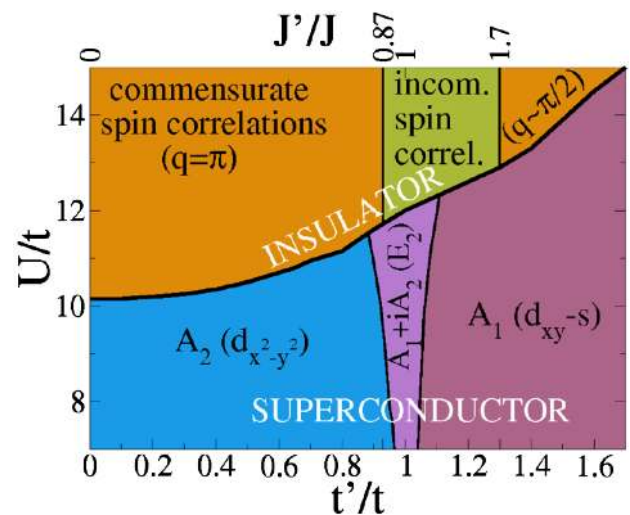

FIG. 39 Phase diagram of the Hubbard model on the anisotropic triangular lattice at half filling and zero temperature calculated from an RVB variational wave function (Powell and McKenzie, 2007). Similar results are found for other strong coupling approaches. The $t'/t = 0$, $t'/t = 1$ and $t'/t \to \infty$ correspond to the square lattice, the isotropic triangular lattice and decoupled chains, respectively. For large $U/(t + t')$ the ground state is a Mott insulator. The type of magnetic ordering varies with $J'/J = (t'/t)^2$. Near the metal-insulator phase boundary superconductivity occurs and the symmetry of the superconducting order parameter is correlated with the dominant spin correlations in the neighbouring Mott insulating phase. [Copyright (2007) by the American Physical Society.]

ing and Mott insulating states shows that these two very different states can have identical energy. This is actually why these materials are so "tuneable" (i.e. one can induce transitions between different phases with "small" changes in the pressure, temperature or magnetic field, and by chemical substitution).

2. Ladder models

Ladder models provide a means to investigate in a controlled manner (e.g., via DMRG, bosonisation, and weak-coupling renormalisation group) physics which it is hoped may be related to what occurs in the two-dimensional limit.

One can characterise different ground states on ladders by n and m, the number of gapless charge and spin modes, respectively. This leads to the notation $CnSm$ and the following identifications. $C2S2$ is the ladder analogue of Fermi liquid metal, $C1S0$ is a superconductor, $C1S2$ is a spin Bose metal, $C0S0$ is a spin gapped Mott insulator, and $C0S2$ is a spin liquid Mott insulator. At half filling a two-leg ladder without frustration has a $C0S0$ ground state, which upon doping changes to $C1S0$ consistent with Anderson's RVB ideas (Balents

and Fisher, 1996).

A weak-coupling renormalisation group analysis has been performed on the zig-zag ladder with longer-range Coulomb repulsion (Lai and Motrunich, 2010). The longer-range interaction stabilises the $C2S2$ phase and leads to a subtle competition between all the different phases listed above. Indeed it is interesting to compare Figure 8 in (Lai and Motrunich, 2010) with our Figure 39.

VII. EMERGENCE OF GAUGE FIELDS AND FRACTIONALISED QUASI-PARTICLES

For a given phase the key question (or assumption) is: what are the quantum numbers of the quasi-particles describing the lowest lying excited states? The answer determines the nature and symmetries of an effective field theory for the low-energy physics. Field theories for magnons (bosonic triplets), spinons (spin-1/2 bosonic or fermionic excitations), and visons (bosonic singlets) have all been considered in various different theories of the organic charge transfer salts.

In a "round table discussion" about the theory of the cuprate superconductors (Zaanen, 2006) Patrick Lee stated that the genuinely new idea that has been developed is "the notion of emergence of gauge fields and fractionalized particles as low-energy phenomena in systems that did not contain them in the starting model." He suggested that this idea is of comparable importance in condensed matter theory to that of Goldstone bosons associated with spontaneously broken symmetry.

Gauge fields emerge when the electron or spin operators are represented in terms of Schwinger bosons (Auerbach, 1994), slave fermions, slave bosons (Lee et al., 2006), or slave rotors (Florens and Georges, 2004). These alternative representations introduce an over-complete description of the problem which requires a constraint so that the canonical commutation (or anti-commutation) relations are preserved.

A nice discussion (for the specific case of Schwinger bosons) is contained in a review (Sachdev, 2008), which we now follow closely. It shows clearly how the effect of gauge field fluctuations leads to qualitative differences in the quantum disordering of commensurate and incommensurate magnetic states. In particular, deconfinement of bosonic spinons is possible in the latter but not the former.

We illustrate this now by showing how, if the spin-1/2 operators are represented by Schwinger bosons (Auerbach, 1994), there is a redundancy because the phase of each boson field can be shifted by an arbitrary amount without affecting the spin degree of freedom. The spin $1/2$ field $\mathbf{N}$ can be written in terms of a $S = 1/2$ complex spinor boson field z_α, where $\alpha = \uparrow, \downarrow$ by

$$\mathbf{N} = z_\alpha^* \boldsymbol{\sigma}_{\alpha\beta} z_\beta \tag{41}$$

where $\boldsymbol{\sigma}$ are the 2×2 Pauli matrices. The spin commu-

tation relations are preserved provided that[16]

$$\sum_\alpha z_\alpha^* z_\alpha = 1. \tag{42}$$

As an aside, we note that there is no problem having spin-1/2 bosons. The spin statistics theorem in relativistic quantum field theory (which requires bosons to have integer spin) does not apply here because in this field theory there is no Lorentz invariance. Also, in what follows we are always considering $\mathbf{N}$ to be a slowly varying field which defines the spin at site j relative to the commensurate wave vector for Neel ordering $\mathbf{Q} = (\pi, \pi)$,

$$\langle \mathbf{S}_j \rangle = \mathbf{N} \cos(\mathbf{Q} \cdot \mathbf{r}_j). \tag{43}$$

where $\mathbf{r}_j$ is the position of site j.

But, note that the representation (41) of $\mathbf{N}$ in terms of z_α has some redundancy. In particular, a change in the phase of both fields z_α by the same space and time dependent field $\theta(x, \tau)$

$$z_\alpha \rightarrow z_\alpha \exp(i\theta) \tag{44}$$

leaves $\mathbf{N}(x, \tau)$ unchanged. All physical properties must then be invariant under the transformation (44), and so any effective Lagrangian for the field z_α has a U(1) gauge invariance, similar to that in quantum electrodynamics. This leads naturally to the introduction of an 'emergent' U(1) gauge field A_μ, where the index μ describes the 2+1 space-time components. Under the gauge transformation (44), $A_\mu \rightarrow A_\mu - i\partial_\mu\theta$. It should be stressed that this gauge field is *not* related to the physical electromagnetic field but rather is an alternative way of describing the interactions between the spinor fields due to the antiferromagnetic fluctuations. Describing the system in terms of the field $\vec{N}$ or the two fields z_α and A_μ is a matter of choice.

The low-energy and long-wavelength action of the quantum field theory for z_α and A_μ is determined by the constraints of spin rotational symmetry and gauge invariance to be

$$\begin{aligned} \mathcal{S}_z = \int d^2r d\tau \Big[&|(\partial_\mu - iA_\mu)z_\alpha|^2 + s_z|z_\alpha|^2 + u(|z_\alpha|^2)^2 \\ &+ \frac{1}{2e_0^2}(\epsilon_{\mu\nu\lambda}\partial_\nu A_\lambda)^2 \Big] \end{aligned} \tag{45}$$

where there is an implicit summation over all indices, $\epsilon_{\mu\nu\lambda}$ is the anti-symmetric tensor and e_0 is the coupling constant, which determines the strength of the coupling between the z_α field and the gauge field.

If the coefficient $s_z < 0$ then the mean-field theory of the action gives a ground state with $\langle z_\alpha \rangle \neq 0$. Substituting this into (41) and (43) we see that this corresponds

---

[16] See page 70 of (Auerbach, 1994).

to a state with commensurate antiferromagnetic order. This also leads to a gap in the spectrum of the A_μ gauge field, and reduces its fluctuations. The case $s_z > 0$ gives $\langle z_\alpha \rangle = 0$. A rather sophisticated analysis is required to show that the gauge field fluctuations are associated with Berry's phases which lead to VBC order (Sachdev, 2008).

A key point is that U(1) gauge fields in 2+1 dimensions are always confining (Kogut, 1979). This is because of instantons which describe the quantum tunneling of the gauge field between alternative classical ground states. The physical consequence of this for commensurate antiferromagnets is that the spinons are always bound together so that the elementary excitations are spin-1 bosons.

A. Spinons deconfine when incommensurate phases are quantum disordered

A ground state with incommensurate magnetic order can be described by two orthogonal vectors, $\mathbf{N}_1$ and $\mathbf{N}_2$ so that the magnetic moment at site j (with position $\mathbf{r}_j$) is (Chubukov et al., 1994a)

$$\langle \mathbf{S}_j \rangle = \mathbf{N}_1 \cos(\mathbf{Q} \cdot \mathbf{r}_j) + \mathbf{N}_2 \sin(\mathbf{Q} \cdot \mathbf{r}_j) \qquad (46)$$

where $\mathbf{Q}$ is the incommensurate ordering wavevector.

The analog of the spinor representation in Eq. (41), is to introduce another spinor w_α, which parameterizes $\mathbf{N}_{1,2}$ by (Chubukov et al., 1994a)

$$\mathbf{N}_1 + i\mathbf{N}_2 = \varepsilon_{\alpha\gamma} w_\gamma \boldsymbol{\sigma}_{\alpha\beta} w_\beta, \qquad (47)$$

where $\varepsilon_{\alpha\beta}$ is the antisymmetric tensor. The physical spin is then invariant under the Z_2 gauge transformation

$$w_\alpha \rightarrow \eta w_\alpha \qquad (48)$$

where $\eta(r, \tau) = \pm 1$. This Z_2 gauge invariance is key to stabilising a spin liquid ground state because it reduces the magnitude of the U(1) gauge field fluctuations which confine the spinons in antiferromagnets with commensurate interactions. In contrast to U(1) gauge theories a Z_2 gauge theory can have a deconfined phase in 2+1 dimensions (Kogut, 1979). We now introduce a Higgs scalar field, the condensation of which, $\langle \Lambda \rangle \neq 0$ can break the U(1) symmetry, in a similar manner to that in which the BCS superconducting state breaks the U(1) gauge invariance associated with electromagnetism. In particular, to break U(1) down to Z_2, requires a Higgs scalar, that carries U(1) charge 2, i.e. $\Lambda \rightarrow e^{2i\theta}\Lambda$, under the transformation (44) (Fradkin and Shenker, 1979).

The physical interpretation of the field Λ becomes clearer by writing down the effective action for Λ. This is constrained only by symmetry and gauge invariance, including its couplings to z_α. One adds to the action (45) the action for the Higgs field,

$$\mathcal{S}_\Lambda = \int d^2 r d\tau \Big[|(\partial_\mu - 2iA_\mu)\Lambda_a|^2 + \tilde{s}|\Lambda_a|^2 + \tilde{u}|\Lambda_a|^4$$
$$- i\Lambda_a \varepsilon_{\alpha\beta} z_\alpha^* \partial_a z_\beta^* + \text{c.c.} \Big]. \qquad (49)$$

Multiple fields Λ_a, with spatial indicies a, are necessary to account for the space group symmetry of the underlying lattice. The crucial term is the last one coupling Λ_a and z_α.

A mean-field treatment of $\mathcal{S}_z + \mathcal{S}_\Lambda$, gives two possible condensates, and hence four possible phases (i.e. neither, either, or both fields condensed), depending on the sign of the two parameters s_z and $\tilde{s}$ (compare Figure 40).

i. $s_z < 0$, $\tilde{s} > 0$: This state has $\langle z_\alpha \rangle \neq 0$ and $\langle \Lambda \rangle = 0$. The modes of the Λ field are gapped and so not relevant. This is a Néel state.

ii. $s_z > 0$, $\tilde{s} > 0$: This state has $\langle z_\alpha \rangle = 0$ and $\langle \Lambda \rangle = 0$. Again the Λ modes are gapped and so not relevant. This is the VBC state.

iii. $s_z < 0$, $\tilde{s} < 0$: This state has $\langle z_\alpha \rangle \neq 0$ and $\langle \Lambda \rangle \neq 0$. Because of the z_α condensate, this state breaks spin rotation invariance, and we determine the spin configuration by finding the lowest energy z_α mode in the background of a non-zero $\langle \Lambda \rangle$ in Eq. (49), which is

$$z_\alpha = \left(w_\alpha e^{i\langle \Lambda \rangle \cdot r} + \varepsilon_{\alpha\beta} w_\beta^* e^{-i\langle \Lambda \rangle \cdot r} \right) / \sqrt{2}, \qquad (50)$$

with w_α a constant spinor. Inserting the above expression (50) into Eq. (41) gives a local moment that is space-dependent so that $\langle \mathbf{S}_i \rangle$ is given by Eq. (46) with $\mathbf{N}_1$ and $\mathbf{N}_2$ given by Eq. (47) and the wavevector $\mathbf{Q} = (\pi, \pi) + 2\langle \boldsymbol{\Lambda} \rangle$. Hence, the field Λ measures the deviation of the spin fluctuations from commensurability.

iv. $s_z > 0$, $\tilde{s} < 0$: This state has $\langle z_\alpha \rangle = 0$ and $\langle \Lambda \rangle \neq 0$. This a Z_2 spin liquid. Spin rotation invariance is preserved, and there is no VBC order because monopoles are suppressed by the Λ condensate (Sachdev, 2008).

We also note that the last term in (49) which couples the incommensurability to the gradient of a field has some similarity to that which occurs in other field theories of incommensurate systems (Klee and Muramatsu, 1996).

B. sp(N) theory

A specific realisation of the above considerations was given (Chung et al., 2001) in a study of the Heisenberg model on the anisotropic triangular lattice [compare equation (38)], in the large N limit of an $sp(N)$ approach (Read and Sachdev, 1991a,b; Sachdev, 1992). In the $N \rightarrow \infty$ limit, mean-field theory is exact and the bosonic spinons are deconfined. The calculated mean-field phase diagram as a function of J'/J and the magnitude of the quantum fluctuations (which can be tuned by varying the ratio of N to the total spin S), exhibits four distinct phases as in Figure 40.

Fluctuations at finite N, however, allow for U(1) gauge field fluctuations, which modify the mean-field results. In

particular, the Berry's phase associated with the instantons in the gauge field confine the spinons in the commensurate phase with short-range magnetic order. However, they do not for the incommensurate phase with short-range order, because their is a non-zero spinon pairing field in the diagonal (J') direction. This field carries a gauge charge of ± 2 making it equivalent to a Higgs field, which prevents confinement in 2+1 dimensions (Fradkin and Shenker, 1979).

The dimerization pattern seen in near the decoupled chain limit ($J' \gg J$) is similar to that found (White and Affleck, 1996) for a ladder with zigzag coupling. Furthermore, spinon excitations are confined into pairs by the $U(1)$ gauge force. This phase is believed to be an analogue of the RVB state found on the isotropic triangular lattice quantum dimer model (Moessner et al., 2001). The phase has topological order; i.e., if the lattice is placed on a torus, the ground state becomes four-fold degenerate in the thermodynamic limit.

C. Experimental signatures of deconfined spinons

Thermal properties will reflect the presence of deconfined spinons and fluctuating gauge fields. These have been calculated for a spinon Fermi surface coupled to a $U(1)$ gauge field (Nave and Lee, 2007). The low-temperature specific heat is dominated by a term $\sim T^{2/3}$ due to gauge field fluctuations (Motrunich, 2005). The thermal conductivity is dominated by the contribution due to spinons, which give a term $\sim T^{1/3}$ (Nave and Lee, 2007).

The low temperature specific heat data for κ-$(ET)_2Cu_2(CN)_3$ (Yamashita et al., 2008) can be fit to either the form expected for gauge fluctuations or for a spinon Fermi surface without the gauge fluctuations (Ramirez, 2008). Hence, it is not possible from the experimental data to definitely conclude that there are gapless fermionic spinon excitations.

One question is: is the spin susceptibility simply related to the spinon susceptibility? This would imply that gauge fluctuations do not modify the spin susceptibility. If so one might expect that the NMR relaxation may exhibit a Korringa-like temperature dependence, i.e., $1/T_1 \sim T$, a temperature independent $1/T_2$ and Knight shift, and a Korringa ratio of unity if there are deconfined spinons.

It has recently been argued that a definitive signature of deconfined spinons in a Mott insulator would be a sizeable thermal Hall effect (Katsura et al., 2010). In an external magnetic field for the Hubbard model on a triangular lattice there is an orbital interaction between the field and the spin chirality (Motrunich, 2005; Sen and Chitra, 1995). This leads to a thermal Hall effect (Katsura et al., 2010) which is estimated to be larger than that due to conventional mechanisms by a factor of order $(J\tau/\hbar)^2$, where τ is the spinon scattering lifetime. The latter is estimated to be about 10^{-12} s from the magnitude of the low temperature thermal conductivity. However, as noted in Section IV this thermal Hall effect is not seen in the candidate spin liquid material Sb-1 (Yamashita et al., 2010).

D. Non-linear sigma models for magnons

The schematic phase diagram shown in Figure 3 provides a means to understand the different qualitative behaviours that can occur in non-linear sigma models, resulting from the presence of a quantum phase transition between ordered and disordered (i.e., spin liquid) phases.

Antiferromagnets which classically exhibit non-collinear magnet order, such as the Heisenberg model on the triangular lattice, may be described by a non-linear sigma model with $SU(N) \times O(2)$ symmetry (Chubukov et al., 1994a). A large N expansion treatment has been given of such a non-linear sigma model, including fluctuations to order $1/N$. The physical spin-1/2 model has $N = 2$. The temperature dependence of the correlation length $\xi(T)$ in the renormalised classical regime (Azaria et al., 1992; Chubukov et al., 1994a), is given by

$$\xi(T) = 0.021 \left(\frac{c}{\rho_s} \right) \left(\frac{4\pi\rho_s}{T} \right)^{1/2} \exp\left(\frac{4\pi\rho_s}{T} \right) \quad (51)$$

where c is a spin wave velocity and ρ_s is a zero-temperature spin stiffness. The static structure factor at the ordering wavevector is (Chubukov et al., 1994a)

$$S(Q) \simeq 0.85 \left(\frac{T}{4\pi\rho_s} \right)^4 \xi(T)^2. \quad (52)$$

The above equations show that ρ_s sets the temperature scale for the development of antiferromagnetic spin correlations. For the isotropic triangular lattice non-linear spin wave theory (to order $1/S^2$) (Chubukov et al., 1994b) gives $c = Ja$ and $\rho_s = 0.06J$. The above expressions are quite similar to those for the $O(3)$ non-linear sigma model that is relevant to the Heisenberg model on the square lattice (Auerbach, 1994; Chakravarty et al., 1989), but with the factor $2\pi\rho_s$ replaced by $4\pi\rho_s$.

A monotonic increase in the NMR relaxation rates with decreasing temperature occurs for a non-linear sigma model in the renormalised classical regime (Azaria et al., 1992; Chubukov et al., 1994a), which occurs as a magnetically ordered state is approached at zero temperature. It is found that $1/T_1 \propto T^{7/2}\xi(T)$ and $1/T_2 \propto T^3\xi(T)$, when the correlation length $\xi(T) \gg a$.

In the quantum critical regime, close to a quantum critical point, the temperature dependence of the NMR rates is (Chubukov et al., 1994a)

$$1/T_1 \sim T^\eta, \qquad 1/T_2 \sim T^{(\eta-1)}, \quad (53)$$

where η is the anomalous critical exponent associated with the spin-spin correlation function. Generally, for $O(N)$ non-linear sigma models (e.g., that are appropriate

for collinear antiferromagnets), this exponent is much less than one (Chakravarty et al., 1989). For example, for $N = 3$, $\eta = 0.04$.

E. Field theories with deconfined spinons

Field theories with deconfined spinons can have $\eta > 1$ (Alicea et al., 2006; Chubukov et al., 1994a; Isakov et al., 2005). Then $1/T_1 T$ *decreases* with decreasing temperature, *opposite* to what occurs when the spinons are confined, because then $\eta \ll 1$. Hence, this is a significant experimental signature. To leading order in $1/N$, the $SU(N) \times O(2)$ model (Chubukov et al., 1994a), has $\eta = 1 + 32/(3\pi^2 N)$. For $N = 2$ this gives $\eta \simeq 1.5$, comparable to the value deduced from NMR experiments on κ-(BEDT-TTF)$_2$Cu$_2$(CN)$_3$ (Figure 13).

F. Field theories with bosonic spinons and visons

Qi, Xu, and Sachdev (Qi et al., 2009; Xu and Sachdev, 2009) propose that the ground state of κ-(BEDT-TTF)$_2$Cu$_2$(CN)$_3$ is a Z_2 spin liquid close to a quantum critical point with quasiparticles that are spin-1/2 bosons (spinons) and spinless bosons (visons). The visons correspond to low-energy singlet excitations and can be viewed as vortices in the Z_2 gauge field associated with a liquid of resonating valence bonds. They showed that at low temperatures spinons dominate the NMR relaxation rate and that visons dominate the thermal conductivity. The visons form a dilute Boltzmann gas with a bandwidth of about 8 K, which the authors claim corresponds to the peak observed in the heat capacity and thermal conductivity. Note that this bandwidth is only about 3 per cent of the exchange interaction J, which sets the energy scale for the spinons. Figure 40 shows the phase diagram of one of the field theories considered (Xu and Sachdev, 2009). The "doubled Chern-Simons theory" used implements the mutual semionic statistics of the visons and spinons.

G. Field theories with fermionic spinons and gauge fields

An alternative approach (Lee and Lee, 2005) starts with the slave rotor representation (Florens and Georges, 2004) and derives an effective Lagrangian describing fermionic spinons and 'X bosons' coupled to U(1) gauge fields. In the Mott insulating phase the X bosons are gapped and the ground state has a spinon Fermi surface coupled to a U(1) gauge field. Although it is known that a compact U(1) pure gauge field is confining, it is controversial as to whether such a field coupled to a matter field can be deconfining. At low temperatures there is the possibility of an Amperean instability (Lee et al., 2007b) which leads to pairing of the spinons.
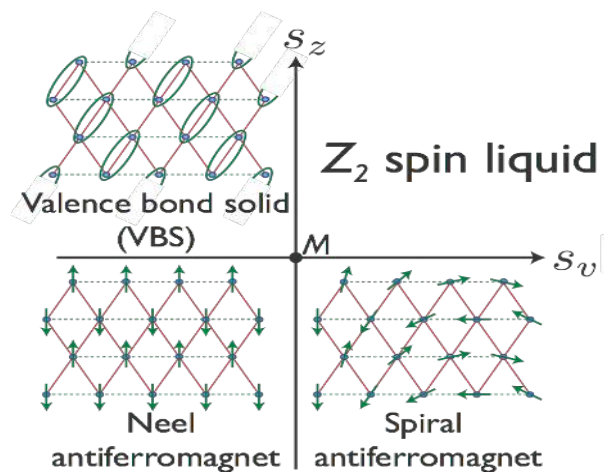

FIG. 40   Phase diagram of a specific field theory with spinons (spin-1/2 bosons) and visons (spinless bosons) (Xu and Sachdev, 2009). The vertical and horizontal axes describe the "mass" of the visons and spinons, respectively. A similar mean-field phase diagram is obtained for the field theory described by the action $\mathcal{S}_z + \mathcal{S}_\Lambda$ given by (45) and (49) with $s_v = \tilde{s}$. M denotes a multi-critical point. One sees competition between phases similar to those found from series expansion studies of the Heisenberg model on the anisotropic triangular lattice (Zheng et al., 1999) (cf. Figure 36). [Copyright (2009) by the American Physical Society].

H. Effective field theories for quasi-particles in the metallic phase

There have been many papers written about possible field theories for the metallic phase of doped Mott insulators (Lee et al., 2006). A common ingredient of many of these theories is that the quasi-particles interact strongly via fluctuations in the gauge field associated with representions of the electron operators in terms of the slave bosons. However, in contrast little work has been done for the metallic state associated with the bandwidth controlled Mott metal-insulator transition.

Qi and Sachdev (Qi and Sachdev, 2008) consider field theories on the triangular lattice which describe transitions from an insulating Z_2 spin liquid state (with bosonic spinon excitations) to metallic states with Fermi surfaces. They argue that near this insulator-metal transition an excitonic condensate can form. This condensate involves pairing of charge neutral pairs of charge $+e$ and charge e fermions. This condensate breaks the lattice space group symmetry. They propose this state as an explanation of an anomaly in thermodynamic properties seen near temperatures of about 6 K in κ-(BEDT-TTF)$_2$Cu$_2$(CN)$_3$. They also discuss the superconductivity associated with the pairing of fermions of the same charge.

An alternative approach (Lee and Lee, 2005; Lee et al., 2007b) starts with the slave rotor representation (Florens and Georges, 2004) and derives an effective Lagrangian describing fermionic spinons and X bosons coupled to U(1) gauge fields. Compared to traditional (Kotliar-

Ruckenstein) slave bosons the X boson is relativistic. In the Mott insulating phase it is gapped and the holon and doublon are bound.

The corresponding field theory has been used to describe a continuous transition from a Fermi liquid to paramagnetic Mott insulator with a spinon Fermi surface (Senthil, 2008). At the critical point the quasiparticle weight Z vanishes and the effective mass m^* diverges. Nevertheless, there is still a sharply defined Fermi surface. Also, the product Zm^* tends to zero as the transition is approached, whereas for dynamical mean-field theory it tends to a non-zero constant. As the temperature increases on the metallic side there is a crossover from the Fermi liquid to a marginal Fermi liquid and then to a quantum critical non-Fermi liquid. A universal jump in the intralayer resistivity of order h/e^2 is predicted. It is suggested that this theory is particularly relevant to κ-(BEDT-TTF)$_2$Cu$_2$(CN)$_3$. However, as discussed in Section III the transition appears to be first order experimentally. A logarithmic correction to the Fermi liquid quadratic temperature dependence of the resistivity is found, whereas a power closer to 2.5 is observed experimentally (cf. section IV.F).

VIII. RELATION TO OTHER FRUSTRATED SYSTEMS

In the search for general organising principles we briefly review other classes for frustrated materials and models. Some of the systems discussed below have been more extensively reviewed elsewhere (Balents, 2010; Normand, 2009).

A. β-(BDA-TTP)$_2$X

A combined experimental and theoretical study was made of these organic charge transfer salts with the two anions X=SbF$_6$ and AsF$_6$ (Ito et al., 2008). An extended Hückel calculation was used to argue that the relevant effective Hamiltonian was a Hubbard model on an anisotropic triangular lattice with three unequal hopping integrals, t_0, t_1, t_2. (If two of these three hopping integrals are equal one obtains the $t - t'$ model discussed extensively in this review). These were calculated for the different crystal structures obtained as a function of uniaxial stress. All were found to vary within the range, 0.03-0.05 eV. Hence, these materials involve significant frustration. The superconducting transition temperature T_c measured as a function of uniaxial stress was compared to that calculated from from a fluctuation exchange approximation (Ito et al., 2008). The parameterisation of the band structure needs to be compared to the actual Fermi surface determined from angle-dependent magnetoresistance (Choi et al., 2003).

B. λ-(BETS)$_2$X

This family of materials has attracted considerable interest due to the discovery of magnetic-field induced superconductivity in the X=FeCl$_4$ material (Uji et al., 2001). At ambient pressure and zero magnetic field it has a Mott insulating ground state, whereas the X=GaCl$_4$ material is a superconductor. Applying a magnetic field parallel to the layers creates a metal, and for sufficiently high magnetic fields, superconductivity. This can be explained in terms of the exchange interaction between the localised magnetic Fe^{3+} ions in the anion layer and the itinerant electrons in the layers of BETS molecules. When this exchange interaction is cancelled by the applied field the electron spins effectively see zero magnetic field (Balicas et al., 2001; Cépas et al., 2002). One can also tune between Mott insulating, metallic, and superconducting states by varying the temperature or the relative concentration of magnetic Fe^{3+} ions and non-magnetic Ga^{3+} ions (which effectively tunes the magnitude of the exchange interaction). (For a review see (Uji and Brooks, 2006)).

The simplest possible lattice model Hamiltonian to describe this family of materials is a Hubbard-Kondo model with a Hubbard model on an anisotropic triangular lattice at half filling with an exchange interaction between the electrons and localised spin-5/2 spins (Cépas et al., 2002). However, there are questions about the role of dielectric fluctuations and charge ordering in these materials (Toyota and Suzuki, 2007). The fact that one can tune between ground states with perturbations involving energy scales of the order of 1 meV (e.g. exchange interactions, fields of order 10 Tesla and temperatures of order 10 Kelvin) underscores how the interplay of frustration and strong correlations leads to competition between different ground states with very similar energies. Given this tuneability more systematic studies of the role of frustration and possible spin liquid states in this family is worthy of further study.

C. Sodium cobaltates

The material Na$_x$CoO$_2$ has attracted considerable interest because of its large thermopower and rich phase diagram which contains metallic, superconducting, insulating, charge ordered, and various magnetic phases (Ong and Cava, 2004). The $x = 0$ member of the family should be described by a single band Hubbard model on the isotropic triangular lattice, at half filling (Merino et al., 2006). Due to the large geometric frustration of magnetic ordering and the absence of Fermi surface nesting the ground state is metallic below a critical value of $U/t \simeq 8$ (Section VI.B). NMR measurements on CoO$_2$ found that the Knight shift is weakly temperature dependent and the spin relaxation rate $1/T_1$ could be fitted to a Curie-Weiss form (de Vaulx et al., 2007). There is also significant particle-hole symmetry and properties of

the model depend significantly on the sign of t.

It turns out that to describe the $x \neq 0$ materials, particularly those with x a rational number (e.g., $x = 1/3, 1/2, 2/3$), one needs to take into account the spatial ordering of the Na^+ ions and the associated periodic potential experienced by electrons in the cobalt layers (Merino et al., 2009a,b; Powell et al., 2010).

D. Cs_2CuCl_4

The best evidence for deconfined spinon excitations in an actual quasi-two-dimensional material is for this one. Both Cs_2CuCl_4 and Cs_2CuBr_4 can be described by a Heisenberg model on the anisotropic triangular lattice. From a range of experiments it is estimated that the value of J'/J is about 3 and 2 for Cs_2CuCl_4 and Cs_2CuBr_4, respectively (Fjærestad et al., 2007; Zheng, Singh, McKenzie and Coldea, 2005). A very detailed analysis of the effect of small residual interactions such as a Dzyaloshinskii-Moriya interaction and an external magnetic field on the ground state has been performed (Starykh et al., 2010).

E. Monolayers of solid ^{3}He

A single monolayer of helium atoms can be adsorbed on graphite plated with HD molecules. At the appropriate areal density the atoms form a solid with a hexagonal lattice. The ^{3}He atoms have nuclear spin-1/2 and the spin degrees of freedom can be described by a Heisenberg model on the triangular lattice with multiple ring exchange. No spin gap was observed down to temperatures as low at 10 μK (Masutomi et al., 2004).

At the density at which the monolayer solidifies into a $\sqrt{7} \times \sqrt{7}$ commensurate solid, a Mott-Hubbard transition between a Fermi liquid and a magnetically disordered solid is observed. This is signified by a diverging linear co-efficient of the specific heat and and a diverging magnetization (Casey et al., 2003). This transition has also been investigated in bilayers; it is found that the interband coupling associated with the two layers vanishes as the insulating phase is approached (Neumann et al., 2007). The experimental results are well described by a cluster DMFT treatment of a bilayer Hubbard model on the triangular lattice (Beach and Assaad, 2009).

F. Pyrochlores

The pyrochlore lattice consists of a three-dimensional network of corner sharing tetrahedra. In a number of transition metal oxides the metal ions are located on a pyrochlore lattice. The ground state of the antiferromagnetic Heisenberg model on a pyrochlore lattice is a gapped spin liquid (Canals and Lacroix, 2000). The ground state consists of weakly coupled RVB (resonating valence bond) states on each tetrahedra. However, Dzyaloshinskii-Moriya interactions have a significant effect, leading to the formation of long-range magnetic order (Elhajal et al., 2005). The conditions necessary for deconfined spinons has been explored in Klein type models (Nussinov et al., 2007). The repeat unit in this lattice consists of a tetrahedron of four spins (giving an integer total spin) and so the Lieb-Schultz-Mattis-Hastings theorem (Hastings, 2004) which can preclude gapped spin liquid ground states does not apply.

The material KOs_2O_6 has a pyrochlore structure and is found to be superconducting with a transition temperature of about 10 K (Yonezawa et al., 2004). Originally it was thought that the superconductivity might be intimately connected to RVB physics (Aoki, 2004). However, it now seems that the superconductivity is s-wave and can be explained in terms of strong electron-phonon interactions which arise because of anharmonic phonons associated with "rattling" vibrational modes of the K ions which are located inside relatively large spatial regions within the cage of Os and O ions (Hattori and Tsunetsugu, 2010).

G. Kagome materials

The material herbertsmithite $ZnCu_3(OH)_6Cl_2$ has generated considerable interest as a realisation of the spin-1/2 Heisenberg model on the Kagome lattice. However, it turns out that analysis of the experimental results is significantly complicated by the presence of a small number of impurities and by the Dzyaloshinskii-Moriya interaction (Gregor and Motrunich, 2008).

$Na_4Ir_3O_8$ is a material in which the Ir ions have spin-1/2 and are located on a three-dimensional "hyperkagome" lattice of corner-sharing triangles. It has been proposed that the ground state of the Heisenberg model on this lattice may be a quantum spin liquid with spinon Fermi surface (Lawler et al., 2008).

The antiferromagnetic spin-1/2 Heisenberg model on the Kagome lattice has at times been thought to be a prime candidate for a quantum spin model with a spin liquid ground state. This is partly because the classical model has an infinite number of degenerate ground states. However, a few years ago a series expansion study (Singh and Huse, 2007) found that the ground state was actually a valence bond crystal with a unit cell of 36 spins. This result was confirmed by a completely different numerical method based on entanglement renormalisation (Evenbly and Vidal, 2010). However, very recent numerical results using the density matrix renormalisation group (DMRG) (Yan et al., 2010) found a spin liquid ground state, with a gap to both singlet and triplet excitations.

H. Spin-1 materials

The spin-1 Heisenberg model on the anisotropic triangular lattice has been studied in the weakly coupled chain limit ($J' \gg J$) using zero-temperature series expansions about magnetically ordered spiral states (Pardini and Singh, 2008). There is a critical interchain coupling $J/J' \sim 0.3 - 0.6$ required to overcome the Haldane spin gap (which occurs in the decoupled chain limit, $J = 0$). This critical coupling is an order of magnitude larger than that required for the case of unfrustrated coupling between chains (i.e. an anisotropic square lattice). Hence, it may be that a Haldane phase can exist in a two-dimensional system. This raises an interesting question about whether this model has topological order.

The family of materials LiVX_2 ($X = $ O, S, Se) can be viewed as spin-1 systems on a triangular lattice. The $X = $ O material has an insulating valence bond solid (VBS) ground state. Upon cooling the $X = $ S compound undergoes a first-order phase transition from a paramagnetic metal (possibly with a pseudogap) to a VBS insulator at 305 K (Katayama et al., 2009). The $X = $ Se material is a paramagnetic metal down to 2 K.

The material NiGa$_2$S$_4$ can be described by spin-1 antiferromagnet on a triangular lattice. There is no sign of magnetic order (Nakatsuji et al., 2005) and it has been proposed that the ground state is a spin nematic phase which is stabilised by bilinear–biquadratic interactions (Tsunetsugu and Arikawa, 2007).

I. Cuprates

One might not expect frustration to be important in these materials, particularly because the parent material clearly undergoes antiferromagnetic Neel ordering. However, a correlation has been found between the magnitude of next-nearest neighbour hopping on the square lattice, which frustrates the system, and the superconducting transition temperature, T_c (Pavarini et al., 2001).

J. $J_1 - J_2$ model

This a Heisenberg model on a square lattice where J_1 and J_2 are the nearest- and next-nearest- neighbour interactions, respectively. Thus, J_2 acts along *both* diagonals of each placquette and is a frustrating interaction. The model has been very widely studied with diverse techniques, motivated by the hope that it would be model case of a two-dimensional model where frustrations produce a spin liquid ground state. For small and for large J_2/J_1 the model has Neel order with wave vector (π, π) and $(0, \pi)$, respectively. For intermediate $0.5 < J_2/J_1 < 0.7$ various studies have found a ground statewith no magnetic order; some are VBC states (Becca et al., 2009). Figure 35 shows how the true ground state is close to an RVB state without magnetic order.
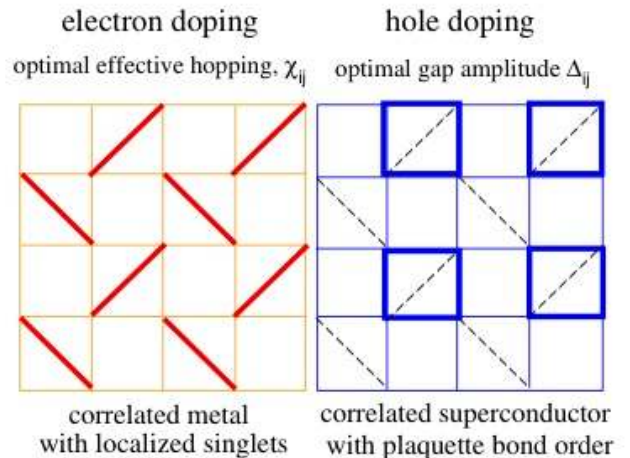

FIG. 41 Particle-hole asymmetry of doped Mott insulators on the Shastry-Sutherland lattice (Liu et al., 2007). The ground state of the Mott insulator is a valence bond crystal with spin singlets along the diagonals shown as heavy lines on the left part of the figure. Electron doping produces a metal with these same spin singlet correlations preserved. In contrast, hole doping produces a d-wave superconductor with co-existing plaquette bond order. [Copyright (2007) by the American Physical Society.]

The corresponding Hubbard model exhibits a subtle competition between $d_{x^2-y^2}$ superconductivity, a Mott insulating phase, different magnetic orders, and a spin liquid state. See for example (Nevidomskyy et al., 2008).

K. Shastry-Sutherland lattice

It has been argued that SrCu$_2$(BO$_3$)$_2$ is a Mott insulator on this lattice (Shastry and Kumar, 2002). The corresponding Heisenberg model has an exchange interaction J along all vertical and horizontal bonds and a diagonal interaction J' along every other plaquette (Shastry and Kumar, 2002). It can be shown that for $J'/J > 1.44 \pm 0.02$ that the exact ground state is a product of singlets along the same diagonals that the J' interaction occurs (Koga and Kawakami, 2000). A variational Monte Carlo study (Liu et al., 2007) was made of the corresponding $t - J$ model (including three site hopping terms) away from half-filling using a projected BCS wave function with $t' = \pm 1.25t$ and $J = 0.3t$. The results are summarised in Figure 41 and in the four points below.

i. There is significant particle-hole asymmetry. The authors point out that one sign of t' corresponds to electron doping and the other to hole doping while t does not change. This is because, for $t' = 0$ the lattice is bipartite. The sign of the hopping integrals only matters when the electrons (or holes) can traverse closed loops consisting of an odd number of lattice sites. On the Shastry-Sutherland lattice (and,

indeed the triangular lattice) all closed loops consisting of an odd number of hops contain an odd number of hops with amplitude t' (and hence an even number of hops with amplitude t; cf. Fig. 41). Hence, only the sign of t' matters for determining particle-hole asymetry.

ii. Hole doping produces d-wave superconductivity. But, this is *not* the result of delocalisation of the pre-existing singlets in the Mott insulator since the latter were along the diagonals.

iii. Electron doping does not produce superconductivity, but only a correlated metal with singlet pairing along the diagonal, as in the parent Mott insulator.

iv. The hole-doped superconducting state co-exists with plaquette bond order where all the nearest neighbour spins have antiferromagnetic correlations. Thus the spin correlations are qualitatively different from those in the parent Mott insulator.

This shows that the competition between superconductivity and antiferromagnetism and resonating valence bonds that occurs when doping a frustrated Mott insulator is more subtle (and confusing) than suggested by Anderson's original conjecture (Anderson, 1987). On the other hand, one might argue that the parent Mott insulator is very different from the cuprates and organics because there are *no* resonating valence bonds in the parent insulators for those classes of material.

L. Surface of 1T-TaSe$_2$

This can be described by the Hubbard model on the isotropic triangular lattice (Perfetti et al., 2005). As the temperature decreases the bandwidth also decreases leading to a metal-insulator transition. The observed ARPES spectrum was found to be comparable to that calculated from the Hubbard model using dynamical mean-field theory (Perfetti et al., 2005).

M. Honeycomb lattice

A recent study presented the results of Quantum Monte Carlo simulations on the Hubbard model at half-filling on the honeycomb lattice (Meng et al., 2010). This is the relevant lattice for graphene and Pb and Sn on Ge(111). As U/t increases there is a phase transition from a semi-metal (which has gapless excitations at corners of the Brillouin zone, Dirac fermions) to a Mott insulating phase, for $U \simeq 3.5t$. More importantly, the authors also find that there is a spin liquid phase with a spin gap before entering a phase with antiferromagnetic order. The latter is what one expects from a strong coupling expansion (i.e. $U \gg t$) which is described by an unfrustrated Heisenberg model (Paiva et al., 2005). The spin liquid state has dimer-dimer correlations similar to that in a single hexagon which can be described by the RVB states of benzene.

Although the honeycomb lattice is bi-partite and so is not frustrated the authors suggest that near the Mott transition effective frustrating interactions occur. For example, the ratio of the next-nearest neighbour exchange interaction to the nearest-neighbour interaction is $(t/U)^2$ (Delannoy et al., 2005).

In passing we note that the spin gap is very small, $\Delta_s \simeq t/40 \simeq J/40$. The single-particle charge gap is also quite small in the spin liquid state being about $t/10 \simeq U/40$. This illustrates the emergence of new low-energy scales due to the presence of large quantum fluctuations.

IX. ALTERNATIVE MODELS OF ORGANIC CHARGE TRANSFER SALTS

We have presented above the evidence that organic charge transfer salts are an experimental realisation of the half-filled anisotropic triangular lattice. We have argued that all of the important phenomena observed can be explained in terms of frustration and strong electronic correlations. This, of course, requires some objective judgement. For example, in which experimental results one views as important and which one views are mere details. Therefore, it is both natural and healthy that others working in these fields have introduced a number of alternative hypotheses. In this section we briefly discuss some of these ideas.

A. Quarter filled models

In order to construct effective low-energy half-filled models of κ-(BEDT-TTF)$_2X$ or $Et_nMe_{4-n}Pn[Pd(dmit)_2]_2$ one has to integrate out all of the internal degrees of freedom within the (BEDT-TTF)$_2X$ or $[Pd(dmit)_2]_2$ dimer. Several authors have considered models where one of these internal degrees of freedom is retained, i.e., models where a lattice site is a single BEDT-TTF or Pd(dmit)$_2$ molecule and the lattice is quarter filled with holes. We note that such models must still integrate out all of the internal degrees of freedom within the molecule. Thus, it is not clear *a priori* that even these models will contain all the physics relevant to the materials. However, all of the phenomena that are correctly described by half-filled models should be contained in the corresponding quarter-filled model. Therefore, one would not wish to argue that there is no description of these materials in quarter filled models. But, it may be that such a description is unnecessarily complicated. On the other hand, some of the papers discussed below argue that the correct description of the relevant physics is not captured by half-filled models, and that quarter-filled models are essential for the correct description of the low-energy physics.

Hotta has recently presented a model that interpolates between a range of different polymorphs of (BEDT-

TTF)$_2X$ in terms of the degree of dimerisation and the splitting of the two bands nearest to the Fermi energy (Hotta, 2003). This model is, in principle, quarter-filled, but becomes half-filled in appropriate limits. Hotta studied this Hamiltonian in the mean-field approximation. Her calculations found antiferromagnetic, charge ordered and metallic states, but lacked superconductivity and exotic insulating states such as spin-liquids and valence bond crystals. This may, of course, be due to the inadequacies of the Hartree-Fock approximation.

Very recently Li *et al.* (Li et al., 2010) have proposed that a number of the exotic phases (spin-liquids, valence bond crystals, etc.) observed in the charge transfer salts can be understood in terms of single phase, which they call the 'paired electron crystal'. The paired electron crystal phase has both charge order and spin order, and is reminiscent of the spin-Peierls phase observed in 1D chains and ladders. This proposal is based on the results of exact diagonalisation calculations for a quarter-filled model on the anisotropic triangular lattice, which is not dissimilar from Hotta's model. This model has a large number of free parameters, including the hopping integrals, on-site and neighbouring site Coulomb repulsion, intra- and inter-site electron-phonon couplings and the spring constants of the relevant phononic modes. Li *et al.* only reported numerical results for a limited parameter set but state that similar results were obtained for a "broad range" of parameters. Li *et al.* have given a qualitative description of how a number of experimental results in κ-(BEDT-TTF)$_2X$, Et$_n$Me$_{4-n}Pn$[Pd(dmit)$_2$]$_2$ and other organic charge transfer salts might be explained in terms of the paired electron crystals. It will be interesting to see whether this idea can be developed into a fully quantitative theory of the experiments in the coming years.

B. The role of phonons

The role of phonons and the interplay between electron-phonon coupling and electronic correlations have received less attention. Other than the work of Li *et al.* (Li et al., 2010), discussed above, and studies that conclude that the phonons play only a relatively minor role (Hassan et al., 2005; Merino and McKenzie, 2000b) most of the discussion of phonons has focused on the superconducting state (Mazumdar and Clay, 2008; Varelogiannis, 2002). A proposal to use Raman scattering to rule out pairing via electron-phonon coupling in the cuprates (Chubukov et al., 2006) may also be relevant to the organics.

C. Weak-coupling, spin fluctuations, and the Fermi surface

We have taken a strong coupling (i.e. large U) perspective where the key physics is that associated with the RVB spin singlet fluctuations in the Mott insulat-

ing phase. From this perspective, geometric frustration destabilises magnetic order and enhances RVB correlations. The opposite weak-coupling (i.e. small U) perspective starts from a Fermi liquid metallic state which becomes unstable due to enhanced spin fluctuations associated with imperfect nesting of the Fermi surface. Theoretical work on the organic charge transfer salts, which has taken such a weak-coupling point of view, has been reviewed previously (Moriya and Ueda, 2003).

A weak-coupling spin fluctuation treatment (e.g., the fluctuation-exchange approximation (FLEX)) of the relevant Hubbard model can produce some aspects of the phenomenology observed in the organic charge transfer salts. These include a transition from a Fermi liquid metal, to d-wave superconductivity, to an antiferromagnetic Mott insulator (Kino and Kontani, 1998; Kondo and Moriya, 1998; Schmalian, 1998). But it is not clear that the weak coupling approach can produce the following:

1. Large effective masses associated with proximity to the Mott insulating state;

2. The first-order phase transition from a superconductor to a non-magnetically ordered Mott insulator;

3. The first-order phase transition between an antiferromagnetic insulator with a large magnetic moment (as opposed to a small moment spin-density wave) to a d-wave superconductor;

4. A $d + id$ superconductor near $t' = t$;

5. A Mott insulating valence bond crystal insulator;

6. A Mott insulating spin liquid.

In contrast, the strong coupling approach gives a natural description of these phenomena, cf. Figure 39.

However, a widely held view is that the RVB and spin-fluctuation theories are just the strong and weak coupling limits of a more general theory that has yet to be articulated. This argument certainly has some merits, for example the weak coupling theory seems to give a reasonable account of the cuprates in the overdoped regime, where correlations are weaker than in more lightly doped cuprates.

This issue of a weak versus strong-coupling perspective is intimately connected with the question of a "glue" for superconductivity (Anderson, 2007). The issue can be nicely summarised as follows (Maier et al., 2008):

> The question of whether one should speak of a pairing glue in the Hubbard and $t - J$ models is basically a question about the dynamics of the pairing interaction. If the dynamics of the pairing interaction arises from virtual states, whose energies correspond to the Mott gap, and give rise to the exchange coupling J,

the interaction is instantaneous on the relative time scales of interest. In this case, while one might speak of an instantaneous glue, this interaction differs from the traditional picture of a retarded pairing interaction. However, if the energies correspond to the spectrum seen in the dynamic spin susceptibility, then the interaction is retarded and one speaks of a spin-fluctuation glue which mediates the d-wave pairing.

Norman has reviewed the difficulty of distinguishing between these points of view in the cuprates, particularly with regard to the observation of Fermi surface like properties in the underdoped state (Norman, 2010).

X. CONCLUSIONS

We have reviewed the significant progress that has been made in understanding frustrated materials in general and of organic charge transfer salts in particular. We are now in a position to partially answer some of the questions posed in the introduction:

1. *Is there a clear relationship between superconductivity in organic charge transfer salts and in other strongly correlated electron systems?*

   Yes. Superconductivity occurs in proximity to a Mott insulating phase. There is substantial evidence that the superconducting state is unconventional in that there are nodes in the energy gap. The superfluid stiffness becomes vanishingly small at high pressures in the organics and at low dopings in the cuprates.

2. *Are there materials for which the ground state of the Mott insulating phase is a spin liquid?*

   Yes. The strongest candidate materials are κ-(BEDT-TTF)$_2$Cu$_2$(CN)$_3$ and Sb-2. Neither of these materials show any evidence of magnetic ordering down to temperatures four orders of magnitude smaller than the antiferromagnetic coupling between neighbouring spins.

3. *What is the relationship between spin liquids and superconductivity? In particular, does the same fermionic pairing occur in both?*

   With increasing pressure there is a first order-phase transition from the spin liquid state to a superconducting state. There is no definitive evidence yet that the same fermionic pairing occurs in both states. A possible hint that this is the case is the similarity between the temperature dependence and magnitude of the thermal conductivity in the spin-liquid phase of κ-(BEDT-TTF)$_2$Cu$_2$(CN)$_3$ and the superconducting state of κ-(BEDT-TTF)$_2$-Cu(NCS)$_2$.

4. *What are the quantum numbers (charge, spin, statistics) of the quasiparticles in each phase?*

   These appear to be quite conventional in the Neel ordered Mott insulating states, the superconducting states, and the metallic state away from the Mott transition. This question remains open in the spin liquid phases of κ-(BEDT-TTF)$_2$Cu$_2$(CN)$_3$ and Sb-1.

5. *Are there deconfined spinons in the Mott insulating spin liquid phase?*

   The strongest evidence comes from the temperature dependence of the NMR relaxation rate and the thermal conductivity at low temperatures. This seems to suggest that there are deconfined spinons in Sb-1, but that κ-(BEDT-TTF)$_2$Cu$_2$(CN)$_3$ is fully gapped. However, the statistics of these spinons is an open question.

6. *Can spin-charge separation occur in the metallic phase?*

   There is no evidence of spin-charge separation in the metallic state yet.

7. *In the metallic phase close to the Mott insulating phase is there an anisotropic pseudogap, as in the cuprates?*

   NMR measurements suggest there is a pseudogap in the less frustrated materials. The anisotropy of this pseudogap in momentum space has not yet been mapped out experimentally. How the formation of the pseudogap may be related to the crossover with decreasing temperature from a bad metal to a Fermi liquid metal is not clear.

8. *What is the simplest low-energy effective quantum many-body Hamiltonian on a lattice that can describe all possible ground states of these materials?*

   There is no evidence yet that one needs to go beyond the Hubbard model on the anisotropic triangular lattice at half filling.

9. *Is a RVB variational wave function an appropriate theoretical description of the competition between the Mott insulating and the superconducting phase?*

   The Gossamer-RVB hypothesis is qualitatively consistent with experimental data reported so far.

10. *Is there any significant difference between destroying the Mott insulator by hole doping and by reducing correlations?*

    Perhaps. This question is only beginning to receive attention. It does seem that in the organics that the effective mass of the quasi-particles m^* increases significantly as the Mott insulator is approached whereas in the cuprates there is little variation in m^* with doping.

11. *For systems close to the isotropic triangular lattice, does the superconducting state have broken time-reversal symmetry?*

   There are no experimental studies of this question yet. Resolving the question theoretically will require high level computational studies beyond what is currently possible. To put this in perspective, there is still no consensus as to whether the doped Hubbard model on the square lattice has a superconducting ground state (Scalapino, 2006).

12. *How can we quantify the extent of frustration? Are there differences between classical and quantum frustration? If so what are the differences?*

   A number of different measures of frustration have been proposed. A clear example of quantum frustration is kinetic energy frustration in, say, the tight binding model, which has no classical analogue. For spin models the differences between quantum and classical frustration are less clear cut and may be a purely taxonomic question.

13. *What is the relative importance of frustration and static disorder due to impurities?*

   This question has not yet received significant attention. The destruction of the non-magnetic state in Sb-2 by, non-magnetic, Et_3MeSb^+ impurities provides a particularly dramatic case to study.

14. *Is the "chemical pressure" hypothesis valid?*

   For the weak frustrated BEDT-TTF salts a number of experimental features collapse onto a single curve, to within experimental error when plotted against the superconducting critical temperature for a range of materials (Powell et al., 2009). This is a success for the chemical pressure hypothesis. The more strongly frustrated κ-(BEDT-TTF)$_2$Cu$_2$(CN)$_3$ behaves differently.

   Recent DFT calculations are also consistent with the hypothesis. A definitive microscopic explanation of the chemical pressure hypothesis will require further characterisation of the pressure and anion dependence of the Hubbard model Hamiltonian parameters t, t', and U. A powerful approach to this problem would be to combine state-of-the-art band structure calculations with experimental characterisation of the Fermi surfaces using AMRO.

15. *Is there quantum critical behaviour associated with quantum phase transitions in these materials?*

   This is not clear. The most compelling evidence may be the temperature dependence of the NMR relaxation rate in κ-(BEDT-TTF)$_2$Cu$_2$(CN)$_3$(Figure 13).

16. *Do these materials illustrate specific "organising principles" that are useful for understanding other frustrated materials?*

   (a) Frustration suppresses long range fluctuations, which improves the the accuracy of mean field theories, such as DMFT, in the normal state.

   (b) In frustrated systems small changes in parameters can lead to dramatic changes in physical properties of the system. For example, a wide range of insulating phases are seen in the $Et_nMe_{4-n}Pn[Pd(dmit)_2]_2$ salts, despite their similar chemistry.

A. Some open questions

There remain many questions still to be answered. Here we outline some of the most important issues still to be resolved:

1. Does the excitation spectrum change as one moves between phases? And, if so, how? There is significant evidence in the cuprates that the excitation spectrum has essentially the same form "d-wave" form in the pseudogap and superconducting phases. This is seen in ARPES (Shi et al., 2009), STM (Lee et al., 2009), and thermal conductivity (Doiron-Leyraud et al., 2006).

2. Quite different physical pictures of the spin liquid state has been proposed for κ-(BEDT-TTF)$_2$Cu$_2$-(CN)$_3$. In particular, Sachdev and collaborators argue that the spinons are bosonic, whereas Lee and collaborators argue that the spinons are fermions and there is a well-defined Fermi surface. We need a "smoking gun" experiment to distinguish these two proposals.

3. The observation of a valence bond crystal in EtMe$_3$P[Pd(dmit)$_2$]$_2$ (P-1 in our notation) is exciting. On the one hand, this may be a realisation of a long sought after state of matter. The fact that this state can be transformed into a superconducting state with pressure is even more interesting. On the other hand, there remains an open question as to whether coupling to the lattice is necessary for stabilisation of this state. Therefore, understanding the role of the lattice in stabilising the VBC phase is a clear pirority.

4. Thermal conductivity measurements provide a sensitive probe of the quasi-particle excitation spectrum. Measurements in materials such as κ-(BEDT-TTF)$_2$Cu[N(CN)$_2$]Br which are close to the Mott transition should be a priority.

5. Observation of deviations from the Weidemann-Franz law (which gives a universal value for the ratio of the thermal and charge conductivities in a Fermi liquid metal) is a potential signature of spin-charge separation. However, both theoretically and experimentally finding such deviations has proven

to have a convoluted and confusing history (Smith and McKenzie, 2008; Smith et al., 2005). A careful study of the Weidemann-Franz law in the organic charge transfer salts could, however, provide significant new insights into the question of spin-charge separation in these materials.

6. What is the origin of the very different temperature dependences of the Nernst effects in κ-(BEDT-TTF)$_2$Cu[N(CN)$_2$]Br and κ-(BEDT-TTF)$_2$Cu(NCS)$_2$? What are the roles of superconducting fluctuations, electronic nematic order and proximity to the Mott transition?

7. Is the superfluid stiffness at high chemical pressures as small as μSR experiments suggest? Does hydrostatic pressure have the same effect?

8. What is the underlying physical cause of this small superfluid stiffness? Is it the same as for the overdoped cuprates, where the decreasing stiffness with increasing doping has been proposed to be due to pair breaking from impurities (Tallon et al., 2006)?

9. What is the symmetry of the superconducting state in the superconducting states derived from the spin liquid or a valence bond crystal? There are strong correlations between ferromagnetic fluctuations and p-wave superconductivity and nascent Néel order and d-wave superconductivity. Presumably the spin fluctuations are rather different in the spin liquid and VBC phases. Therefore, it is possible that they would lead to different superconducting orders.

10. Is time-reversal symmetry broken in the superconducting state of any of these frustrated materials? The superconducting phases which occur upon applying pressure to the spin liquids κ-(BEDT-TTF)$_2$Cu$_2$(CN)$_3$ and EtMe$_3$Sb[Pd(dmit)$_2$]$_2$ and the valence bond crystal EtMe$_3$P[Pd(dmit)$_2$]$_2$ would seem to be particularly promising systems to exhibit superconductivity that breaks time reversal symmetry.

11. If large enough single crystals could be grown inelastic neutron scattering could provide direct measurement of the spin excitation spectrum and the signatures of deconfined spinons such as a high energy continuum. Also, observation of an analogue of the neutron resonance mode seen in the cuprate and pnictide superconductors (Christianson et al., 2008) could be important.

12. We have seen that the precise value of the parameter t'/t has a dramatic effect on the ground state of the system. Hence, it is desirable to have DFT calculations for the Pd(dmit)$_2$ family of charge transfer salts. Experimental measurements that test the accuracy of such calculations, such as AMRO in the normal state, would also be of significant value.

13. The deviation of t'/t from unity is a measure of how far the electronic structure deviates from the isotropic triangular lattice. Hence, it is worth asking whether there is some structural parameter (e.g. deviation of the shape of the first Brillouin zone from a hexagon) which can be correlated with this ratio. There have been previous attempts to provide a unified view of structural trends (cf. (Mori, 1998, 2004; Shao et al., 2009; Yamochi et al., 1993)) but more work is needed to relate these trends in a definitive manner to electronic properties.

14. In the presence of a constant magnetic field B perpendicular to the layers a fluctuating $U(1)$ gauge field will modify the effect of B on transport properties. A significant amount of analysis of the related problem for the fractional quantum Hall liquid near filling factor $\nu = 1/2$ (Evers et al., 1999; Wolfle, 2000) has been performed. Recently, corrections to the Lifshitz-Kosevich form for the temperature dependence of the magnitude of quantum oscillations were calculated (Fritz and Sachdev, 2010). More general results for a non-Fermi liquid associated with quantum criticality were then derived using the holographic correspondence (Hartnoll and Hofman, 2010). A similar analysis of the effect of gauge fluctuations on AMRO may provide measurable signatures of a fluctuating $U(1)$ gauge field in these materials.

15. It is desirable to obtain a better understanding of the thermal expansion anomalies associated with the superconducting, pseudogap, and spin liquid transitions (Manna et al., 2010). These anomalies may reveal the spatial symmetry breaking associated with the transitions. With this goal, a Ginzburg-Landau theory for the acoustic anomalies associated with the superconducting transition has been developed (Dion et al., 2009).

Finally, we stress that in seeking to explain the rich physics still to be understood in frustrated materials in general and organic charge transfer salts in particular an important task for the community is to generate multiple hypotheses that may explain the data (Platt, 1964). It is then important to design and execute experiments that clearly distinguish between these hypotheses.

References

Abdel-Jawad M, Kennett M P, Balicas L, Carrington A, Mackenzie A P, McKenzie R H and Hussey N E 2006 *Nat. Phys.* **2**, 821.

Alet F, Walczak A M and Fisher M P 2006 *Physica A* **369**, 122.

Alicea J, Motrunich O I and Fisher M P A 2006 *Phys. Rev. B* **73**, 174430.

Altman E and Auerbach A 2002 *Phys. Rev. B* **65**, 104508.

Analytis J G, Ardavan A, Blundell S J, Owen R L, Garman E F, Jeynes C and Powell B J 2006 *Phys. Rev. Lett.* **96**, 177002.

Anderson P 1973 *Materials Research Bulletin* **8**, 153.

Anderson P W 1972 *Science* **177**, 393.

Anderson P W 1987 *Science* **235**, 1196.

Anderson P W 2007 *Science* **316**, 1705.

Anderson P W 2008 *Physics Today* **61**(4), 8.

Annett J F 1990 *Adv. Phys.* **39**, 83.

Annett J F, Goldenfeld N D and Renn S R 1990 World Scientific Singapore.

Aoki H 2004 *J. Phys.: Cond. Matter* **16**, V1.

Aonuma S, Sawa H and Kato R 1997 *Synth. Met.* **86**, 1881.

Apel W, Wintel M and Everts H 1992 *Z. Phys. B* **86**, 139.

Arai T, Ichimura K, Nomura K, Takasaki S, Yamada J, Nakatsuji S and Anzai H 2000 *Solid State Commun.* **116**, 679.

Ashcroft N W and Mermin N D 1976 *Solid State Physics* Holt, Rinehart and Winston New York.

Auerbach A 1994 *Interacting Electrons and Quantum Magnetism* Springer.

Augustyniak-Jablokow M A, Borshch S A, Daniel C, Hartl H and Yablokov Y V 2005 *New J. Chem.* **29**, 1064.

Azaria P, Delamotte B and Mouhanna D 1992 *Phys. Rev. Lett.* **68**, 1762.

Balents L 2010 *Nature* **464**, 199.

Balents L and Fisher M P A 1996 *Phys. Rev. B* **53**, 12133.

Balicas L, Brooks J S, Storr K, Uji S, Tokumoto M, Tanaka H, Kobayashi H, Kobayashi A, Barzykin V and Gor'kov L P 2001 *Phys. Rev. Lett.* **87**, 067002.

Barford W and Kim J H 1991 *Phys. Rev. B* **43**, 559.

Bartosch L, de Souza M and Lang M 2010 *Phys. Rev. Lett.* **104**, 245701.

Baskaran G 1989 *Phys. Rev. Lett.* **63**, 2524.

Baskaran G 2003 *Phys. Rev. Lett.* **90**, 197001.

Beach K and Assaad F 2009 *arXiv:0905.1127v1* .

Becca F, Capriotti L, Parola A and Sorella S 2009 *arXiv:0905.4854* .

Becca F and Mila F 2002 *Phys. Rev. Lett.* **89**, 037204.

Behnia K 2009 *J. Phys.: Condens. Matter* **21**, 113101.

Belin S, Behnia K and Deluzet A 1998 *Phys. Rev. Lett.* **81**, 4728.

Berg E, Altman E and Auerbach A 2003 *Phys. Rev. Lett.* **90**, 147204.

Bernu B and Misguich G 2001 *Phys. Rev. B* **63**, 134409.

Block M S, Sheng D N, Motrunich O I and Fisher M P A 2010 *arXiv:1009.1179* .

Boyer M C, Wise W D, Chatterjee K, Yi M, Kondo T, Takeuchi T, Ikuta H and Hudson E W 2007 *Nature Phys.* **3**, 802.

Brocks G, van den Brink J and Morpurgo A F 2004 *Phys. Rev. Lett.* **93**, 146405.

Buravov L I, Kushch N D, Merzhanov V A, Osherov M V, Khomenko A G and Yagubskii E B 1992 *J. Phys. I* **2**, 1257.

Canadell E 1999 *Coord. Chem. Rev.* **185-186**, 629.

Canals B and Lacroix C 2000 *Phys. Rev. B* **61**, 1149.

Cano-Cortés L, Dolfen A, Merino J, Behler J, Delley B, Reuter K and Koch E 2007 *Eur. Phys. J. B* **56**, 173.

Casey A, Patel H, Nyéki J, Cowan B P and Saunders J 2003 *Phys. Rev. Lett.* **90**, 115301.

Castellani C, Castro C D, Feinberg D and Ranninger J 1979 *Phys. Rev. Lett.* **43**, 1957.

Caulfield J, Lubczynski W, Pratt F L, Singleton J, Ko D Y K, Hayes W, Kurmoo M and Day P 1994 *J. Phys.: Condens. Matter* **6**, 2911.

Cépas O, Fong C M, Leung P W and Lhuillier C 2008 *Phys. Rev. B* **78**, 140405.

Cépas O, McKenzie R H and Merino J 2002 *Phys. Rev. B* **65**, 100502.

Chakravarty S, Halperin B I and Nelson D R 1989 *Phys. Rev. B* **39**, 2344.

Chandra P, Coleman P and Larkin A I 1990 *J. Phys.: Condensed Matter* **2**, 7933.

Cho S Y and McKenzie R H 2006 *Phys. Rev. A* **73**, 012109.

Choi E S, Jobilong E, Wade A, Goetz E, Brooks J S, Yamada J, Mizutani T, Kinoshita T and Tokumoto M 2003 *Phys. Rev. B* **67**, 174511.

Christianson A D, Goremychkin E A, Osborn R, Rosenkranz S, Lumsden M D, Malliakas C D, Todorov I S, Claus H, Chung D Y, Kanatzidis M G, Bewley R I and Guidi T 2008 *Nature* **456**, 930.

Chubukov A V, Devereaux T P and Klein M V 2006 *Phys. Rev. B* **73**, 094512.

Chubukov A V and Jolicoeur T 1992 *Phys. Rev. B* **46**, 11137.

Chubukov A V, Sachdev S and Senthil T 1994a *Nucl. Phys. B* **426**, 601.

Chubukov A V, Sachdev S and Senthil T 1994b *J. Phys.: Cond. Matter* **6**, 8891.

Chung C H, Marston J B and McKenzie R H 2001 *J. Phys.: Cond. Matt.* **13**, 5159.

Clay R T, Li H and Mazumdar S 2008 *Phys. Rev. Lett.* **101**, 166403.

Coldea R, Hayden S M, Aeppli G, Perring T G, Frost C D, Mason T E, Cheong S W and Fisk Z 2001 *Phys. Rev. Lett.* **86**, 5377.

Coldea R, Tennant D A and Tylczynski Z 2003 *Phys. Rev. B* **68**, 134424.

Coleman P 2003 *Ann. Henri Poincare* **4**, 559.

Coleman P and Schofield A J 2005 *Nature* **433**, 226.

Cross M C and Fisher D S 1979 *Phys. Rev. B* **19**, 402.

Cuk T, Shen Z X, Gromko A D, Sun Z and Dessau D S 2004 *Nature* **432**.

Dai D and Whangbo M H 2004 *J. Chem. Phys.* **121**, 672.

Daou R, Chang J, LeBoeuf D, Cyr-Choinière O, Laliberté F, Doiron-Leyraud N, Ramshaw B J, Liang R, Bonn D A, Hardy W N and Taillefer L 2010 *Nature* **463**, 519.

de Soto S M, Slichter C P, Kini A M, Wang H H, Geiser U and Williams J M 1995 *Phys. Rev. B* **52**, 10364.

de Vaulx C, Julien M H, Berthier C, Herbert S, Pralong V and Maignan A 2007 *Phys. Rev. Lett.* **98**, 246402.

Delannoy J Y P, Gingras M J P, Holdsworth P C W and Tremblay A M S 2005 *Phys. Rev. B* **72**, 115114.

Demishev S V, Kondrin M V, Glushkov V V, Sluchanko N E and Samarin N A 1998 *JETP* **86**, 182.

Ding H Q and Makivic M S 1990 *Phys. Rev. Lett.* **64**, 1449.

Dion M, Fournier D, Poirier M, Truong K D and Tremblay A M S 2009 *Phys. Rev. B* **80**, 220511.

Doiron-Leyraud N, Sutherland M, Li S Y, Taillefer L, Liang R, Bonn D A and Hardy W N 2006 *Phys. Rev. Lett.* **97**, 207001.

Doniach S 1968 *J. Appl. Phys.* **39**, 483.

Doniach S and Sondheimer E H 1998 *Greens Functions for Solid State Physics* Imperial College Press London.

Dressel M, Grüner G, Eldridge J E and Williams J M 1997 *Synth. Met.* **85**, 1503.

Dressel M, Klein O, Grüner G, Carlson K D, Wang H H and Williams J M 1994 *Phys. Rev. B* **50**, 13603.

Dumm M, Faltermeier D, Drichko N, Dressel M, Mézière C and Batail P 2009 *Phys. Rev. B* **79**, 195106.

Dumoulin B, Bourbonnais C, Ravy S, Pouget J P and Coulon C 1996 *Phys. Rev. Lett.* **76**, 1360.

Eldridge J E, Kornelsen K, Wang H H, Williams J M, Crouch A V S and Watkins D M 1991 *Solid State Commun.* **79**, 583.

Elhajal M, Canals B, Sunyer R and Lacroix C 2005 *Phys. Rev. B* **71**, 094420.

Elstner N, Singh R R P and Young A P 1993 *Phys. Rev. Lett.* **71**, 1629.

Elstner N, Singh R R P and Young A P 1994 *J. Appl. Phys.* **75**, 5943.

Emery V J and Kivelson S A 1995 *Nature* **374**, 434.

Evenbly G and Vidal G 2010 *Phys. Rev. Lett.* **104**, 187203.

Evers F, Mirlin A D, Polyakov D G and Wölfle P 1999 *Phys. Rev. B* **60**, 8951.

Falicov L M and Proetto C 1993 *Phys. Rev. B* **47**, 14407.

Falicov L M and Victora R 1984 *Phys. Rev. B* **13**, 1695.

Faltermeier D, Barz J, Dumm M, Dressel M, Drichko N, Petrov B, Semkin V, Vlasova R, Mézière C and Batail P 2007 *Phys. Rev. B* **76**, 165113.

Fazekas P and Anderson P 1974 *Phil. Mag.* **30**, 1478.

Ferrero M, Cornaglia P S, Leo L D, Parcollet O, Kotliar G and Georges A 2009 *Phys. Rev. B* **80**, 064501.

Ferrero M, Leo L D, Lecheminant P and Fabrizio M 2007 *J. Phys.: Cond. Matt.* **19**, 433201.

Fischer Ø, Kugler M, Maggio-Aprile I, Berthod C and Renner C 2007 *Rev. Mod. Phys.* **79**, 353.

Fjærestad J O, Zheng W, Singh R R P, McKenzie R H and Coldea R 2007 *Phys. Rev. B* **75**, 174447.

Florens S and Georges A 2004 *Phys. Rev. B* **70**, 035114.

Foury-Leylekian P, Bolloch D L, Hennion B, Ravy S, Moradpour A and Pouget J P 2004 *Phys. Rev. B* **70**, 180405(R).

Fradkin E, Kivelson S A, Lawler M J, Eisenstein J P and Mackenzie A P 2010 *Ann. Rev. Cond. Matt. Phys.* **1**, 153.

Fradkin E and Shenker S H 1979 *Phys. Rev. D* **19**, 3682.

Freed K F 1983 *Acc. Chem. Res.* **16**, 137.

Freericks J K, Falicov L M and Rokhsar D S 1991 *Phys. Rev. B* **44**, 1458.

French S A and Catlow C R A 2004 *Journal of Physics and Chemistry of Solids* **65**, 39.

Fritz L and Sachdev S 2010 *Phys. Rev. B* **82**, 045123.

Fulde P 1995 *Electron correlations in molecules and solids* Springer Berlin.

Galitski V and Kim Y B 2007 *Phys. Rev. Lett.* **99**, 266403.

Gan J Y, Chen Y, Su Z B and Zhang F C 2005 *Phys. Rev. Lett.* **94**, 067005.

Gan J Y, Chen Y and Zhang F C 2006 *Phys. Rev. B* **74**, 094515.

Georges A, Kotliar G, Krauth W and Rozenberg M J 1996 *Rev. Mod. Phys.* **68**, 13.

Gregor K and Motrunich O I 2008 *Phys. Rev. B* **77**, 184423.

Gregor K and Motrunich O I 2009 *Phys. Rev. B* **79**, 024421.

Grover T, Trivedi N, Senthil T and Lee P A 2010 *Phys. Rev. B* **81**, 245121.

Gulley J, Hone D, Scalapino D and Silbernagel B G 1970 *Phys. Rev. B* **1**, 1020.

Gunnarsson O 2004 *Alkali-Doped Fullerides: Narrow-Band Solids with Unusual Properties* World Scientific Singapore.

Gunnarsson O, Calandra M and Han J E 2003 *Rev. Mod. Phys.* **75**, 1085.

Hackl A and Vojta M 2009 *Phys. Rev. B* **80**, R220514.

Hackl A, Vojta M and Sachdev S 2010 *Phys. Rev. B* **81**, 045102.

Haldane F D M 1991 *Phys. Rev. Lett.* **67**, 937.

Hao Z and Chubukov A V 2009 *Phys. Rev. B* **79**, 224513.

Hartnoll S A and Hofman D M 2010 *Phys. Rev. B* **81**, 155125.

Hassan S, Georges A and Krishnamurthy H R 2005 *Phys. Rev. Lett.* **94**, 036402.

Hastings M B 2004 *Phys. Rev. B* **69**, 104431.

Hattori K and Tsunetsugu H 2010 *Phys. Rev. B* **81**, 134503.

Hayashi A, Shiga M and Tachikawa M 2006 *J. Chem. Phys.* **125**, 204310.

Hayashi Y and Ogata M 2007 *J. Phys. Soc. Japan* **76**, 053705.

Heidarian D, Sorella S and Becca F 2009 *Phys. Rev. B* **80**, 012404.

Herring C 1968 *Physics Today* **21**(9), 27.

Hotta C 2003 *J. Phys. Soc. Japan* **72**, 840.

Huang H X, Li Y Q, Gan J Y, Chen Y and Zhang F C 2007 *Phys. Rev. B* **75**, 184523.

Hwang J, Timusk T and Gu G 2004 *Nature* **427**, 714.

Imada M 2005*a* *J. Phys. Soc. Japan* **74**, 859.

Imada M 2005*b* *Phys. Rev. B* **72**, 075113.

Imada M, Fujimori A and Tokura Y 1998 *Rev. Mod. Phys.* **70**, 1039.

Imai Y and Kawakami N 2002 *Phys. Rev. B* **65**, 233103.

Isakov S V, Senthil T and Kim Y B 2005 *Phys. Rev. B* **72**, 174417.

Ishiguro T, Yamaji K and Saito G 1998 *Organic Superconductors* Springer Berlin.

Ishii Y, Tamura M and Kato R 2007 *J. Phys. Soc. Japan* **76**, 033704.

Itaya M, Eto Y, Kawamoto A and Taniguchi H 2009 *Phys. Rev. Lett.* **102**, 227003.

Ito H, Ishihara T, Tanaka H, Kuroda S i, Suzuki T, Onari S, Tanaka Y, Yamada J i and Kikuchi K 2008 *Phys. Rev. B* **78**, 172506.

Itoh M, Hirashima S and Motoya K 1995 *Phys. Rev. B* **52**, 3410.

Itou T, Oyamada A, Maegawa S, Kubo K, Tamura M and Kato R 2009 *Phys. Rev. B* **79**, 174517.

Itou T, Oyamada A, Maegawa S, Tamura M and Kato R 2008 *Phys. Rev. B* **77**, 104413.

Iwata S and Freed K F 1992 *J. Chem. Phys.* **96**, 1304.

Jacko A C, Fjærestad J O and Powell B J 2009 *Nature Phys.* **5**, 422.

Kadowaki K and Woods S B 1986 *Solid State Commun.* **58**, 507.

Kagawa K, Itou T, Miyagawa K and Kanoda K 2004 *Phys.*

Rev. Lett. **93**, 127001.

Kagawa K, Miyagawa K and Kanoda K 2005 *Nature* **436**, 534.

Kagawa K, Miyagawa K and Kanoda K 2009 *Nature Phys.* **5**, 880.

Kagoshima S and Kondo R 2004 *Chem. Rev.* **104**, 5593.

Kandpal H C, Opahle I, Zhang Y Z, Jeschke H O and Valentì R 2009 *Phys. Rev. Lett.* **103**, 067004.

Kanoda K 1997 *Physica C* **282287**, 299.

Kanoda K 2006 *J. Phys. Soc. Japan* **75**, 051007.

Kartsovnik M V 2004 *Chem. Rev.* **104**, 5737.

Kasowski R and Whangbo M H 1990 *Inorg. Chem.* **29**, 360.

Katayama N, Uchida M, Hashizume D, Niitaka S, Matsuno J, Matsumura D, Nishihata Y, Mizuki J, Takeshita N, Gauzzi A, Nohara M and Takagi H 2009 *Phys. Rev. Lett.* **103**, 146405.

Kato R 2004 *Chem. Rev.* **104**, 5319.

Kato R, Kashimura Y, Aonuma S, Hanasaki N and Tajima H 1998 *Solid State Commun.* **105**, 561.

Kato R, Liu Y L, Aonuma S and Sawa H 1996 *Solid State Commun.* **98**, 1021.

Kato R, Tajima A, Nakao A and Tamura M 2006 *J. Am. Chem. Soc.* **128**, 10016.

Kato R, Tajima N, Tamura M and Yamura J I 2002 *Phys. Rev. B* **66**, 020508(R).

Katsura H, Nagaosa N and Lee P A 2010 *Phys. Rev. Lett.* **104**, 066403.

Kawakami T, Shibauchi T, Terao Y, Suzuki M and Krusin-Elbaum L 2005 *Phys. Rev. Lett.* **95**, 017001.

Kawamoto A, Honma Y, Kumagai K I, Matsunaga N and Nomura K 2006 *Phys. Rev. B* **74**, 212508.

Kawamoto A, Miyagawa K, Nakazawa Y and Kanoda K 1995*a* *Phys. Rev. Lett.* **74**, 3455.

Kawamoto A, Miyagawa K, Nakazawa Y and Kanoda K 1995*b* *Phys. Rev. Lett.* **74**, 3455.

Kennett M P and McKenzie R H 2007 *Phys. Rev. B* **76**, 054515.

Kézsmárki I, Shimizu Y, Mihály G, Tokura Y, Kanoda K and Saito G 2006 *Phys. Rev. B* **74**, 201101.

Kikuchi J, Yasuoka H, Hase M, Sasago Y and Uchinokura K 1994 *J. Phys. Soc. Japan* **63**, 034704.

Kino H and Fukuyama H 1996 *J. Phys. Soc. Japan* **65**, 2158.

Kino H and Kontani H 1998 *J. Phys. Soc. Japan* **67**, 3691.

Kino H and Miyazaki T 2006 *J. Phys. Soc. Japan* **75**, 034704.

Klee S and Muramatsu A 1996 *Nucl. Phys. B* **473**, 539.

Koga A and Kawakami N 2000 *Phys. Rev. Lett.* **84**, 4461.

Kogut J B 1979 *Rev. Mod. Phys.* **51**, 659.

Kohno M, Starykh O and Balents L 2007 *Nat. Phys.* **3**, 790.

Komatsu T, Matsukawa N, Inoue T and Saito G 1996) *J. Phys. Soc. Jpn.* **65**, 1340.

Kondo H and Moriya T 1998 *J. Phys. Soc. Japan* **67**, 3695.

Kondo H and Moriya T 2004 *J. Phys. Soc. Jpn.* **73**, 812.

Koretsune T, Motome Y and Furusaki A 2007 *Journal of the Physical Society of Japan* **76**, 074719.

Kornelsen K, Eldridge J E, Homes C C, Wang H H and Williams J M 1989 *Solid State Commun.* **72**, 475.

Korringa J 1950 *Physica* **16**, 601.

Kotetes P and Varelogiannis G 2010 *Phys. Rev. Lett.* **104**, 106404.

Kotliar G, Lange E and Rozenberg M J 2000 *Phys. Rev. Lett.* **84**, 5180.

Kotliar G and Vollhardt D 2004 *Phys. Today* **57**, 53.

Krusin-Elbaum L, Blatter G and Shibauchi T 2004 *Phys. Rev. B* **69**, R220506.

Kubler J, Weger M and Sommers C 1987 *Solid State Commun.* **62**, 801.

Kurosaki K, Shimizu Y, Miyagawa K, Kanoda K and Saito G 2005 *Phys. Rev. Lett.* **95**, 177001.

Kyung B 2007 *Phys. Rev. B* **75**, 033102.

Kyung B and Tremblay A M S 2006 *Phys. Rev. Lett.* **97**, 046402.

Lacorre P 1987 *Journal of Physics C: Solid State Physics* **20**, L775.

Lai H H and Motrunich O I 2010 *Phys. Rev. B* **81**, 045105.

Lang M and Müller J 2003 Springer Verlag Berlin.

Larkin A I 1965 *JETP Lett.* **2**, 130.

Laughlin R B and Pines D 2000 *Proc. Nat. Acad. Sci. (USA)* **97**, 28.

Lawler M J, Paramekanti A, Kim Y B and Balents L 2008 *Phys. Rev. Lett.* **101**, 197202.

Lax M J 1974 *Symmetry Principles in Solid State and Molecular Physics* Wiley New York.

Lechermann F, Georges A, Kotliar G and Parcollet O 2007 *Phys. Rev. B* **76**, 155102.

Lee H, Li G and Monien H 2008 *Phys. Rev. B* **78**, 205117.

Lee J, Fujita K, Schmidt A R, Kim C K, Eisaki H, Uchida S and Davis J C 2009 *Science* **325**, 1099.

Lee P 2008 *Science* **321**, 1306.

Lee P, Nagaosa N and Wen X G 2006 *Rev. Mod. Phys.* **78**, 17.

Lee S S and Lee P 2005 *Phys. Rev. Lett.* **95**, 036403.

Lee S S, Lee P A and Senthil T 2007*a* *Phys. Rev. Lett.* **98**, 067006.

Lee S S, Lee P and Senthil T 2007*b* *Phys. Rev. Lett.* **98**, 067006.

Lee Y J, Nieminen R M, Ordejon P and Canadell E 2003 *Phys. Rev. B* **67**, 180505.

Lefebvre S, Wzietek P, Brown S, Bourbonnais C, Jérome D, Mézirè C, Fourmigué M and Batail P 2000 *Phys. Rev. Lett.* **85**, 5420.

Li H, Clay R T and Muzumdar S 2010 *J. Phys.: Condens. Matter* **22**, 272201.

Liebsch A, Ishida H and Merino J 2009 *Phys. Rev. B* **79**, 195108.

Limelette P, Georges A, Jérome D, Wzietek P, Metcalf P and Honig J M 2003 *Science* **302**, 89.

Limelette P, Wzietek P, Florens S, Georges A, Costi T A, Pasquier C, Jérome D, Mézière C, and Batail P 2003 *Phys. Rev. Lett.* **91**, 016401.

LiMing W, Misguich G, Sindzingre P and Lhuillier C 2000 *Phys. Rev. B* **62**, 6372.

Liu J, Schmalian J and Trivedi N 2005 *Phys. Rev. Lett.* **94**, 127003.

Liu J, Trivedi N, Lee Y, Harmon B N and Schmalian J 2007 *Phys. Rev. Lett.* **99**, 227003.

MacDonald A, Girvin S and Yoshioka D 1990 *Phys. Rev. B* **41**, 2565.

Maier T A, Poilblanc D and Scalapino D J 2008 *Phys. Rev. Lett.* **100**, 237001.

Manna R S, de Souza M, Brühl A, Schluter J A and Lang M 2010 *Phys. Rev. Lett.* **104**, 016403.

Masutomi R, Karaki Y and Ishimoto H 2004 *Phys. Rev. Lett.* **92**, 025301.

Mayaffre H, Wzietek P, Jérome D, Lenoir C and Batail P 1994 *Europhys. Lett.* **25**, 208.

Mazumdar S and Clay R T 2008 *Phys. Rev. B* **77**, 180515.

McKenzie R H 1998 *Comments Cond. Matt. Phys.* **18**, 309.

McKenzie R H 2007 *Nature Phys.* **3**, 756.

McWhan D B, Menth A, Remeika J P, Brinkman W F and Rice T M 1973 *Phys. Rev. B* **7**, 1920.

Meng Z, Lang T C, Wessel S, Assaad F F and Muramatsu A 2010 *Nature* **464**, 847.

Merino J, Dumm M, Drichko N, Dressel M and McKenzie R H 2008 *Phys. Rev. Lett.* **100**, 086404.

Merino J and McKenzie R H 2000a *Phys. Rev. B* **61**, 7996.

Merino J and McKenzie R H 2000b *Phys. Rev. B* **62**, 16442.

Merino J and McKenzie R H 2000c *Phys. Rev. B* **62**, 16442.

Merino J, McKenzie R H, Marston J and Chung C 1999 *J. Phys.: Condens. Matter* **11**, 2965.

Merino J, Powell B J and McKenzie R H 2006 *Phys. Rev. B* **73**, 235107.

Merino J, Powell B J and McKenzie R H 2009a *Phys. Rev. B* **79**, 161103.

Merino J, Powell B J and McKenzie R H 2009b *Phys. Rev. B* **80**, 145116.

Millis A, Monien H and Pines D 1990a *Phys. Rev. Lett.* **42**, 167.

Millis A, Monien H and Pines D 1990b *Phys. Rev. B* **42**, 167.

Mineev V P and Samokhin K V 1999 *Introduction to Unconventional Superconductivity* Gordan and Breach Amsterdam.

Misawa T, Yamaji Y and Imada M 2006 *J. Phys. Soc. Japan* **75**, 083705.

Misguich G and L'huillier C 2005 *Frustrated spin systems* World Scientific.

Mitrović V F, Bachman H N, Halperin W P, Reyes A P, Kuhns P and Moulton W G 2002 *Phys. Rev. B* **66**, 014511.

Miyagawa K, Kanoda K and Kawamoto A 2004 *Chem. Rev.* **104**, 5635.

Miyagawa K, Kawamoto A and Kanoda K 2002 *Phys. Rev. Lett.* **89**, 017003.

Miyagawa K, Kawamoto A, Nakazawa Y and Kanoda K 1995 *Phys. Rev. Lett.* **75**, 1174.

Miyazaki T and Kino H 2003 *Phys. Rev. B* **68**, 220511(R).

Miyazaki T and Kino H 2006 *Phys. Rev. B* **73**, 035107.

Miyazaki T and Ohno T 1999 *Phys. Rev. B* **59**, R5269.

Moessner R, Sondhi S L and Fradkin E 2001 *Phys. Rev. B* **65**, 024504.

Monthoux P, Pines D and Lonzarich G G 2007 *Nature* **450**, 1177.

Montrunich O I 2005 *Phys. Rev. B* **72**, 045105.

Moret R, Ravy S, Pouget J P, Comes R and Bechgaard K 1986 *Phys. Rev. Lett.* **57**, 1915.

Mori T 1998 *Bull. Chem. Soc. Japan* **71**, 2509.

Mori T 2004 *Chem. Rev.* **104**, 4947.

Morita H, Watanabe S and Imada M 2002 *J. Phys. Soc. Japan* **71**, 2109.

Moriya T 1956 *Progress of Theoretical Physics* **16**, 23.

Moriya T 1963 *J. Phys. Soc. Japan* **18**, 516.

Moriya T and Ueda K 2000 *Adv. Phys.* **49**, 555.

Moriya T and Ueda K 2003 *Rep. Prog. Phys.* **66**, 1299.

Morozov N, Krusin-Elbaum L, Shibauchi T, Bulaevskii L N, Maley M P, Latyshev Y I and Yamashita T 2000 *Phys. Rev. Lett.* **84**, 1784.

Moses P and McKenzie R 1999 *Phys. Rev. B* **60**, 7998.

Motrunich O I 2005 *Phys. Rev. B* **72**, 045105.

Motrunich O I 2006 *Phys. Rev. B* **73**, 155115.

Mott N F 1949 *Proc. Roy. Soc.* **62**, 416.

Murata K, Ishibashi M, Honda Y, Fortune N A, Tokumoto M, KInoshita N and Anzai H 1990 *Solid State Commun.* **76**, 377.

Nakamura A, Yoshimoto Y, Kosugi T, Arita R and Imada M 2009 *J. Phys. Soc. Japan* **78**, 083710.

Nakamura T, Takahashi T, Aonumac S and Kato R 2001 *J. Mat. Chem.* **11**, 2159.

Nakao A and Kato R 2005 *J. Phys. Soc. Japan* **74**, 2754.

Nakatsuji S, Nambu Y, Tonomura H, Sakai O, Jonas S, Broholm C, Tsunetsugu H, Qiu Y and Maeno Y 2005 *Science* **309**, 1697.

Nam M S, Ardavan A, Blundell S J and Schlueter J A 2007 *Nature* **449**, 584.

Nave C P and Lee P A 2007 *Phys. Rev. B* **76**, 235124.

Neumann M, Nyeki J, Cowan B and Saunders J 2007 *Science* **317**, 1356.

Nevidomskyy A H, Scheiber C, Sénéchal D and Tremblay A M S 2008 *Phys. Rev. B* **77**, 064427.

Ng T K and Lee P A 2007 *Phys. Rev. Lett.* **99**, 156402.

Noce C and Cuoco M 1996 *Phys. Rev. B* **54**, 13047.

Norman M 2006 *The Handbook of Magnetism and Advanced Magnetic Materials* Vol. 5 Wiley. cond-mat/0609559.

Norman M 2010 *Physics* **3**, 86.

Normand B 2009 *Contemp. Phys.* **50**, 533.

Nussinov Z, Batista C D, Normand B and Trugman S A 2007 *Phys. Rev. B* **75**, 094411.

Ohashi T, Momoi T, Tsunetsugu H and Kawakami N 2008 *Phys. Rev. Lett.* **100**, 076402.

Ohmichi E, Ito H, Ishiguro T, Komatsu T and Saito G 1997 *Journal of the Physical Society of Japan* **66**, 310.

Ohmichi E, Ito H, Ishiguro T, Saito G and Komatsu T 2009 *Phys. Rev. B* **57**, 7481.

Ong N and Cava R 2004 *Science* **305**, 5680.

Paiva T, Scalettar R T, Zheng W, Singh R R P and Oitmaa J 2005 *Phys. Rev. B* **72**, 085123.

Papanikolaou S, Fernandes R M, Fradkin E, Phillips P W, Schmalian J and Sknepnek R 2008 *Phys. Rev. Lett.* **100**, 026408.

Parcollet O, Biroli G and Kotliar G 2004 *Phys. Rev. Lett.* **92**, 226402.

Pardini T and Singh R R P 2008 *Phys. Rev. B* **77**, 214433.

Pavarini E, Dasgupta I, Saha-Dasgupta T, Jepsen O and Andersen O K 2001 *Phys. Rev. Lett.* **87**, 047003.

Perfetti L, Gloor T A, Mila F, Berger H and Grioni M 2005 *Phys. Rev. B* **71**, 153101.

Phillips P 2003 *Advanced Solid State Physics* Westview Boulder.

Pintschovius L, Rietschel H, Sasaki T, Mori H, Tanaka S, Toyota N, Lang M and Steglich F 1997 *Europhys. Lett.* **37**, 627.

Platt J 1964 *Science* **146**, 347.

Powell B J 2006 *J. Phys.: Condens. Matter* **18**, L575.

Powell B J 2008 *J. Phys.: Condens. Matter* **20**, 345234.

Powell B J 2011 *An introduction to effective low-energy Hamiltonians in condensed matter physics and chemistry* in J. R. Reimers (Ed.), *Computational Methods for Large Systems: Electronic Structure Approaches for Biotechnology and Nanotechnology*, (Wiley, Hoboken), in press, preprint arXiv:0906.1640.

Powell B J and McKenzie R H 2004a *J. Phys.: Condens. Matter* **16**, L367.

Powell B J and McKenzie R H 2004b *Phys. Rev. B* **69**, 024519.

Powell B J and McKenzie R H 2005 *Phys. Rev. Lett.* **94**, 047004.

Powell B J and McKenzie R H 2006 *J. Phys.: Condens. Matter* **18**, R827.

Powell B J and McKenzie R H 2007 *Phys. Rev. Lett.* **98**, 027005.

Powell B J, Yusuf E and McKenzie R H 2009 *Phys. Rev. B* **80**, 054505.

Powell B, Merino J and McKenzie R H 2010 *Phys. Rev. B* **80**, 085113.

Pratt F L 2010 *Physica B* **405**, S205.

Pratt F L and Blundell S J 2005 *Phys. Rev. Lett.* **94**, 097006.

Pratt F L, Blundell S J, Marshall I M, Lancaster T, Lee S L, Drew A, Divakar U, Matsui H and Toyota N 2003 *Polyhedron* **22**, 2307.

Pruschke T, Jarrell M and Freericks J K 1995 *Adv. Phys.* **44**, 187.

Qi Y and Sachdev S 2008 *Phys. Rev. B* **77**, 165112.

Qi Y, Xu C and Sachdev S 2009 *Phys. Rev. Lett.* **102**, 176401.

Rahal M, Chasseau D, Gaulthier J, Ducasse L, Kurmoo M and Day P 1997 *Acta Crystallogr. B* **53**, 159.

Ramirez A 2008 *Nature Phys.* **4**, 442.

Ramirez A P 1994 *Annu. Rev. Mater. Sci.* **24**, 453.

Read N and Sachdev S 1991a *Phys. Rev. Lett.* **66**, 1773.

Read N and Sachdev S 1991b *Int. J. Mod. Phys. B* **5**, 219.

Reuther J and Thomale R 2010 *arXiv:1006.3622* .

Rice M J 1968 *Phys. Rev. Lett.* **20**, 1439.

Sachdev S 1992 *Phys. Rev. B* **45**, 12377.

Sachdev S 1999 *Quantum Phase Transitions* Cambridge University Press.

Sachdev S 2000 *Science* **288**, 475.

Sachdev S 2008 *Nature Phys.* **4**, 173.

Sachdev S 2009a *arXiv:0901.4103* .

Sachdev S 2009b *Physics* **2**, 90.

Sahebsara P and Senechal D 2006 *Phys. Rev. Lett.* **97**, 257004.

Sahebsara P and Sénéchal D 2008 *Phys. Rev. Lett.* **100**, 136402.

Sandvik A W and Scalapino D J 1995 *Phys. Rev. B* **51**, 9403.

Sasaki T, Oizumi H, Yoneyama N and Kobayashi N 2010 arXiv:1004.4406.

Sasaki T, Yoneyama N, Suzuki A, Kobayashi N, Ikemoto Y and Kimura H 2005 *J. Phys. Soc. Japan* **74**, 2351.

Scalapino D J 2006 *arXiv:condmat/0610.710* .

Scalapino D J, Loh E and Hirsch J E 1986 *Phys. Rev. B* **34**, 8190.

Scalapino D J and Trugman S A 1996 *Phil. Mag. B* **74**, 607.

Schiffer P and Daruka I 1997 *Phys. Rev. B* **81**, 4232.

Schmalian J 1998 *Phys. Rev. Lett.* **56**, 13712.

Schumann R 2002 *Ann. Phys. (Leipzig)* **11**, 49.

Schumann R 2008 *Ann. Phys. (Leipzig)* **17**, 221.

Scriven E and Powell B J 2009a *J. Chem. Phys.* **130**, 104508.

Scriven E and Powell B J 2009b *Phys. Rev. B* **80**, 085113.

Sen D and Chitra R 1995 *Phys. Rev. B* **51**, 1922.

Senthil T 2008 *Phys. Rev. B* **78**, 045109.

Seo H, Merino J, Yoshioka H and Ogata M 2006 *J. Phys. Soc. Japan* **75**, 051009.

Shaik S S and Hiberty P C 2008 *A chemist's guide to valence bond theory* Wiley Hoboken.

Shao X, Yoshida Y, Nakano Y, Yamochi H, Sakata M, Maesato M, Otsuka A, Saito G and Koshihara S y 2009 *Chemistry of Materials* **21**, 1085.

Shastry B S and Kumar B 2002 *Progress of Theoretical Physics Supplement* **145**, 1.

Sheng D N, Motrunich O I and Fisher M P A 2009 *Phys. Rev. B* **79**, 205112.

Shi M, Bendounan A, Razzoli E, Rosenkranz S, Norman M R, Campuzano J C, Chang J, Monsson M, Sassa Y, Claesson T, Tjernberg O, Patthey L, Momono N, Oda M, Ido M, Guerrero S, Mudry C and Mesot J 2009 *Europhys. Lett.* **88**, 27008.

Shibauchi T, Krusin-Elbaum L, Li M, Maley M P and Kes P H 2001 *Phys. Rev. Lett.* **86**, 5763.

Shimizu Y, Akimoto H, Tsuji H, Tajima A and Kato R 2007a *Phys. Rev. Lett* **99**, 256403.

Shimizu Y, Akimoto H, Tsuji H, Tajima A and Kato R 2007b *J. Phys.: Condens. Matter* **19**, 145340.

Shimizu Y, Kasahara H, Furuta T, Miyagawa K, Kanoda K, Maesato M and Saito G 2010 *Phys. Rev. B* **81**, 224508.

Shimizu Y, Miyagawa K, Kanoda K, Maesato M and Saito G 2003 *Phys. Rev. Lett.* **91**, 107001.

Shimizu Y, Miyagawa K, Kanoda K, Maesato M and Saito G 2006 *Phys. Rev. B* **73**, 140407(R).

Sigrist M and Ueda K 1991 *Rev. Mod. Phys.* **63**, 239.

Simonov S V, Shevyakova I Y, Zorina L V, Khasanov S S, Buravov L I, Emelyanov V A, Canadell E, Shibaeva R P and Yagubskii E B 2005 *J. Mater. Chem.* **15**, 2476.

Sindzingre P, Lecheminant P and Lhuillier C 1994 *Phys. Rev. B* **50**, 3108.

Singh R R P 2010 *Physics* **3**, 35.

Singh R R P and Gelfand M P 1990 *Phys. Rev. B* **42**, 996.

Singh R R P and Huse D A 2007 *Phys. Rev. B* **76**, 180407.

Singleton J 2000 *Rep. Prog. Phys.* **63**, 1111.

Singleton J, Goddard P, Ardavan A, Harrison N, Blundell S, Schluter J and Kini A 2002 *Phys. Rev. Lett.* **88**, 037001.

Singleton J and Mielke C 2002 *Contemp. Phys.* **43**, 63.

Smith D F, Slichter C P, Schlueter J A, Kini A M and Daugherty R G 2004 *Phys. Rev. Lett.* **93**, 167002.

Smith M F and McKenzie R H 2008 *Phys. Rev. Lett.* **101**, 266403.

Smith M F and McKenzie R H 2009 *Phys. Rev. B* **80**, 214528.

Smith M F, Paglione J, Walker M B and Taillefer L 2005 *Phys. Rev. B* **71**, 014506.

Sondheimer E H 1948 *Proc. R. Soc. A* **193**, 484.

Starykh O A, Zhitomirsky M E, Khomskii D I, Singh R R P and Ueda K 1996 *Phys. Rev. Lett.* **77**, 2558.

Starykh O, Katsura H and Balents L 2010 *Physical Review B* **82**, 014421.

Strack C, Akinci C, Pashchenko V, Wolf B, Uhrig E, Assmus W, Lang M, Schreuer J, Wiehl L, Schlueter J A, Wosnitza J, Schweitzer D, Müller J and Wykhoff J 2005 *Phys. Rev. B* **72**, 054511.

Sushko Y V, Shirakawa N, Murata K, Kubo Y, Kushch N D and Yabubskii E B 1997 *Synth. Met.* **85**, 1541.

Suzuki T, Negishi E, Uozaki H, Matsui H and Toyota N 2006 *J. Low Temp. Phys.* **142**, 567.

Takigawa M, Starykh O A, Sandvik A W and Singh R R P 1997 *Phys. Rev. B* **56**, 13681.

Tallon J, Cooper J, Naqib S and Loram J 2006 *Physical Review B* **73**, 180504.

Tamura M and Kato R 2002 *J. Phys.: Condens. Matter* **14**, L729.

Tamura M and Kato R 2004 *Chem. Phys. Lett.* **387**, 448.

Tamura M, Nakao A and Kato R 2006 *J. Phys. Soc. Japan* **75**, 093701.

Tamura M, Tajima A and Kato R 2005 *Synth. Met.* **152**, 397.

Tamura M, Tajima H, Yakushi K, Kuroda H, Kobayashi A, Kato R and Kobayashi H 1991 *J. Phys. Soc. Jpn.* **60**, 3861.

Tamura M, Takenaka K, Takagi H, Sugai S, Tajima A and Kato R 2005 *Chem. Phys. Lett.* **411**, 133.

Tanatar M A, Ishiguro T, Ito H, Kubota M and Saito G 1997 *Phys. Rev. B* **55**, 12529.

Taniguchi H, Kanoda K and Kawamoto A 2003 *Phys. Rev. B* **67**, 014510.

Taniguchi H, Sato R, Satoh K, Kawamoto A, Okamoto H and Kobayasi T a K 2006 *J. Low. Temp. Phys.* **142**, 437.

Taylor O J, Carrington A and Schlueter J A 2007 *Phys. Rev.*

Lett. **99**, 057001.

Tennant D A, Cowley R A, Nagler S E and Tsvelik A M 1995 *Phys. Rev. B* **52**, 13368.

Thouless D J 1965 *Proc. Phys. Soc.* **86**, 893.

Timusk T and Statt B 1999 *Rep. Prog. Phys.* **62**, 61.

Tinkham M 1992 *Group Theory and Quantum Mechanics* McGraw-Hill New York.

Tocchio L F, Parola A, Gros C and Becca F 2009 *Phys. Rev. B* **80**, 064419.

Toyota N, Sbimazub T, Sasakib T, SItibatab K, Kajitani T, Ian M and Ikeda S 1997 *Synth. Met.* **86**, 2009.

Toyota N and Suzuki T 2007 *Comptes Rendus Chimie* **10**, 37.

Trumper A E 1999 *Phys. Rev. B* **60**, 2987.

Tsai S W and Marston J 2001 *Can. J. Phys.* **79**, 1463.

Tsiper E and Soos Z 2003 *Phys. Rev. B* **68**, 085301.

Tsunetsugu H and Arikawa M 2007 *J. Phys.: Cond. Matter* **19**, 145248.

Ueda K, Kontani H, Sigrist M and Lee P A 1996 *Phys. Rev. Lett.* **76**, 1932.

Uji S and Brooks J S 2006 *J. Phys. Soc. Japan* **75**, 051014.

Uji S, Shinagawa H, Terashima T, Yakabe T, Terai Y, Tokumoto M, Kobayashi A, Tanaka H and Kobayashi H 2001 *Nature* **410**, 908.

Underhill A E, Clark R A, Marsden I, Friend R H, Tajima H, Naito T, Tamura M, Kuroda H, Kobayashi A, Kobayashi H, Canadell E, Ravy S and Pouget J P 1991 *J. Phys.: Condens. Matter* **3**, 933.

Valkov V, Misskan V and Petrakovskii G 2006 *JETP* **102**, 234.

Varelogiannis G 2002 *Phys. Rev. Lett.* **88**, 117005.

Visser R J J, Oostra S, Vettier C and Voiron J 1983 *Phys. Rev. B* **28**, 2074.

Wang Y, Li L and Ong N P 2006 *Phys. Rev. B* **73**, 024510.

Watanabe T, Yokoyama H, Ogata M, Tanaka Y and Inoue J 2006 *J. Phys. Soc. Japan* **75**, 074707.

Watanabe T, Yokoyama H, Tanaka Y and Inoue J 2008 *Phys. Rev. B* **77**, 214505.

Welp U, Fleshler S, Kwok W K, Crabtree G W, Carlson K D, Wang H H, Geiser U, Williams J M and Hitsman V M 1992 *Phys. Rev. Lett.* **69**, 840.

Wen X G 2002 *Phys. Rev. B* **65**, 165113.

Wen X G 2004 *Quantum Field Theory of Many-Body Systems* third edn Oxford University Press. Chapter 1.

Weng M Q, Sheng D N, Weng Z Y and Bursill R J 2006 *Phys. Rev. B* **74**, 012407.

Werner P and Millis A J 2010 arXiv:1001.1377.

White S R and Affleck I 1996 *Phys. Rev. B* **54**, 9862.

Williams J M, Ferraro J R, Thron R J, Carlson K D, Geiser U, Wang H H, Kini A A and Whangbo M H 1992 *Organic Superconductors (Including Fullerenes): Synthesis, Structure, Properties, and Theory* Prentice Hall Englewood Cliffs.

Wolfle P 2000 *Adv. Solid State Phys.* **40**, 77.

Wosnitza J 2007 *J. Low Temp. Phys.* **164**, 641.

Wosnitza J, Goll G, Beckmann D, Wanka S, Schweitzer D and Strunz W 1996 *J. Phys. I* **6**, 1597.

Wosnitza J, Hagel J, Qualls J S, Brooks J S, Balthes E, Schweitzer D, Schlueter J A, Geiser U, Mohtasham J, Winter R W and Gard G L 2002 *Phys. Rev. B* **65**, 180506.

Wrobel P and Suleja W 2007 *Phys. Rev. B* **76**, 214509.

Xu C and Sachdev S 2009 *Phys. Rev. B* **79**, 064405.

Yamaguchi K, Kawakami T, Taniguchi T, Nakano S, Kitagawa Y, Nagao H, Ohsaku T and Takeda R 2003 *Polyhedron* **22**, 2077.

Yamashita M, Nakata N, Kasahara Y, Sasaki T, Yoneyama N, Kobayashi N, Fujimoto S, Shibauchi T and Matsuda Y 2009 *Nature Phys.* **5**, 44.

Yamashita M, Nakata N, Senshu Y, Nagata M, Yamamoto H M, Kato R, Shibauchi T and Matsuda Y 2010 *Science* **328**, 1246.

Yamashita S, Nakazawa Y, Oguni M, Oshima Y, Nojiri H, Shimizu Y, Miygawa K and Kanoda K 2008 *Nature Phys.* **4**, 459.

Yamaura J I, Nakao A and Kato R 2004 *J. Phys. Soc. Japan* **73**, 976.

Yamochi H, Komatsu T, Matsukawa N, Saito G, Mori T, Kusunoki M and Sakaguchi K 1993 *J. Am. Chem. Soc.* **115**, 11319.

Yan S, Huse D A and White S R 2010 *arXiv:1011.6114* .

Yang H Y, Laeuchli A, Mila F and Schmidt K 2010 *arXiv:1006.5649* .

Yonezawa S, Muraoka Y, Matsushita Y and Hiroi Z 2004 *J. Phys.: Cond. Matter* **16**, L9.

Yu R C, Williams J M, Wang H H, Thompson J E, Kini A M, Carlson K D, Ren J, Whangbo M H and Chaikin P M 1991 *Phys. Rev. B* **44**, 6932.

Yunoki S and Sorella S 2006 *Phys. Rev. B* **74**, 014408.

Yusuf E, Powell B J and McKenzie R H 2007 *Phys. Rev. B* **75**, 214515.

Yusuf E, Powell B J and McKenzie R H 2009 *J. Phys.: Condens. Matter* **21**, 195601.

Zaanen J 2006 *Nat. Phys.* **2**, 138.

Zaanen J, Sawatzky G A and Allen J W 1985 *Phys. Rev. Lett.* **55**, 418.

Zheng G Q, Kuhns P L, Reyes A P, Liang B and Lin C T 2005 *Phys. Rev. Lett.* **94**, 047006.

Zheng W, Fjærestad J O, Singh R R, McKenzie R H and Coldea R 2006 *Phys. Rev. B* **74**, 224420.

Zheng W, McKenzie R H and Singh R R P 1999 *Phys. Rev. B* **59**, 14367.

Zheng W, Singh R R P, McKenzie R H and Coldea R 2005 *Phys. Rev. B* **71**, 134422.

Ziman J M 1960 *Electrons and Phonons* Oxford University Press Oxford.

Zuo F, Schlueter J A and Williams J M 1999 *Phys. Rev. B* **60**, 574.